UC Davis

UC Davis Electronic Theses and Dissertations

Title

Dissecting tumor-associated macrophage-driven resistance to immunotherapy in the complex melanoma microenvironment

Permalink

https://escholarship.org/uc/item/48g3b7wk

Author

Kirane, Amanda

Publication Date

2024

Peer reviewed|Thesis/dissertation

eScholarship.org Powered by the California Digital Library
University of California

Dissecting Tumor-Associated Macrophage-Driven Resistance to Immunotherapy in the Complex Melanoma Microenvironment

By
AMANDA KIRANE
DISSERTATION

Submitted in partial satisfaction of the requirements for the degree of

DOCTOR OF PHILOSOPHY

in

Immunology

in the

OFFICE OF GRADUATE STUDIES

of the

UNIVERSITY OF CALIFORNIA

DAVIS

Approved:

Emanual Maverakis, Chair

Jamal Lewis

Athena Soulika

Nicholas Mitsiades

Committee in Charge

2024

Acknowledgements

I would like to express my heartfelt gratitude to the remarkable individuals who have supported me through this adventure. This journey has taught me resilience, empathy, and the importance of staying true to oneself. First, I want to thank the patients and melanoma community who inspired my work in Immunotherapy – without their willingness to participate in medical research, our advances in translational science would not be possible.

It would take me many pages to properly thank all the advisors, mentors, and teachers that have helped me to complete this work: Thank you to all who have contributed to my growth and success, this dissertation is a testament to our collective efforts and support. A special thank you to my dissertation committee: Athena Soulika, Jamal Lewis, Nicholas Mitsiades, and Michiko Shimoda. Your wisdom and expertise have shaped my academic and research path, and I am grateful for the opportunities you have provided me.

To my Major Professor, Emanual Maverakis, thank you for your guidance, encouragement, and belief in my abilities. Thank you for normalizing the pain points, persisting against highly unfavorable odds, making magic out of very little substrate, and demonstrating that “no” is just a starting offer. Academic medicine, translational research, and the efforts of a clinician-scientist are a Sishyphean undertaking and require tremendous mental training in seeing the world for its opportunities and possibilities, not for its tragedies.

To my former PI: Rolf Brekken, I have no idea what my career would look like without your mentorship. A single conversation, sitting on the curb outside your house, changed my trajectory forever. I had always been regarded as too ambitious by the circle of those close to me then – you were the first to suggest I should be aiming even higher. Thank you for giving me inspiration, opportunity, and second (third, fourth) chances to actualize those goals.

To my mentor and friend, Banafshe Larijani, thank you for being willing to inherit me as a mentee. I have it on good authority that I am certainly not the easiest to train – between the stubborn convictions and the constant flight of ideas. It takes a special perserverence to see thos qualities for their equal potential in being relentless in pursuit of answers and creative, out-of-the-box (sometimes, not just out-of-the-box but out-of-this-world) perspective. Learning from you and partnering you was true serendipity and I look forward to all we have to come!

I would like to extend my heartfelt appreciation to my incredible lab team for their collaborative spirit and willingness to pivot, adapt, and get creative in our research endeavors. You all have been instrumental in overcoming challenges and achieving milestones. Your expertise, commitment to excellence, and innovative thinking have not only enriched our scientific discoveries but have also fostered a dynamic and inspiring work environment. I am grateful for each member's unique contributions, camaraderie, and shared passion for advancing knowledge in Immunology. Together, we have navigated obstacles, celebrated successes, and grown both personally and professionally.

I would like to extend a special thank you to my partner, Andrew, for his unwavering support, love, and sacrifice over the last five years. Your understanding, perspective, and encouragement have been my anchor during the tumultuous times of balancing school, work, and family responsibilities. Your confidence in me has been a constant source of strength and

motivation. I am truly grateful to have you by my side, thank you for being my rock and for always believing in our shared dreams and aspirations.

To Aoife: You are my constant inspiration. Thank you for tagging along, voluntarily or not, for hugs on long days, coffee dates on early mornings, your endless humor, and your patience. There was not a minute I did not miss being with you. I can only hope to support you actualizing the dreams that make you happy the way you have honored mine and I hope I have made you proud. I love being able to share our enthusiasm for science, curiosity, making magic, and exploring the world in both very abstract and very precise ways. You embody both the family motto, “Hugs everyday” and the family mission statement, “when the going gets tough, we get creative.” I love you beyond words and owe you my deepest gratitude for sharing the world with me.

Abstract

Despite the advancements in immunotherapies for cancer having profound impact on survival for some patients, the lack of consistent, predictive markers of treatment response and adverse event risk remains a significant clinical challenge. Checkpoint inhibitors targeting programmed cell death protein 1 (PD-1), cytotoxic T-lymphocyte-associated protein 4 (CTLA-4), and other immune checkpoints, have significantly altered the landscape of melanoma care, but a substantial portion of patients still face inadequate responses, underscoring the critical need for improved biomarker tools that offer high distinguishability, single to subcellular resolution, and high throughput with low-cost preparation. The work presented here focuses on the imperative need for precision medicine in cancer treatment, particularly to resolve the complexities in harnessing the immune system's potential for therapeutic benefits.

The diverse and heterogeneous nature of melanoma, characterized by high mutational burden and adaptive resistance mechanisms, complicates the identification of effective biomarkers for best treatment selection. One focus of this research lies in exploring neoadjuvant intra-tumoral therapy in high-risk melanoma, revealing promising results in generating systemic immune responses with less severe adverse event profiles compared to systemic treatments, such as immune checkpoint blockade (ICB). Studying the immune cell dynamics related to therapy responses has identified potential novel markers that shed critical light on the inconsistencies of patient responses and the importance of innate immune cell contributions. Novel technical approaches incorporating immune time-resolved Förster resonance energy transfer (iFRET) technology are utilized to capture molecular properties of the tumor microenvironment beyond traditional expression profiling. This innovative method allows for the interrogation of the function of multiple checkpoints and signaling pathways, enabling a deeper understanding of tumor activity and response to therapies.

Second, investigations presented here delved into the role of AXL tyrosine kinase in melanoma and its complex interactions in the tumor microenvironment, particularly with tumor-associated macrophages (TAMs). Prior research focused on oncolytic viruses (OV) and ICB, particularly in relationship to the multi-faceted roles of TAMs, have highlighted significant gaps in understanding the intricate interactions within the tumor-immune microenvironment (TiME), ultimately affecting treatment outcomes. Studies presented in this thesis elucidated the function of AXL in multiple melanoma models, providing novel insights into immune responses impacted by AXL function and the potential to exploit these mechanisms to improve immunotherapeutic strategies. These mechanistic studies, utilizing *in vivo* and *in vitro* models of multicellular dynamics and multiple AXL inhibition strategies, reveal context-dependent relationships between AXL activity, macrophage functions, and immune recognition of tumors. The synergistic effects of AXL inhibition and anti-PD-1 immunotherapy may offer promising avenues for enhancing tumor control in anti-PD-1-resistant melanoma.

Further investigations are needed to enhance predictive accuracy and refine patient stratification strategies for immunotherapy. In parallel, exploring the neoadjuvant setting and leveraging advances in regional therapies offer promising avenues to augment immune responses, control tumor growth, and foster durable therapeutic outcomes. By delving into checkpoint ligand-receptor engagements involving non-tumor immune cells and TAMs, functional assessments of interactive states in tumors stand out as promising tools for enhancing precision immunotherapy and delineating optimal treatment strategies tailored to individual patient profiles. Continued research efforts are vital to unraveling the complexities of melanoma-immune interactions and paving the way for personalized interventions and strategic drug combinations to effectively target immunosuppressive tumor environments and enhance treatment outcomes for patients with melanoma.

Table of Contents

Acknowledgements ii

Abstract iv

Table of Contents vi

List of Figures and Tables viii

List of Abbreviations xi

Copyright Acknowledgements xiv

Chapter 1: Introduction 1

Chapter 2: Literature Review 4

1. Toward Precision Immunotherapy in Melanoma for Improved Patient Outcomes 4
2. Improving the Immune Response and Durability of Cancer Control: Neoadjuvant Therapy and Harnessing the Innate Immune System 7
3. iFRET and Novel Biomarker Development 13

Novel IFRET Imaging for Determining Immune Checkpoint Interaction in *Ex Vivo* Assays 14

PD-1/PD-L1 Interaction State is Indicative of Patient Outcome in Various Cancer Types .. 15

4. Immunotherapy Resistance - Targeting the Immunosuppressive Tumor Environment .. 18
5. Targeting the Melanoma TiME 22

AXL is a Biomarker of Aggressive Melanoma 30

Chapter 3 Methodology 32

1. Human Studies 32
2. *In Vivo* Experiments 41
3. *In Vitro* Experiments 42

Chapter 4: Functional Analysis of Neoaduvant Oncolytic Virus 47

1. Trial Design and Clinical Analysis 47
2. Shifts in the TiME 51
3. iFRET Functional Immune Engagement 51
4. Immune Monitoring 53
5. Variability in Innate Systemic Response 58

Chapter 5: Macrophage-Dependent Synergy of AXL Tyrosine Kinase Inhibition with Anti-PD-1 Therapy 61

1. The Clinical Landscape of AXL Expression in Melanoma 61
2. AXL Inhibition in Models of Anti-PD-1-Resistant Melanoma 68
3. AXL Inhibition Augments Anti-PD-1 Therapy 70
4. TiME Shifts with AXL and PD-1 Inhibition 73
5. Selective Depletion of TAMs Impacts Anti-AXL-mediated Inhibition of Tumor Growth 75
6. TiME Impact of Myeloid Cell Depletion 78
7. AXL expression and activity related to macrophage polarization 80
8. AXL-related Checkpoint Expression is Context-dependent 82
9. AXL-related Macrophage Function 84
10. Environmental context impacts AXL and PD-1 synergistic function 86
11. AXL-inhibition induces changes in the secretome 88

Chapter 6: Discussion 91

Chapter 7: Conclusion and Future Directions 105

References 109

Appendix: Copyright documentation 121

List of Figures and Tables

Chapter 2: 4

Figure 2-1: Survival in advanced melanoma 5

Figure 2-2: Neoadjuvant immunotherapy in melanoma 8

Figure 2-3: TVEC mechanism of action 10

Figure 2-4: Neoadjuvant TVEC improves durable tumor control over surgery alone 10

Figure 2-5: Potentially divergent mechanisms of response may facilitate therapeutic selection 12

Figure 2-6: Successful biomarkers will allow precision therapeutic stratification for patients with high-risk disease 13

Figure 2-7: iFRET methodology 14

Figure 2-8: Median iFRET efficiency as a biomarker 16

Figure 2-9: iFRET efficiency is spatially heterogenous and does not correlate to T cell infiltrate 17

Figure 2-10: PD-L1:PD-1 beyond tumor:T cell interactions 18

Figure 2-11: Macrophage:effector cell crosstalk 20

Figure 2-12: Proposed paradoxical impact of TAMs in response to OV 20

Figure 2-13: GM-CSF rheostat 21

Figure 2-14: AXL signaling and inhibition strategies 23

Figure 2-15: AXL inhibition in pancreatic cancer depletes TAMs, shifts inflammatory profile 29

Figure 2-16: AXL expression is associated with PD-1 therapy nonresponse 31

Table 2-1: Recent clinical trials with AXL inhibitor Bemcentinib 24

Table 2-2: Ongoing development of AXL-targeted therapy: Preclinical and clinical trials 25

Chapter 3 32

Table 3-1: Flow cytometry gating strategy 36

Chapter 4 47

Figure 4-1: Trial Design and clinical analysis 48

Figure 4-2: iFRET functional receptor analysis corresponds to treatment response, not PD-L1 expression 54

Figure 4-3: Total immune population changes over treatment course 57

Figure 4-4: Immune cell subset shifts with TVEC therapy differ amongst responders, non-responders, and metastatic disease 59

Table 4-1: Clinicopathologic features 49

Chapter 5 61

Figure 5-1: The clinical landscape of AXL in melanoma 63

Figure 5-2: AXL expression in melanoma 64

Figure 5-3: AXL expression and cellular association in advanced melanoma 67

Figure 5-4: Diversity of AXL family receptor and ligands expression in the melanoma TiME 68

Figure 5-5: AXL targeting in PD-1-resistant melanoma 70

Figure 5-6: AXL inhibition synergizes with anti-PD-1 therapy 72

Figure 5-7: TiME shifts with AXL and PD-1 inhibition 74

Figure 5-8: AXL and PD-1 targeting in multiple models of macrophage depletion 77

Figure 5-9: TiME alterations in response to macrophage depletion 79

Figure 5-10: *In vitro* macrophage differentiation and AXL expression 81
Figure 5-11: Direct influence of AXL inhibition and Gas6 activation on macrophage polarity 83
Figure 5-12: Shifts in macrophage phenotype and checkpoint expression with AXL and anti-PD-1 inhibition 84
Figure 5-13: Impact of AXL inhibition and macrophage phenotype on phagocytosis and efferocytosis 85
Figure 5-14: Impact of AXL inhibition and macrophage phenotype on T cell proliferation .. 87
Figure 5-15: Impact of AXL inhibition on the microenvironmental secretome 89

Table 5-1: Baseline demographics of patients with invasive melanoma relative to warfarin usage 62

List of Abbreviations

ADC	Antibody-drug conjugate
AEs	Adverse events
aHR	Adjusted hazard ratio
APCs	Antigen-presenting cells
BEM	Bemcentinib
BMDM	Bone marrow-derived macrophages
BMI	Body mass index
BSA	Bovine serum albumin
CAFs	Cancer-associated fibroblasts
CI	Confidence interval
CLL	Chronic lymphocytic leukemia
CTLA-4	Cytotoxic T-lymphocyte-associated protein 4
CyTOF	Cytometry by time of flight
CSF1R	Colony-stimulating factor 1 receptor
DC	Dendritic cells
EDTA	Ethylenediaminetetraacetic acid
EMT	Epithelial-to-mesenchymal transition
FFPE	Formalin-fixed paraffin-embedded
FLIM	Fluorescence Lifetime Imaging
GCP	Good Clinical Practice
GM-CSF	Granulocyte-macrophage colony-stimulating factor
HPF	High-powered fields
HRP	Horseradish peroxidase
ICB	Immune checkpoint blockade
IFN-y	Interferon-gamma
iFRET	Immune-Förster-resonance-energy transfer
IHC	Immunohistochemistry
IL	Interleukin
IL-1RA	IL-1 receptor antagonist
irAE	Immune-related adverse events
IRB	Institutional Review Board
LPS	Lipopolysaccharide

mAb	Monoclonal antibody
MBM	Melanoma brain metastases
mDC	Myeloid DC
MDSC	Myeloid-derived suppressor cells
MHC	Major histocompatibility complex
MITF	Melanocyte-inducing transcription factor
MRC1	Mannose receptor C-type 1
MSI	Microsatellite instability
MSI-H	Microsatellite instability-high
MSS	Melanoma-specific survival
NIVO	Nivolumab
NK	Natural killer
NSCLC	Non-small cell lung cancer
OS	Overall survival
OV	Oncolytic virus
PBMC	Peripheral blood mononuclear cells
PBS	Phosphate-buffered saline
PBST	PBS-tween
pCR	Pathologic complete response
PD-1	Programmed cell death protein 1
pDC	Plasmacytoid DC
PD-L1	Programmed cell death ligand 1
PDX	Patient-derived xenograft
PFS	Progression-free survival
PR	Partial response
RCC	Renal cell carcinoma
RFS	Recurrence-free survival
ROI	Regions of interest
sAXL	soluble AXL
SD	Standard deviation
SKCM	skin cutaneous melanoma
SLNB	Sentinel lymph node biopsy
TAMs	Tumor-associated macrophages
TCGA	The Cancer Genome Atlas

TILs	Tumor-infiltrating lymphocytes
TiME	Tumor immune microenvironment
TK	Tyrosine kinase
TKI	Tyrosine kinase inhibitor
TMA	Tissue microarray
TMB	Tumor mutational burden
TNF	Tumor necrosis factor
Tregs	Regulatory T cells
TSA	Tyramide signal amplification
tSNE	t-distributed stochastic neighbor embedding
TVEC	Talimogene Laherparepvec
UCDCCC	UC Davis Comprehensive Cancer Center
UMAP	Uniform manifold approximation and projection
VEGF	Vascular endothelial growth factor

Copyright Acknowledgements

Chapter 2 contains material originally published in scientific journals

- Figure 2-1 was originally published in Clinical Oncology:
  Hanna TP, Nguyen P, Baetz T, Booth CM, Eisenhauer E. A Population-based Study of Survival Impact of New Targeted and Immune-based Therapies for Metastatic or Unresectable Melanoma. Clin Oncol (R Coll Radiol). 2018;30(10):609-17; 10.1016/j.clon.2018.05.005.
- The two panels in Figure 2-2 were originally published in Annals of Surgical Oncology; reproduced with permission from Springer Nature:
  Holder AM, Wargo JA, Ross MI. Timing is Everything: Neoadjuvant Versus Adjuvant Immunotherapy in Patients with Resectable Metastatic Melanoma. Ann Surg Oncol. 2023;30(12):6953-7; 10.1245/s10434-023-14133-8.
- Figure 2-4 was originally published in Nature Medicine; reproduced with permission from Springer Nature:
  Dummer R, Gyorki DE, Hyngstrom J, Berger AC, Conry R, Demidov L, et al. Neoadjuvant talimogene laherparepvec plus surgery versus surgery alone for resectable stage IIIB-IVM1a melanoma: a randomized, open-label, phase 2 trial. Nature Medicine. 2021;27(10):1789-96; 10.1038/s41591-021-01510-7.
- Figure 2-5 was originally published in Frontiers in Molecular Biosciences:
  Kaufman HL, Shalhout SZ, Iodice G. Talimogene Laherparepvec: Moving From First-In-Class to Best-In-Class. Frontiers in Molecular Biosciences. 2022;9:834841; 10.3389/fmolb.2022.834841.
- Figure 2-8 was reprinted from Cancer Research, 2020,
  80(19), 4244-57, Sánchez-Magraner L et al., High PD-1/PD-L1 Checkpoint Interaction Infers Tumor Selection and Therapeutic Sensitivity to Anti-PD-1/PD-L1 Treatment, with permission from AACR.
- Figure 2-9 was reprinted from Cancer Research, 2020,
  80(19), 4244-57, Sánchez-Magraner L et al., High PD-1/PD-L1 Checkpoint Interaction Infers Tumor Selection and Therapeutic Sensitivity to Anti-PD-1/PD-L1 Treatment, with permission from AACR.
- Figure 2-10 was originally published in Cancers (Basel):
  Planes-Laine G, Rochigneux P, Bertucci F, Chretien AS, Viens P, Sabatier R, et al. PD-1/PD-L1 Targeting in Breast Cancer: The First Clinical Evidences Are Emerging. A Literature Review. Cancers (Basel). 2019;11(7); 10.3390/cancers11071033.
- Figure 2-12 was originally published in Biomedicines:
  Denton NL, Chen CY, Scott TR, Cripe TP. Tumor-Associated Macrophages in Oncolytic Virotherapy: Friend or Foe? Biomedicines. 2016;4(3); 10.3390/biomedicines4030013.
- Figure 2-13 was originally published in Experimental & Molecular Medicine:
  Hong I-S. Stimulatory versus suppressive effects of GM-CSF on tumor progression in multiple cancer types. Experimental & Molecular Medicine. 2016;48(7):e242; 10.1038/emm.2016.64.
- Figure 2-14 was adapted from a figure originally published in Journal of Thoracic Oncology:
  Levin PA, Brekken RA, Byers LA, Heymach JV, Gerber DE. Axl Receptor Axis: A New Therapeutic Target in Lung Cancer. J Thorac Oncol. 2016;11(8):1357-62; 10.1016/j.jtho.2016.04.015.
- Figure 2-15 was reprinted from Cancer Research, 2018,

78(1), 246-55, Ludwig KF et al., Small-molecule inhibition of Axl targets tumor immune suppression and enhances chemotherapy in pancreatic cancer, with permission from AACR.

Chapter 5 contains material originally published in scientific journals:

- Table 5-1 was published in Surgical Oncology Insight:
  Bateni SB, Walsh AN, Xu AJ, Gingrich AA, Maverakis E, Kirane AR. Association between warfarin and survival in invasive melanoma: a population-based cohort study. Surgical Oncology Insight. 2024;1(3); 10.1016/j.soi.2024.100083.
- Figure 5-1 was published in Surgical Oncology Insight:
  Bateni SB, Walsh AN, Xu AJ, Gingrich AA, Maverakis E, Kirane AR. Association between warfarin and survival in invasive melanoma: a population-based cohort study. Surgical Oncology Insight. 2024;1(3); 10.1016/j.soi.2024.100083.

Chapter 1: Introduction

The advent of immunotherapy with immune checkpoint blockade (ICB) has revolutionized cancer care, proving highly effective in patients with advanced melanoma. However, only half of patients with melanoma show a meaningful response.[1-3] Melanoma presents a particular challenge due to its aggressive behavior in very early stages and wide intra- and inter-tumoral heterogeneity that drives resistance to conventional therapies.[4, 5] Clinically reliable biomarkers predictive of response to facilitate therapeutic selection, and defining divergent molecular features of non-response to immunotherapy, remain a critically important but unmet need, hindering the implementation of precision medicine approaches in melanoma.[6-8] To date, the role of the innate immune system in mitigating responses to ICB—including the definition of pre- and post-therapy shifts in the tumor immune microenvironment (TiME) milieu—has remained underexplored.

As key components of the innate immune system, macrophages play multifaceted roles in cancer progression and response to treatment. Within the TiME, macrophages can exhibit a spectrum of phenotypes ranging from pro-inflammatory (M1-like) to anti-inflammatory (M2-like).[9, 10] The plasticity of macrophages enables them to either support antitumor immunity or facilitate tumor growth and immune evasion. In melanoma, tumor-associated macrophages (TAMs) often skew towards an immunosuppressive M2-like phenotype, contributing to immunotherapy resistance.[11, 12] The heterogeneity and complexity of TAMs in melanoma underscore the necessity for precision medicine approaches that can accurately target and/or reprogram these cells to overcome immunotherapy resistance.[13] The primary objective of this thesis is to elucidate the behavior of macrophages in immunotherapy-resistant melanoma, with the goal of developing precision immunotherapy strategies. By leveraging cutting-edge technologies and experimental models, this research aims to 1) explore the role of TAMs in immunotherapy resistance using a novel strategy exploiting neoadjuvant oncolytic virus (OV), and 2) evaluate the macrophage-

specific role of AXL tyrosine kinase (TK) in cellular polarization and function, and the generation of a durable immune response toward aggressive melanoma.

Talimogene Laherparepvec (TVEC) is an oncolytic virus that mediates tumor regression through selective replication within and lysis of tumor cells, as well as induction of systemic antitumor immunity.[14, 15] TVEC has been demonstrated to stimulate long-term, systemic immunity against melanoma through the bystander effect, a process by which tumors are eradicated at distant, non-injected sites.[14-16] While this bystander effect of OV is observed in advanced melanoma, draining nodal tissue has not been evaluated in prior reports. By assessing the immune response in this tissue, this study presents a unique opportunity to explore the mechanisms by which TVEC induces systemic antitumor immunity. In project 1, I hypothesize that response to neoadjuvant intra-lesional therapy with TVEC in melanoma will be dampened in tumors with a pre-existing, pro-tumorigenic, anti-inflammatory macrophage phenotype. I aim to design and utilize a first-in-class trial of neoadjuvant TVEC in primary melanoma prior to standard surgery to determine TiME features of responders that may be predictive of response, and the mechanisms by which this response may be amplified (NCT04427306).

Second, appreciation of the function and importance of the receptor TK AXL in tumor biology and progression is mounting; however, AXL-related activity has not been well explored in clinical melanoma specimens. Given that AXL can participate in numerous pathways that promote melanoma progression, particularly in relationship to tumor-immune cell crosstalk, it is considered a high-value target with potential specific implications in ICB resistance.[17, 18] Very preliminary data demonstrates AXL expression in advanced melanoma is associated with resistance to ICB.[19, 20] We have previously shown strong evidence that blockade of AXL can suppress tumor growth, metastasis, and drug resistance in other cancer types.[21] However, AXL signaling significantly influences macrophage polarization and the behavior of multiple innate cells in the TiME, resulting in mixed clinical results when inhibited.[19, 20] I aim to evaluate the clinical relevance of AXL as a biomarker of therapy response and explore its potential as a target to augment

immunotherapeutic efficacy in malignant melanoma using ICB-resistant mouse models of melanoma.

The findings obtained with this research will contribute to the growing body of knowledge on the role of macrophages in cancer immunology and provide a foundation for the development of precision immunotherapy approaches tailored to the unique immunosuppressive mechanisms present in immunotherapy-resistant melanoma. By targeting the pivotal role of macrophages, this work aims to enhance immunotherapy effectiveness and improve outcomes for patients with melanoma, as well as deliver rationale for the development of next-generation clinical therapeutic approaches for melanoma.

Chapter 2: Literature Review

1. Toward Precision Immunotherapy in Melanoma for Improved Patient Outcomes

Over the past decade, immunotherapy has revolutionized the treatment landscape for melanoma, offering durable responses and improved survival outcomes for many patients. Melanoma with distant metastases historically had a dismal prognosis with a 5-year overall survival (OS) of 15.7% from the years 1992-2005[22], which has now been improved to up to 52% with use of dual ICB (**Figure 2-1**).[23, 24] Checkpoint inhibitors targeting programmed cell death protein 1 (PD-1), cytotoxic T-lymphocyte-associated protein 4 (CTLA-4), and other immune checkpoints have demonstrated remarkable efficacy in advanced melanoma by invigorating the immune function in tumors, attributed largely to augmentation of cytotoxic T cell responses, and resulting in long-lasting responses in a subset of patients.[25] Despite these advancements, challenges remain in optimizing immunotherapy for patients with melanoma as roughly half of patients do not achieve adequate responses or are unable to fully utilize these therapies due to a high rate of immune-related adverse events (irAEs).[26-28] Additionally, melanoma remains a highly heterogeneous disease hallmarked by high mutational burden and evasive resistance mechanisms, which has challenged not only the identification of clinically relevant biomarkers but also the development of rational, effective approaches to second-line treatment in the setting of anti-PD-1 refractory disease.

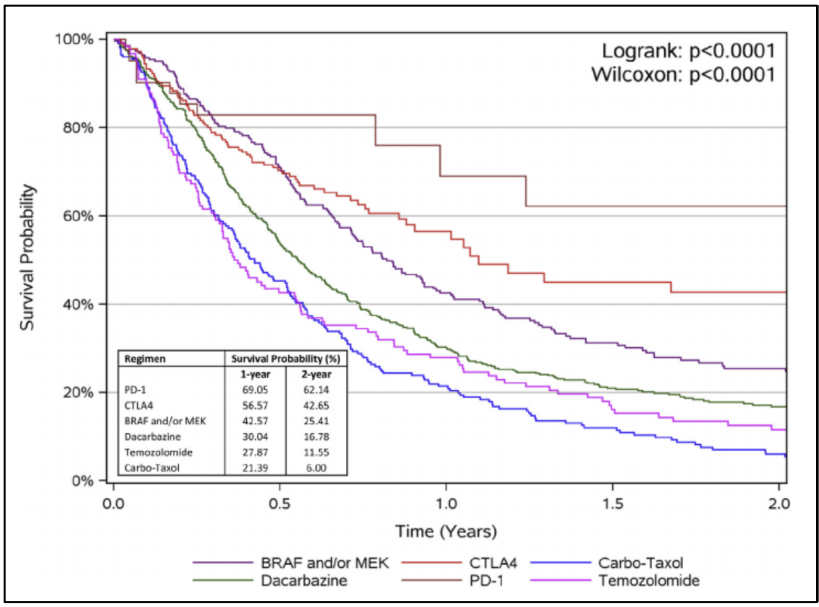

Figure 2-1. Survival in advanced melanoma[24] Overall survival by first-line regimen, where prior chemotherapy-based regimens failed to demonstrate effective disease control with less than 6 month average survival in stage IV melanoma until the development of targeted therapies and ICB. Targeted BRAF therapy and single agent ICB with CTLA-4 inhibition were the first agents to demonstrate meaningful increases in overall survival, with continued improvement demonstrated by anti-PD-1 therapy and combination ICB (not shown) now significantly extending average overall survival to 5 years.

Biomarker development for immunotherapy selection in melanoma has emerged as a critical area of research, as the identification of reliable markers can help stratify patients based on their likelihood of responding to treatment. A central challenge for biomarker development is the heterogeneity of the disease and the complex interactions between tumor cells and the TiME.[29-31] The programmed cell death ligand 1 (PD-L1) score, or the percentage of PD-L1-expressing cells typically assessed through immunohistochemical (IHC) staining, is the most common biomarker evaluated prior to ICB use in various cancers, including melanoma.[32] Use of the PD-L1 score to guide treatment decisions and patient selection for immunotherapy has challenges due to 1) the dynamic nature of PD-L1 expression with significant changes over time and 2) heterogeneity in expression, even across tumor sites in the same patient.[33] Variability in testing methods, including different antibodies and assays used to detect PD-L1 expression, can further complicate the interpretation of PD-L1 scores and limit its reliability as a predictive biomarker.[34] As a result, not all patients with high PD-L1 expression respond to ICB, while some patients with low or negative PD-L1 expression may still benefit from treatment.[35] In current clinical practice, PD-L1 score does not serve as an *a priori* selection criterium for therapy, and even

patients with a negative PD-L1 score will typically utilize a trial of ICB as the mainstay of therapy, with good responses possible.

Tumor mutational burden (TMB) and microsatellite instability (MSI) are emerging biomarkers for immunotherapy selection in cancer treatment. High TMB, representing an increased number of somatic mutations within tumors, has been associated with improved responses to ICB therapy across various cancer types, including melanoma.[36, 37] Meanwhile, microsatellite instability-high (MSI-H) tumors exhibit defects in DNA mismatch repair, leading to an accumulation of genetic mutations and enhanced neoantigen presentation, sensitizing tumors to ICB.[38] Both TMB and MSI provide insights into the tumor's immunogenicity and can help guide treatment decisions by identifying patients who are more likely to benefit from immunotherapy.[39, 40] MSI status is employed as a treatment stratifier in emerging subsets of disease not previously demonstrating significant response to ICB, such as colorectal and gastric cancers.[41, 42] However, neither serves as a clinical prediction tool in melanoma. Molecular profiling of tumors for specific tumor or germline mutations is employed for known targetable mutations, such as BRAF, which is expressed by 50% of melanomas, or NRAS and c-KIT.[43-46] However, response to therapies targeting these mutations is typically limited in duration and ICB has recently demonstrated superior tumor control, remaining the mainstay of therapy with curative intent.[43]

Significant effort has been made to define potential immunologic signatures of response to ICB with the understanding that inflamed, or immune “hot” tumors with high levels of tumor-infiltrating lymphocytes (TILs), are more likely to respond to immunotherapy compared to tumors with low TIL levels, known as immune "cold" tumors.[43, 47] Development of these signatures has included assessment of immune cell infiltrate and interferon-gamma (IFNγ) genes induced in response to IFNγ signaling.[48, 49] The presence of TILs within the TiME is indicative of an ongoing immune response against the tumor. High levels of TILs, particularly cytotoxic T cells, have been associated with improved responses to immunotherapy, including ICB.[50] The OpACIN-neo study showed improved outcomes to ICB in patients with high baseline IFNγ levels leading to significant

interest in utilizing the IFNγ signature as a therapeutic stratifier. This gene expression signature reflects the presence of an active immune response within the tumor, characterized by enhanced T cell activation and pro-inflammatory cytokine production, which are essential for mounting an effective antitumor immune response.[51] The DOMINI study was designed to prospectively test this approach by selecting patients with high IFNγ score tumors for single agent nivolumab (anti-PD-1) versus use of domatinostat, which is used to stimulate conversion of low IFNγ tumors to high, in combination with nivolumab and ipilimumab (anti-CTLA-4).[7, 52] Limitations in study design failed to yield substantial justification of this approach in patients. However, longitudinal tumor sampling showed that, in tumors transitioning from low to high IFNγ scores, therapy induced complete responses in 50-80% of patients, depending on the choice of systemic combination. Notably, tumors remaining at low levels of IFNγ score expression despite treatment had negligible response to immunotherapy at the time of study assessment.[53, 54]

2. Improving the Immune Response and Durability of Cancer Control: Neoadjuvant Therapy and Harnessing the Innate Immune System

One key approach for tackling both the need for improved therapeutic response and biomarker development is the application of immunotherapy in the neoadjuvant setting, prior to surgical removal, to allow for longitudinal survey of the TiME before and after therapy to histologically confirm the therapeutic impact. This approach, combined with rapidly expanding -omics technologies, may enhance biomarker discovery and deepen our mechanistic understanding of treatment response (**Figure 2-2A**).[16, 55, 56] This information can then be used to develop clinical assays for therapeutic selection to 1) maximize therapeutic efficacy, 2) allow for earlier rescue of difficult-to-treat tumors, and 3) avoid severe toxicities in patients less likely to benefit from therapy. Neoadjuvant approaches with ICB in melanoma are rapidly evolving and becoming standard of care.[6] However, there has been limited exploration of this approach in the absence of clinical nodal disease, due in part to the potential for significant adverse events (AEs) with systemic

immunotherapy and the current lack of predictive biomarkers to identify patients likely to respond to therapy.

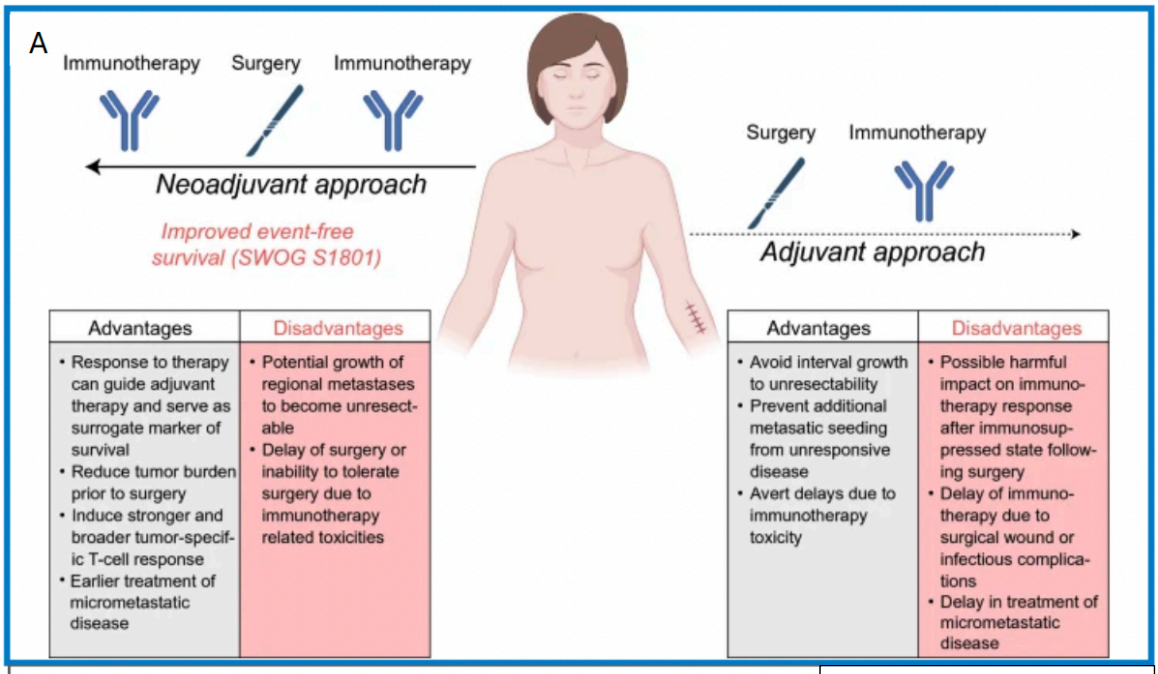

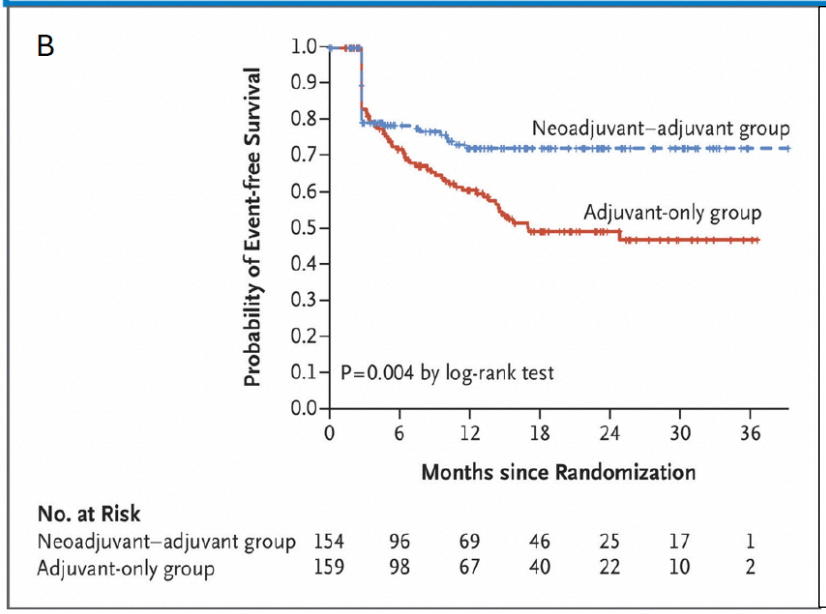

Figure 2-2. A) Neoadjuvant immunotherapy in melanoma Clinical advantages and disadvantages for neoadjuvant approach exist; however, B) the recent SWOG1801 trial demonstrated significantly improved in event free survival for neoadjuvant over adjuvant ICB alone. Assessment of overall survival benefit is ongoing. Loss of surgical opportunity was low, 8%, with most progression events as distant metastases.[55]

Immunotherapies in the neoadjuvant setting may be more efficacious than when used after surgical resection and investigations are underway in advanced disease settings with nodal or metastatic disease (**Figure 2-2B**[55]).[3, 57, 58] The potential for significant AEs with systemic immunotherapy and lack of predictive biomarkers to identify patients likely to respond has made

expansion of this approach into the earlier disease setting extremely limited. Very recently, adjuvant checkpoint blockade was approved in Stage II melanoma but, concerningly, Grade 3/4 AEs were reported in 25.9% of patients and therapy only resulted in a 5.7% reduction in disease recurrence.[59] An intratumoral treatment approach is attractive for the neoadjuvant setting, as it maximizes direct tumor delivery of the drug, potentially minimizing off-target toxicities, and can demonstrate significant abscopal effect in non-injected sites.[60-62]

TVEC is an OV that preferentially replicates in tumor cells and enhances immunity by increased antigen loading of major histocompatibility complex (MHC) class I molecules and expression of granulocyte-macrophage colony-stimulating factor (GM-CSF) to increase tumor antigen presentation by dendritic cells. Mechanistically, TVEC increases infiltration of T cells, decreases immunosuppressing regulatory T cells (Tregs), and may generate lasting immunity, observed as abscopal effect (**Figure 2-3**).[14, 16, 60] Intratumoral TVEC was shown to be safe, and very recent data revealed efficacy of pre-surgical TVEC for late stage, resectable melanoma.[16, 63] Treatment resulted in improved OS and progression-free survival (PFS) and reduced the need for systemic ICB in complete responders.[63] In the open-label, Phase II trial NCT02211131, patients were randomized to 12 weeks of TVEC prior to surgical excision of nodal or metastatic disease vs. surgery alone (**Figure 2-4**).[16] The primary endpoint, 2-year recurrence-free survival (RFS), improved to 29.5% in TVEC-treated patients compared to 16.5% in the control group. Patients who showed complete pathologic response (17.1%) had an exceptionally low recurrence rate with associated lack of progression, reducing subsequent systemic therapy use.[63] Observation of the bystander effect to TVEC in non-injected lesions has been variable and distant sites and draining lymph nodes are not typically sampled in studies of advanced disease.[14, 15, 60] Therefore, little is known about changes in the inflammatory infiltrate downstream of injection sites.

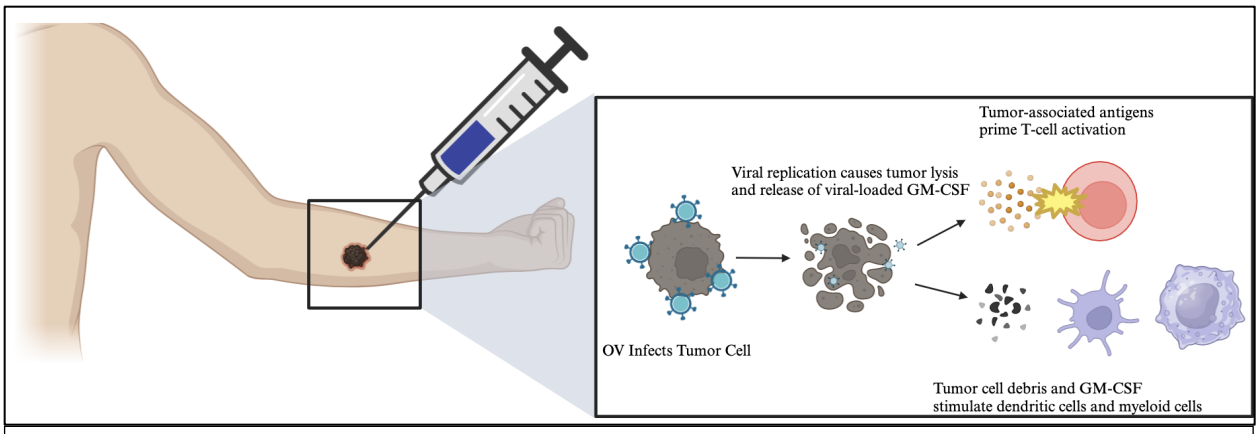

Figure 2-3. TVEC mechanism of action TVEC is an attenuated oncolytic herpes virus that induces direct tumor lysis with preferential infection of tumor cells and minimal off-target activity. The virus is modified to produce GM-CSF to enhance antitumor immune response in both the local injected site and distant, non-injected sites.

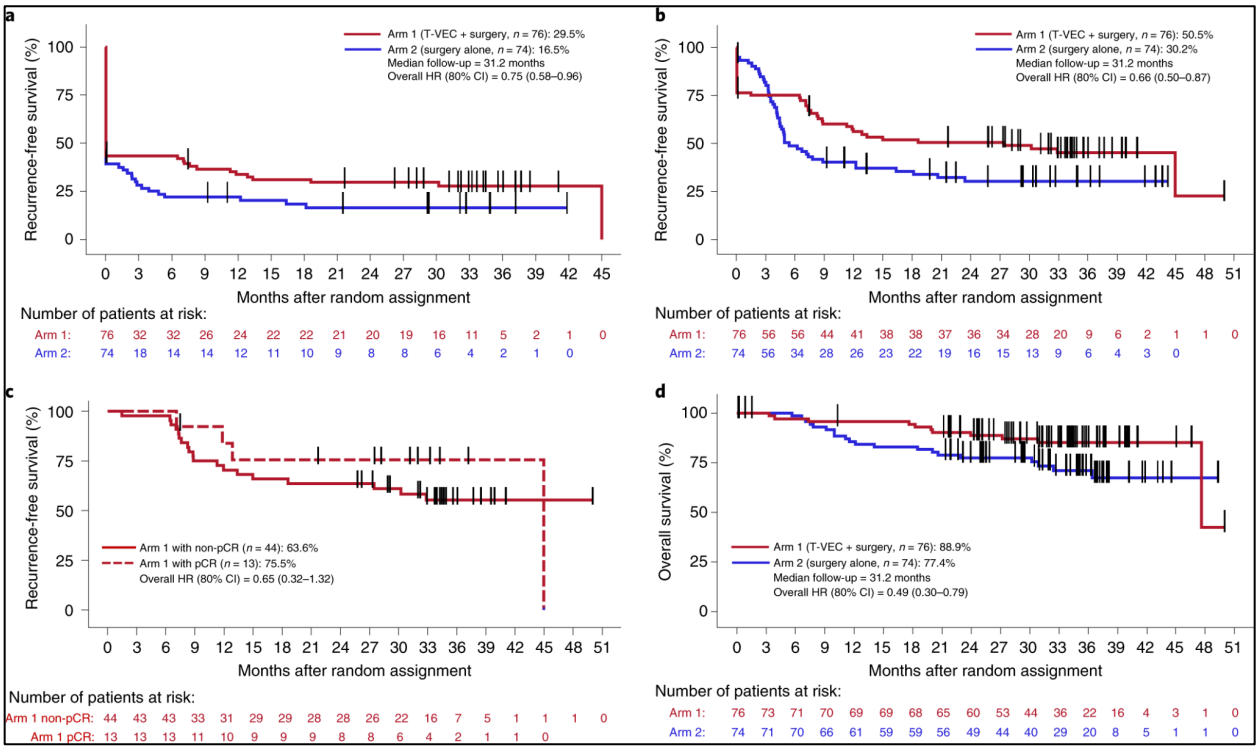

Figure 2-4. Neoadjuvant TVEC improves durable tumor control over surgery alone. Patients were randomized to 12 weeks of therapy (6 doses) prior to surgical resection. A) patients without R0 resection were considered an event and b) surgical outcome is disregarded in sensitivity analysis. C) Pathologic complete response (pCR) was 17% amongst injected tumors with pCR being associated with improved disease control in the 2 years post-surgery and D) durable improvement in OS at 5 years follow-up.[16]

Generally, TVEC is thought to enhance the recruitment and activation of $CD8^+$ T cells within the tumor, leading to increased infiltration of these cytotoxic T cells, as well as increased

PD-L1 expression in tumors as a result of the increased inflammation.[15] As TVEC infects and lyses tumor cells, it can release tumor antigens that further stimulate $CD8^+$ T cell activation, promoting a robust immune response against the tumor. In this way, immunologically "cold" melanoma tumors, which have limited immune cell infiltrates and low levels of antitumor immune activity, can be impacted by TVEC to convert into "hot" tumors by inducing inflammation to enhance immune cell recruitment and activation within the TiME. The change in $CD8^+$ T cell infiltrate with oncolytic virus in melanoma can vary based on the specific characteristics of the TiME and the immune response triggered by the therapy.[47] Tumor genotype, such as RAS mutations, may influence susceptibility to virus-mediated oncolysis.[64]

Given that OV durability relies on the stimulation of innate immune responses to amplify systemic antitumor immune responses, the patient's baseline immune status might predict treatment success.[65] Of note, some biomarkers hypothesized to predict response to OV versus ICB differ, due to the unique mechanisms of action associated with each therapy. Recent studies have highlighted the importance of interferon signaling genes, such as JAK1 and JAK2, as potential biomarkers for OV response, as cells lacking gene expression were more sensitive to OV infection (**Figure 2-5**).[66] Additionally, STING expression has been identified as a predictive biomarker, with low STING-expressing melanoma cells that are resistant to PD-1 blockade showing sensitivity to OV treatment, suggesting a role for STING as a biomarker for OV response.[67, 68] In addition to intracellular factors, potential biomarkers for OV responses also include viral cell entry receptor expression, immune cell profiles, and the TiME status.[69] Limited data on the association of anti-viral immune responses with clinical outcomes in OV trials emphasize the need for further investigation into predictive biomarkers. Incorporating these biomarkers in future OV studies can provide valuable insights to identify markers for prospective validation and optimization of patient selection.[66]

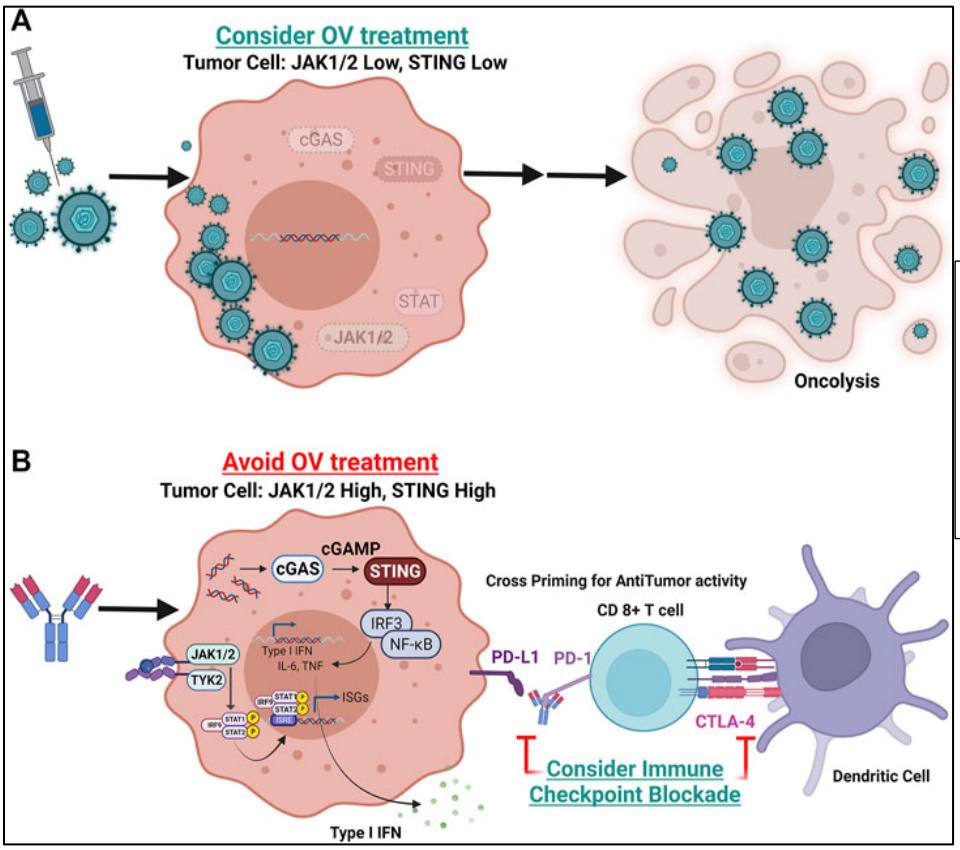

Figure 2-5. Potentially divergent mechanisms of response may facilitate therapeutic selection. Mutations in IFNγ-JAK-STAT pathway may A) confer resistance to ICB therapy but selectivity to OV therapy with B) inverse patterns in OV responses[66]

Patient-specific variations of the innate immune system might impact the heterogeneity of therapeutic response observed with TVEC. However, prior studies of both OV and ICB have under-investigated the contributions of the innate immune system to checkpoint engagement and OV response.[14-16] Traditional assessments, such as PD-L1 expression and T cell phenotyping, have shown highly heterogenous results, which may have contributed to the failure of prior studies to identify biomarkers capable of stratifying patients appropriate for this type of therapy, as well as the failure of the combination of TVEC with ICB in the Phase III setting.[15, 70] Additionally, with the introduction of single cell methodologies, it has become clear that numerous cells in the TiME express conventional checkpoint ligands and receptors beyond tumor cell to T cell communication.[34, 71, 72] The highly immunosuppressive contribution of tumor-associated macrophages (TAMs) to immunotherapy failures has identified these cells as a priority target for reprogramming of the TiME, in sequence or in combination, to rescue immunotherapy responses.[73-75]

3. iFRET and Novel Biomarker Development

As neoadjuvant immunotherapy trials continue to rapidly expand, designing studies capable of delivering highly illustrative ancillary data requires more functional readouts that the traditional proteomic and genomic expression data alone have failed to deliver. **I**mmune time-resolved-**F**örster-**r**esonance-**e**nergy **t**ransfer (iFRET) is a novel discovery tool[4, 76-78] proving to be highly meaningful in multiple cancer types, with higher specificity to clinical outcomes compared to checkpoint expression data, or PD-L1 score, alone.[76, 78] Importantly, the evolution of iFRET measurements in the TiME has not, to date, explored both pre- and post-treatment matched tissues to define longitudinal changes induced by immunotherapy. Further, it has not been assessed in the context of checkpoint ligand-receptor contributions by non-tumor, non-$CD8^+$ T cells in the complex TiME. Contextualizing the dynamic iFRET shifts in immunotherapy responders from those without benefit may delineate a preliminary signal of patients who may be better served by a specific type of therapy or even upfront surgery (**Figure 2-6**).

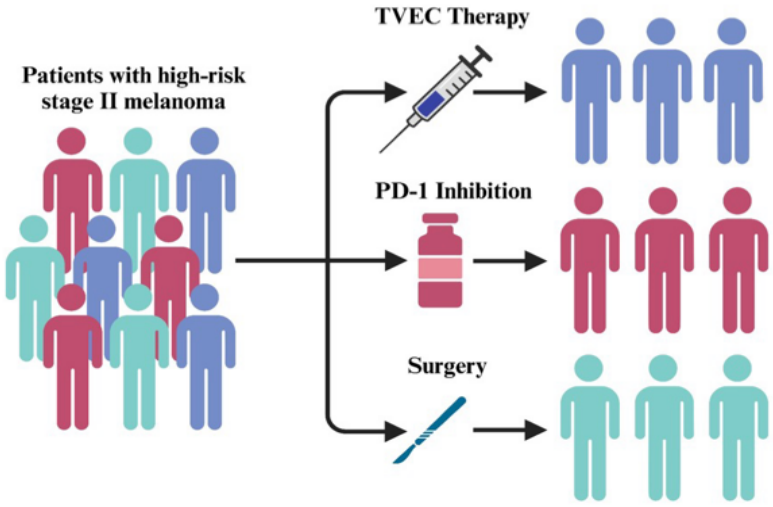

Figure 2-6. Successful biomarkers will allow for precision therapeutic stratification for patients with high-risk disease.

Novel IFRET Imaging for Determining Immune Checkpoint Interaction in *Ex Vivo* Assays

Evaluation of genetic and proteomic expression does not necessarily correlate with oncoprotein activation. Post-translational modifications, such as phosphorylation, lipidation, and methylation, impact protein functionality, contributing to cancer progression.[79, 80] Defining functional actors at play in the TiME is critical to improve assay predictive values and overall patient outcomes. The iFRET assay used to measure the immune checkpoint interaction state is based on time-resolved FRET, a photophysical event whereby energy non-radiatively transfers from a chromophore in an electronic excited state, termed the donor, to a fluorescent acceptor. FRET acts as a "chemical ruler," measuring distances of 1–10 nm to directly elucidate spatial protein activation in single cells and routinely fixed patient tissues **(Figure 2-7)**[3,5,8,12]. Preclinical use of this assay has uncovered mechanisms of molecular signaling and conformational changes that contribute to therapy responses, as well as clinically relevant immune interactive states that are predictive of survival.[78] Our team has developed the use of this assay in multiple cancers and

Figure 2-7. iFRET methodology Schematic of time-resolved immune FRET assay. A) Demonstrates the non-functional distance between receptor ligand complexes that is indistinguishable by colocalization (70 nm) or proximity-ligand assay (10-40 nm). B) Demonstrates the direct interactive state measurable by iFRET assay (<10 nm). Image created in BioRender.

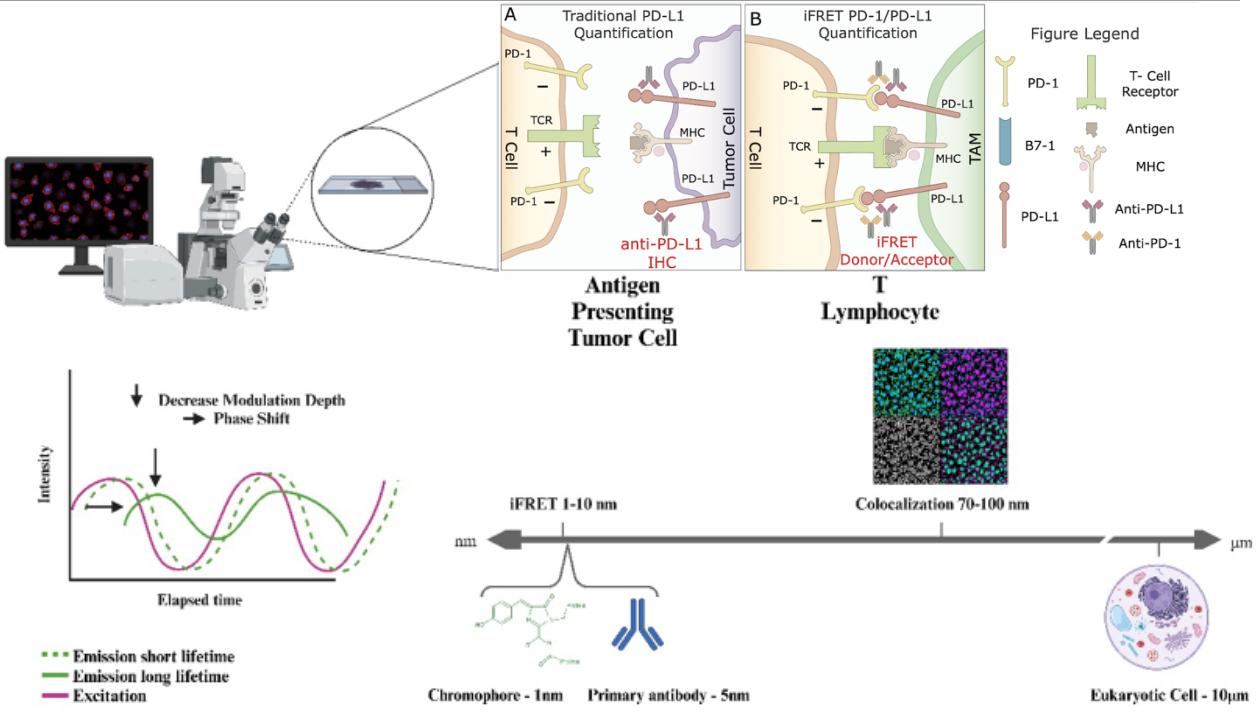

defined strengthened relevance of ligand-receptor interactive states across multiple ligand-receptor pairs, including PD-1:PD-L1, CTLA-4:CD80, Gas6:AXL, and HIF2α:HIF1b.[4, 76, 78, 81] We highlight the wide utility of further interrogation of iFRET as a companion to modern profiling techniques that have failed to yield a reliable biomarker in ICB response.

PD-1/PD-L1 Interaction State is Indicative of Patient Outcome in Various Cancer Types

The PD-1/PD-L1 interaction status in ICB-treated patients has been examined in multiple cancer types, including melanoma, to contextualize the clinical relevance of mean FRET efficiency in comparison to PD-L1 status.[76] Across melanoma, mean FRET efficiencies varied from 0.17% to 26.2%. Crucially, iFRET detected significant interaction states in most patients with PD-L1–negative tumors, a functional state that was not detected by conventional IHC (**Figure 2-8**).[76] Conversely, in patients clinically stratified as PD-L1 positive, 19/42 patients showed no interaction. Survival compared to rank-ordered median FRET efficiency (highest 40%, lowest 60 % efficiency) demonstrated significantly worse OS for those with a low iFRET strata (P = 0.05, **Figure 2-2A**), but no difference was found when patients were stratified based on PD-L1 expression (P = 0.97).[78]

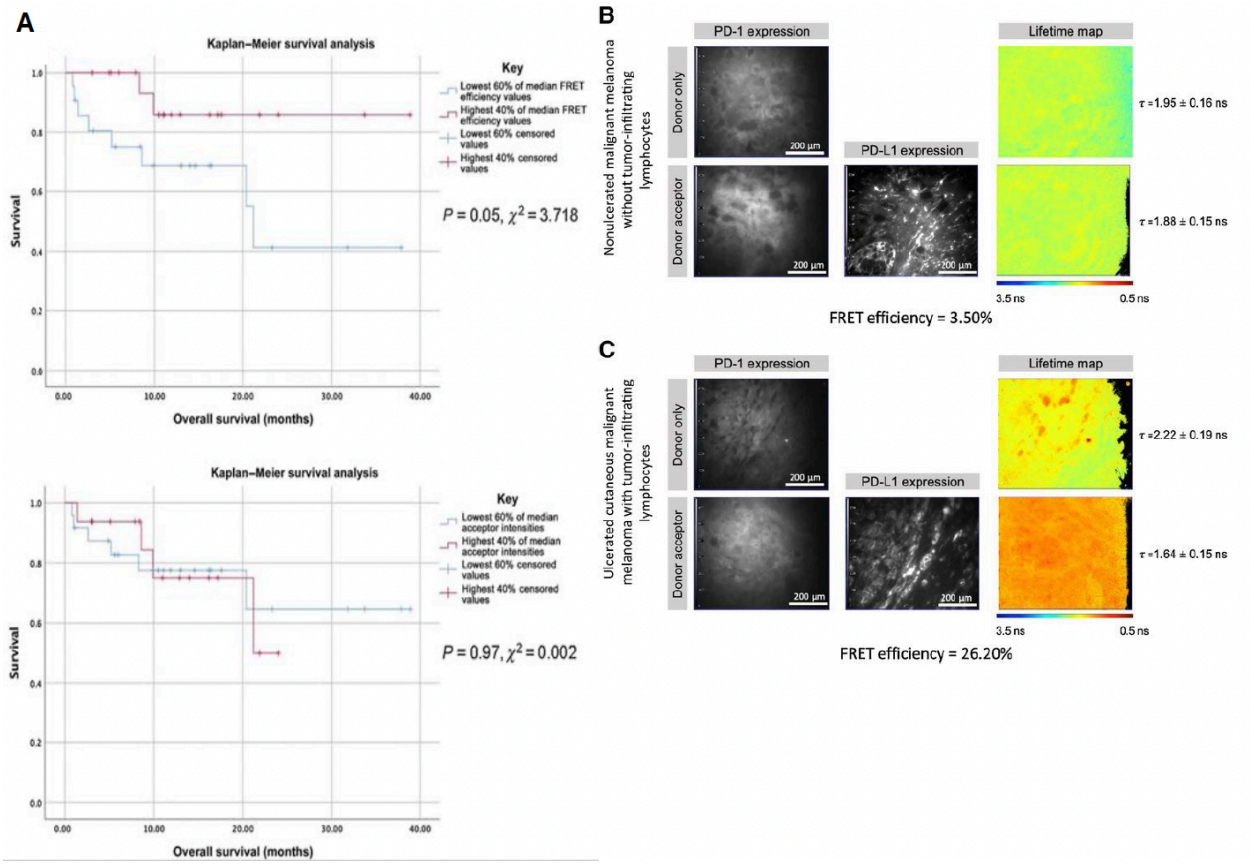

Figure 2-8. Median iFRET efficiency as a biomarker A) iFRET efficiency of PD-L1:PD-1 interaction, classified as highest 40% or lowest 60%, demonstrates improved stratification of clinical outcomes compared to B) Poor correlation of PD-L1 (iFRET donor protein) score. C) Lifetime image shown of tumor demonstrating low versus high interactive state.[76]

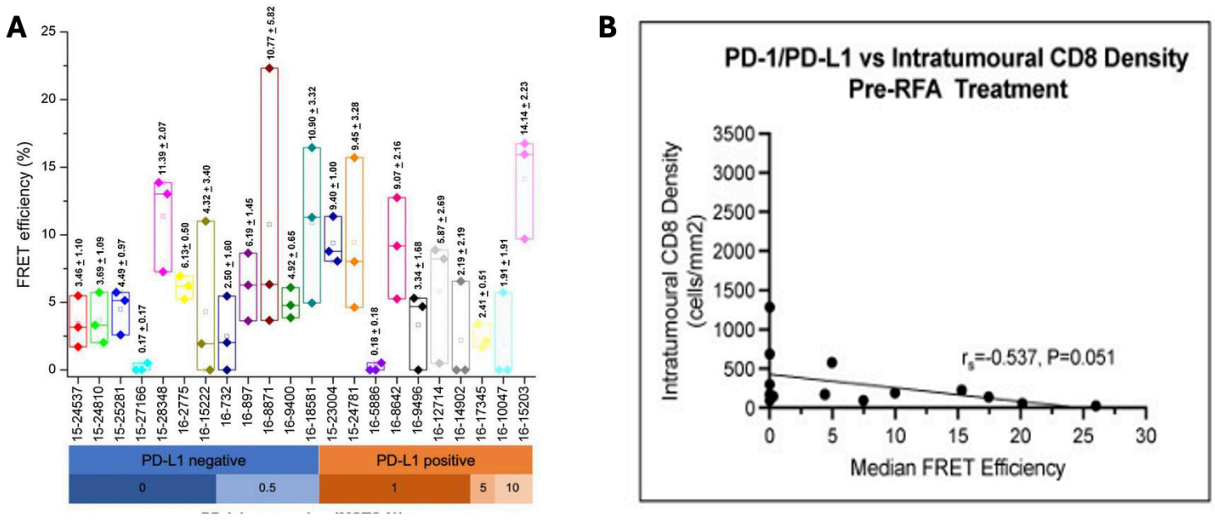

Figure 2-9. iFRET efficiency is spatially heterogenous and does not correlate to T cell infiltrate. A) iFRET efficiency is reported as median efficiency; however, the geographic landscape of the melanoma TiME is complex with regions of high and low efficiency, which may portend partial responses and areas less sensitive to therapy. B) $CD8^+$ T cell infiltrate does not correlate to PD-L1:PD-1 engagement, indicating need to contextualize the TiME to define relevance of interactive state within immune neighborhoods.[76]

Among the myriad factors contributing to immunotherapy resistance, the role of TAMs within the TiME has garnered significant attention.[72] TAMs, through their plasticity and functional heterogeneity, can profoundly influence tumor progression and immune evasion, posing a critical barrier to the efficacy of immunotherapeutic interventions.[73, 82] Interrogation of TAMs and other tumor-residing immune cells contributing to checkpoint receptor-ligand complexes compels investigation of iFRET as a companion diagnostic to improve precision immunotherapy (**Figure 2-9**[76]**, 2-10**[83]). A comprehensive focus on this type of data within a larger cohort could accelerate the unified goal of predictive biomarker discovery. Validating the potential of iFRET as a predictive biomarker to improve outcomes for high-risk melanoma has strong potential to expand precision application of immunotherapy. Future directions of this work should aim to fully characterize all cells contributing to checkpoint interaction, which will better define the mechanisms responsible for the divergence in checkpoint expression and functional checkpoint ligand-receptor interaction.

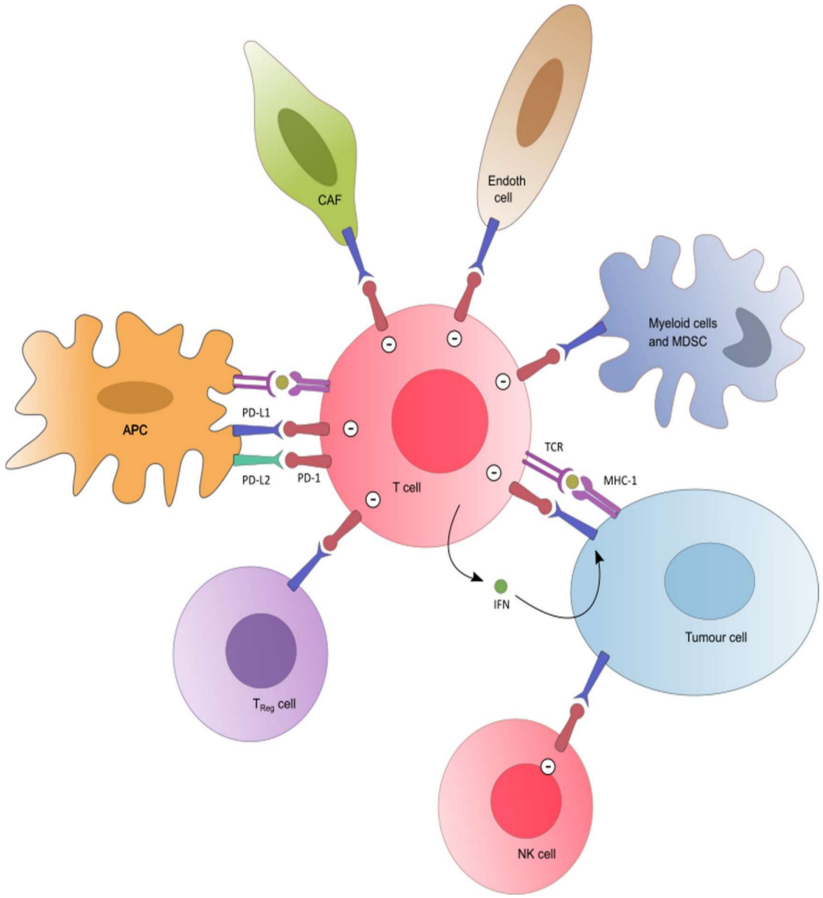

Figure 2-10. PD-L1:PD-1 beyond tumor:T cell interactions. Multiple cells of the tumor-immune microenvironment communicate across immune checkpoints to dynamically amplify or regulate inflammatory signaling. The precise state of these interactions in relationship to overall responses to ICB therapy have been under-explored and may alter the results of ICB action, including generation of irAE by unlocking regulation of autoimmune responses.[83]

4. Immunotherapy Resistance - Targeting the Immunosuppressive Tumor Environment

The TiME is a complex and dynamic ecosystem composed of various cellular and molecular constituents that interact to influence tumor growth and response to therapies. TAMs are among the most abundant immune cells in many tumors, and in melanoma they may comprise 50% of the tumor mass.[12, 84] Macrophages display remarkable plasticity, adopting distinct phenotypes and functions in response to various microenvironmental signals. Previous nomenclature broadly categorized macrophages into classically activated M1 macrophages, which have pro-inflammatory and anti-tumor properties, and alternatively activated M2 macrophages, which promote tissue repair and immunosuppression, with TAMs predominantly exhibiting an M2-like phenotype within the tumor milieu.[13, 85, 86] The recruitment, polarization, and functional reprogramming of TAMs are driven by tumor-derived signals and stromal interactions,

creating a supportive environment for tumor growth and a barrier to effective immune responses. Likewise, these M2-like TAMs contribute to tumor progression through various mechanisms, including the secretion of immunosuppressive cytokines, promotion of angiogenesis, enhancement of tumor cell invasion, and the modulation of other immune cell functions.[12, 87]

Understanding the biology and dynamics of TAMs in the TIME is crucial, as these cells play a pivotal role in mediating resistance to immunotherapy by dampening anti-tumor immunity.[10, 88] At the two phenotypic extremes: classically activated (M1) macrophages, which are induced by pro-inflammatory signals such as IFN-γ and lipopolysaccharide (LPS) and are characterized by their ability to produce pro-inflammatory cytokines, reactive oxygen species, and nitric oxide, contributing to anti-tumor and antimicrobial activities; and alternatively activated (M2) macrophages, which are stimulated by anti-inflammatory signals, such as interleukin (IL)-4 and IL-13 and are involved in wound healing, tissue remodeling, and immunosuppression.[89] In the TME, particularly in melanoma, macrophages often adopt an M2-like phenotype.[12] TAMs facilitate tumor growth and metastasis through multiple mechanisms: they secrete pro-angiogenic factors like vascular endothelial growth factor (VEGF) to promote blood vessel formation, produce matrix metalloproteinases to remodel the extracellular matrix and support invasion, and release immunosuppressive cytokines such as IL-10 and transforming growth factor β (TGF-β) to dampen anti-tumor immune responses.[90, 91] Moreover, TAMs interact with other immune cells, such as T cells, dendritic cells, and natural killer (NK) cells, often leading to an overall immunosuppressive microenvironment that allows tumor cells to evade immune surveillance.[92, 93] The dynamic and multifaceted functions of macrophages in melanoma underscore their importance as a therapeutic target. By reprogramming TAMs or inhibiting their recruitment and polarization, it may be possible to shift the balance towards a more pro-inflammatory and anti-tumor immune milieu, thereby overcoming resistance to immunotherapy and improving patient outcomes (**Figure 2-11**).

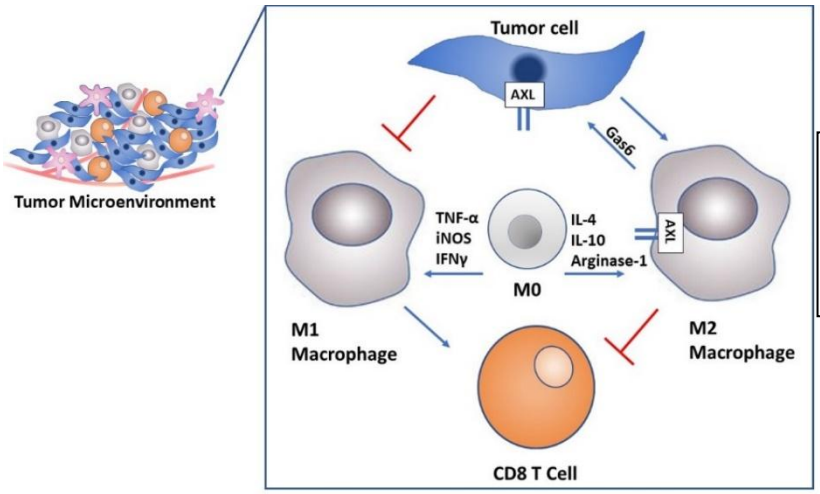

Figure 2-11. Macrophage: effector cell crosstalk. Proposed model of AXL-related function in macrophage polarization and T cell activation.

Importantly, our understanding of the incredible diversity of TAMs has rapidly shifted. Recent advancements in single-cell sequencing, spatial transcriptomics, and sophisticated imaging techniques have provided unprecedented insights into the dynamic interactions between TAMs and other immune cells within the TME.[13] These technologies offer the potential to identify novel biomarkers and therapeutic targets, paving the way for more tailored and effective interventions. Importantly, it remains unknown how these cells may influence the precarious balance between anti-viral responses and anti-tumor responses. Environments with a high number of M2 TAMs may dampen the anti-viral response necessary for oncolysis and immune stimulation *or* overly inflammatory M1-like environments may clear OV too rapidly to maximize

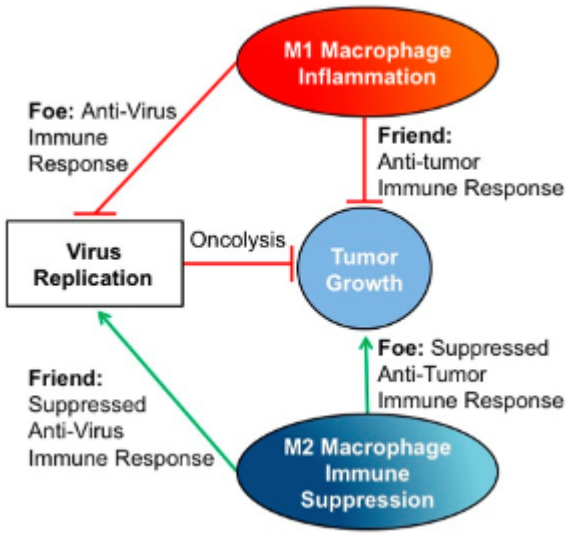

Figure 2-12. Proposed paradoxical impact of TAMs in response to OV. Inflammatory macrophages may facilitate viral clearance before allowing optimal antitumor responses whereas immunosuppressive TAMs may prevent OV responses needed to stimulate anti-tumoral immunity.[94]

necessary immune stimulation **(Figure 2-12**[94]**)**.[95, 96] Likewise, agents such as TVEC that encode for innate stimulation by releasing GM-CSF, have potential to function as a double-edged sword in an environment-specific fashion with both 1) some melanoma lines demonstrating direct stimulatory, proliferative effect of GM-CSF and 2) expansion of both M1 and M2 pre-existing populations (**Figure 2-13**[97]).[97-99] Preclinical modeling of reovirus-based OV demonstrate both oncolysis and anti-tumor T cell immunity are impaired in the presence of M2 TAMs by production of anti-inflammatory cytokines and metabolic dysregulation.[100] This finding has not yet been evaluated in patient specimens and, if validated to be associated with clinical response, presents an important rationale for further investigations of TAM-targeted therapies in combination with other immunotherapies. Further translational work to characterize tumors in the context of response to neoadjuvant therapy will be a critical next step in improving precision application of therapy and overall clinical outcomes for patients with melanoma. Thus, a critical gap in the field is fully characterizing cellular biomarkers beyond CD8 and PD-L1 in both pre- and post-treatment specimens to better illustrate the mechanisms of response and resistance.

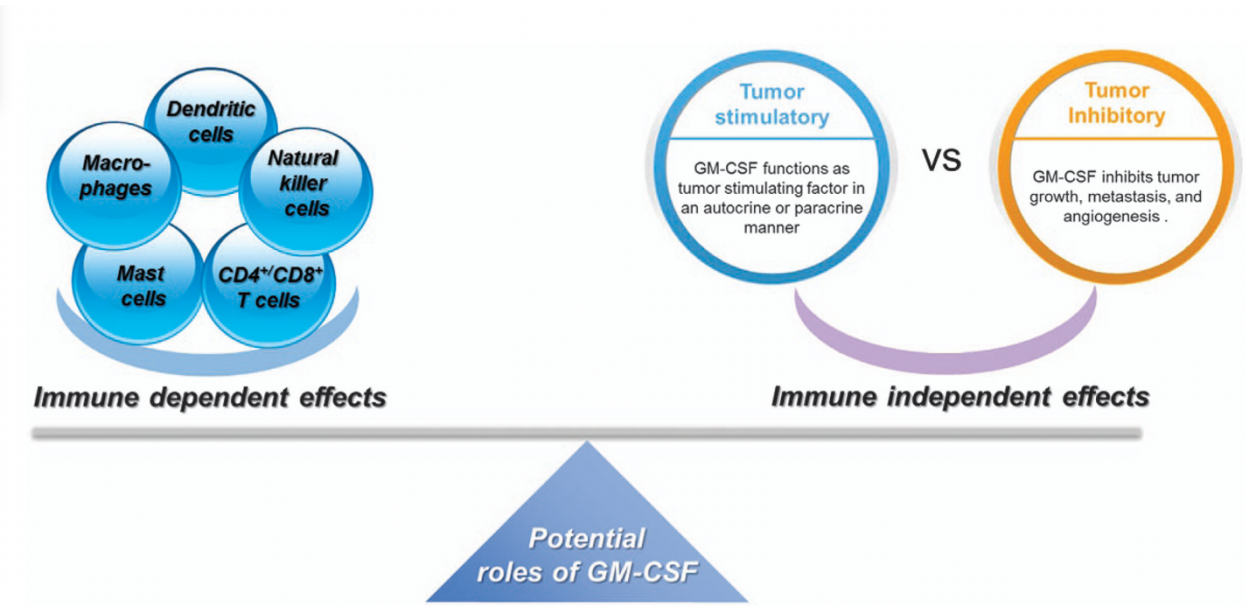

Figure 2-13. GM-CSF rheostat. Conventional function of GM-CSF is linked to expansion of Inflammatory macrophages. However, GM-CSF can play a multi-potent role in the TiME with high dose delivery contributing to expansion of all myeloid cells, beyond M1-like macrophages, and additional direct stimulatory tumor effects in melanoma cells responsive to GM-CSF[97]

5. Targeting the Melanoma TiME

There is a vast array of molecular players involved in mediating resistance to immunotherapy, ranging from tumor epigenetic modifications to aberrations in signaling.[27] The receptor tyrosine kinase AXL[21], along with TAM-family receptors Mer and Tyro3, participates directly in tumor cell invasion and metastasis in multiple tumor types. However, the exact role of AXL in oncogenesis, particularly in relationship to immunogenicity and TiME plasticity remains unclear.[18, 19, 21, 101-104] AXL dimerization and activation is induced by growth arrest-specific factor 6 (Gas6), a protein that requires vitamin K-dependent gamma-carboxylated glutamic residues.[21] When activated, AXL acts on a myriad of downstream pathways through PI3K/AKT, MAPK, and STAT3, leading to cell proliferation, survival, and immune modulation (**Figure 2-14**[20, 105]).[102, 106] There is strong evidence in preliminary work that AXL blockade in tumors with either ligand inhibition via warfarin, a vitamin K carboxylase inhibitor, or a small molecule inhibitor, BGB324, can suppress tumor progression, metastasis, and drug resistance.[21, 107] AXL signaling significantly influences macrophage polarization and inhibition of AXL correlates with tumor control in non-melanoma tumor types.[21, 108-110] The exact contribution of AXL activity to tumor progression remains unknown, as paradoxical oncogenic and anti-inflammatory properties of the AXL receptor have been described, which may have implications for potential anticancer therapy.

While AXL plays a vital physiologic role essential to cellular maintenance, it has been found to be abnormally expressed in patients with multiple types of cancers on both tumor cells and cells within their TiME, such as dendritic cells, macrophages, and NK cells.[111, 112] This activation of AXL within these different cellular subsets is implicated in inflammation-driven oncogenesis by influencing angiogenesis, invasion, proliferation, epithelial-mesenchymal transition, and immune suppression.[102] The mechanism behind the carcinogenic effects of AXL has been characterized in a variety of cancers, including breast, non-small cell lung cancer (NSCLC), and ovarian cancer.[113] Inhibition of AXL-mediated M2 TAM polarization can significantly

sensitize tumors to chemotherapies in resistant breast and pancreatic models, but the critical role of macrophage activation in modern immunotherapies remains underappreciated. In leukemia, inhibition of AXL has been shown to enable PD-1 checkpoint blockade in PD-1-refractory leukemias.[114] However, overall results in clinical trials to date exploring the impact of AXL inhibitors, results have been highly variable with AXL demonstrating a highly variable role in primary tumor control, metastatic control, and immune impact due to the heterogeneity of its function across normal homeostatic and malignant biogeographic functions (**Table 2-1, 2-2**).

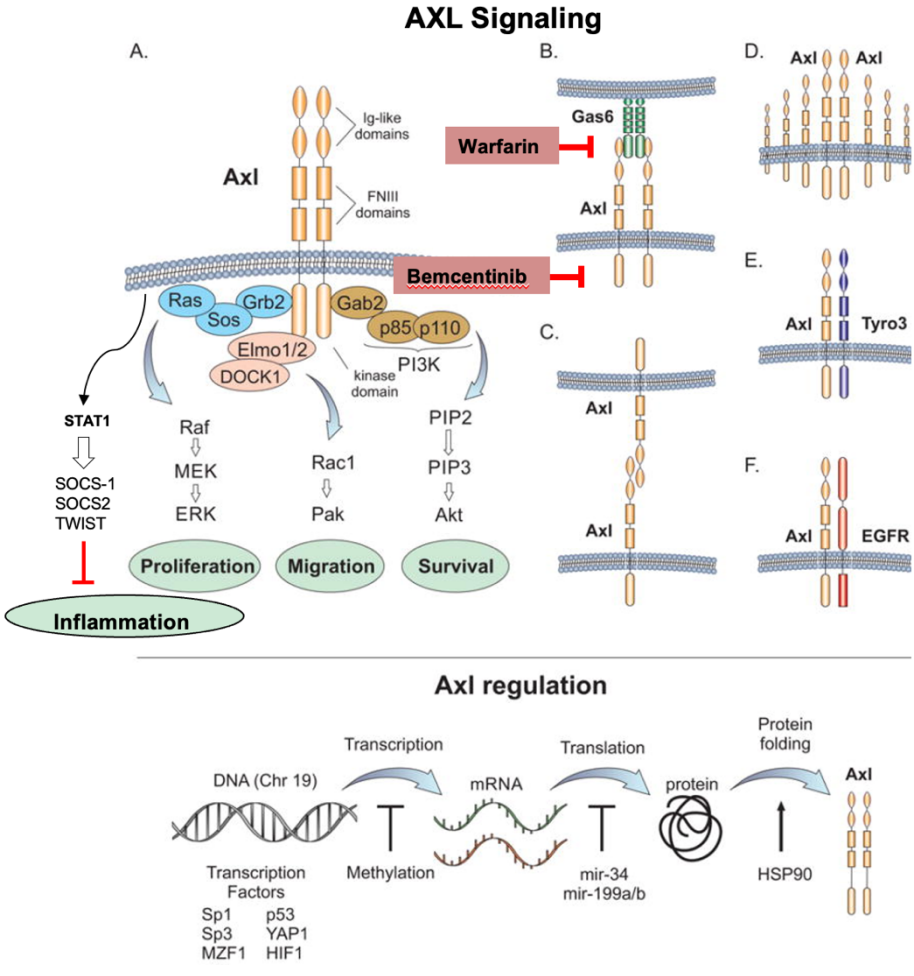

Figure 2.14. AXL signaling and inhibition strategies. A) AXL TK participates in multiple oncogenic pathways. In tumor cells, it has been associated with mesenchymal behavior, invasiveness, metastases, and resistance to therapies. It's role in inflammation is currently an area of intense investigation. B) AXL activation is predominantly by Gas6 ligand activation. Warfarin, an inhibitor of vitamin K-dependent proteins, inhibits primary ligand Gas6 as well as other class ligands, such as Pros1. BGB324/Bemcentinib small molecule inhibitor have been explored as highly specific strategies for direct receptor targeting, C) AXL can also be activated by crosslinking of extracellular domains, D) constitutive overexpression, E) Dimerization with AXL-family receptors, or F) heterodimerization with non-family receptors Adapted from Levin *et al.*[105]

Table: 2-1 Recent clinical trials with AXL inhibitor, Bemcentinib Bergen Bioscience

Disease	Drugs Combinations	Patient Outcome	Phases
AML/MDS	Bemcentinib (BEM) + Low-Dose Cytarabine	BEM + LDAC: mOS 16.5 months in ND AML; Potential for patient's ineligible for intensive chemotherapy.	Phase Ib/2
Metastatic NSCLC	Bemcentinib + Pembrolizumab	BEM + PEM: mOS 13 months, mPFS 6.2 months; Promising for poor-prognosis mutations (LKB1/STK11, KEAP1, SMARCA4, KRAS) irrespective of PD-L1 status.	Phase II
STK11-mutant NSCLC	Bemcentinib + Pembrolizumab	AXL inhibition with bemcentinib+ pembrolizumab beneficial in STK11/KEAP1 mutations; Ongoing Phase Ib/IIa trial (NCT054691) in advanced NSCLC with STK11 mutation.	Phase II
Metastatic Melanoma	Bemcentinib + Dabrafenib/trametinib or pembrolizumab	Bemcentinib + dabrafenib/trametinib or pembrolizumab: AXL's role in drug resistance; Interim analysis (June 2019) indicates tolerability with well-tolerated RP2D.	Phase Ib/II
Non-Squamous NSCLC	Bemcentinib + pembrolizumab	Significant advancement in 2L metastatic NS NSCLC treatment. AXL identified as a resistance mediator. Bemcentinib showed promise as an AXL inhibitor.	Phase II
			Phase I

Advanced NSCLC (Previously treated)	Bemcentinib (BGB324) + docetaxel	Few adverse events such as neutropenia and diarrhea, pharmacokinetic alignment with monotherapies, disease control rate exceeding 80%. demonstration of anti-tumor activity in combination with docetaxel and G-CSF support	
AML	Bemcentinib + low-dose cytarabine	Positive outcomes and specific activation of $CD8^+$ T cells and B cells/plasma cells linked to treatment response	Phase I

Abbreviations: *2L: second-line; AML: acute myeloid leukemia; G-CSF: granulocyte-colony stimulating factor; KEAP1: Kelch-like ECH-associated protein 1; NS: non-squamous; NSCLC: non-small cell lung cancer; PD-L1: programmed cell death ligand 1; RP2D: recommended phase II dose; STK11: serine/threonine kinase 11*

Table 2-2. Ongoing development of AXL-targeted therapy: Preclinical and clinical trials

Drug Name	**Drug Type**	**Mechanism of Action**	**Preclinical Evidence and Clinical Status**
Enapotamab Vedotin	Antibody-Drug Conjugate (ADC)	Utilizes the microtubule-destroying agent MMAE combined with an AXL-targeted immunoglobulin G1.	Demonstrated anti-tumor effects in osimertinib-resistant patient-derived xenograft (PDX) models. Phase I/II trial ongoing for solid tumors, including NSCLC (NCT02988817).
CAB-AXL-ADC	Antibody-Drug Conjugate (ADC)	A conditionally active biologic anti-AXL ADC selectively binding to AXL-expressing cells in the tumor microenvironment.	Induced cytotoxicity in vitro and inhibited tumor growth in various xenograft models. Phase I/II trial ongoing for solid tumors, with a separate

			NSCLC trial (NCT03425279, NCT04681131).
BGB324 (Bemcentinib)	Tyrosine Kinase Inhibitor (TKI)	A small molecule AXL TKI inhibiting AXL signaling.	Demonstrated efficacy in NSCLC and pancreatic cancer preclinical studies. Phase I/II trials ongoing, including combinations with docetaxel, erlotinib, and pembrolizumab (NCT02922777, NCT02424617, NCT03184571).
SLC-391	Small Molecule Inhibitor	A potent inhibitor of AXL/PI3K/AKT-dependent cell proliferation and survival.	Synergistic anti-tumor effect observed with a PD-1 inhibitor. Phase I study ongoing for solid tumors (NCT03990454).
DS-1205c	AXL Inhibitor	A sulfate hydrate with potent anti-tumor effects in AXL-overexpressing NSCLC xenografts.	Phase I trial ongoing in combination with EGFR TKI (gefitinib) (NCT03599518).
ASP2215 (Gilteritinib)	AXL/FLT3 Inhibitor	A highly selective dual AXL/FLT3 inhibitor with anti-leukemic activity.	Regressed tumor size in FLT3 mutated cells and AML xenograft models. ASP2215 and erlotinib combination study terminated due to adverse events (NCT02495233).
BPI-9016M	AXL/c-Met Inhibitor	Potently regressed tumor size in NSCLC PDX models.	Favorable safety profile in phase I trial. Phase I trial ongoing in c-Met

			dysregulated NSCLC patients (NCT02929290).
INCB081776	AXL/MER Inhibitor	A novel inhibitor increasing anti-tumor immune activity.	Potent inhibition of recombinant AXL/MER enzymes in preclinical data. Phase I study ongoing in advanced solid tumors (NCT03522142).
PF-07265807	AXL/MER Inhibitor	Enhances dendritic cell function to cross-prime CD8+ T cells.	Alone showed anti-tumor effects and increased cure rates in combination with PD-1 inhibitor in preclinical assays. Phase I trial ongoing in advanced solid malignancies (NCT04458259).
Q702	AXL/MER/CSF1R Inhibitor	Inhibits multiple kinases leading to tumor regression and immune stimulation.	Potential for tumor regression and immune activity in various syngeneic models. Phase I trial ongoing in advanced solid malignancies (NCT04648254).
RXDX-106	TAM RTK Inhibitor	A pan TAM RTK family inhibitor with enhanced anti-tumor efficacy in combination with ICIs.	Clinical trial terminated in advanced solid tumors (NCT03454243).
TP-0903	AXL Inhibitor	Inhibits AXL phosphorylation, modifies EMT, and induces chronic lymphocytic leukemia (CLL) cell death.	Phase I study ongoing in advanced solid malignancies, including EGFR-mutation NSCLC patients (NCT02729298).

MGCD265 (Glesatinib)	Multi-Target Inhibitor	Inhibits c-Met/VEGFR/Tie-2/Ron action.	Phase II study in Met-altered NSCLC patients conducted. Adverse events reported, but efficacy data not statistically significant (NCT02544633).
MGCD516 (Sitravatinib)	Multi-Target Inhibitor	A small molecule inhibitor with potent anti-tumor effects.	Phase III trial combining MGCD516 and nivolumab ongoing in advanced NSCLC patients (NCT03906071).
YW327.6S2	Monoclonal Antibody (mAb)	A monoclonal antibody (mAb) inhibiting AXL receptor activation and downstream signaling.	Decreased tumor size and increased anti-VEGF treatment efficacy in preclinical study. Research in preclinical stage.
D9 and E8	Monoclonal Antibody (mAb)	Selective anti-AXL mAbs inhibiting Gas6-induced phosphorylation.	Suppression of Gas6-mediated phosphorylation in pancreatic cancer cells and xenograft models. Research in preclinical stage.
MAb173	Monoclonal Antibody (mAb)	Inhibited Kaposi sarcoma cell invasion by inducing receptor degradation.	Reduced tumor size and down-regulated AXL protein levels in Kaposi sarcoma and renal cell carcinoma (RCC) preclinical studies. Research in preclinical stage.
AVB-S6-500	Soluble Receptor (Gas6 Target)	An AXL decoy receptor binding Gas6 ligand, reducing AXL phosphorylation and tumor growth.	Preclinical studies in ovarian, renal, and pancreatic cancer ongoing. Clinical studies ongoing in ovarian, renal, and pancreatic cancer (NCT03639246, NCT04019288, NCT04729608, NCT04300140).

Upon further investigation into how AXL drives resistance to immunotherapy, such as ICB, macrophages have become players of interest. Macrophages make up a significant proportion of the TiME, making up to 50% of tumor mass in melanoma, and their cytokine profiles have been directly implicated in either promoting tumor progression in M2-like immunosuppressive environments or regression by the M1-like proinflammatory infiltrate.[115, 116] Having a higher proportion of M2-like macrophages within the TiME has been associated with a worse prognosis, due to their production of immunosuppressive cytokines allowing tumors to evade immune surveillance.[21, 115] The Gas6/AXL axis has been shown to classically drive an M2-like macrophage phenotype in a variety of systems and disease settings.[117, 118] However, it is also essential for augmenting an M1-like macrophage proinflammatory response and the overall effect of this axis is dependent on the system or microenvironment of interest.[119] Both macrophage depletion and macrophage polarization shifts have been implicated in response AXL inhibition (**Figure 2-15**)[107] and as strategies to augment T-cell therapies, sequencing of immune targeting is a critical area of interest in immunotherapy.[120]

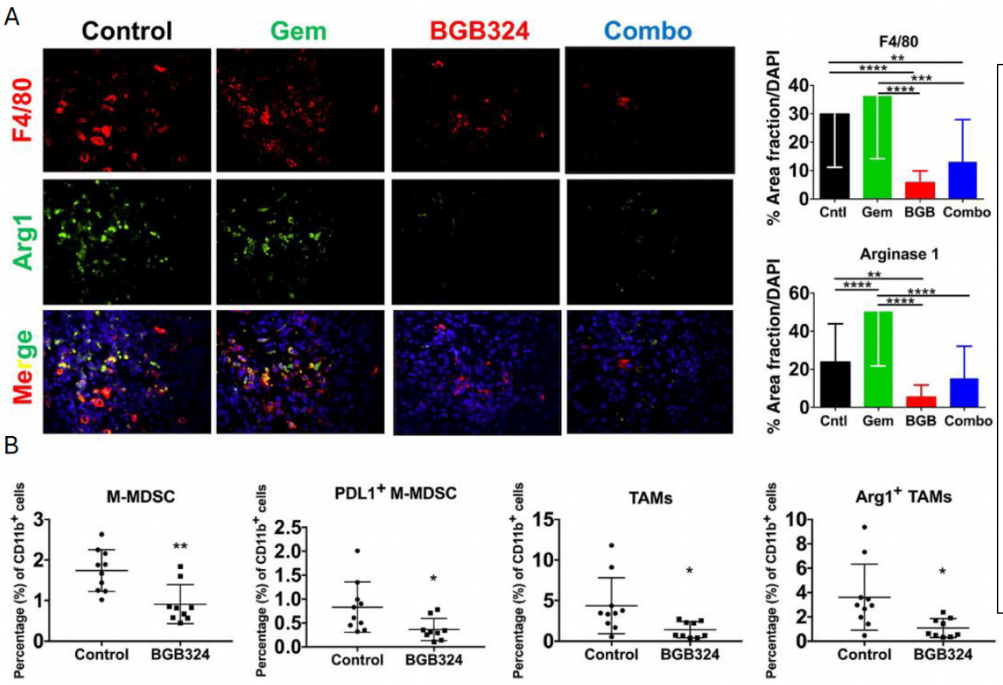

Figure 2-15. AXL inhibition in pancreatic cancer depletes TAMs, shifts inflammatory profile A) BGB324/ Bemcentinib AXL small molecule decreased overall TAM populations in an orthotopic model of pancreatic cancer. B) Amongst remaining TAM populations, AXL inhibition significantly shifted milieu toward M1-like inflammatory profile.[107]

AXL is a Biomarker of Aggressive Melanoma

AXL receptor signaling significantly manipulates epithelial-to-mesenchymal (EMT) plasticity in the TME, by influencing ligand secretion by macrophages. This correlates with significant increases in the metastatic potential of AXL-expressing tumors, and it has shown that metastatic events could be eliminated by multiple strategies of AXL inhibition.[21] The complex interplay of AXL signaling in immune cells at the TME interface is emerging with multiple targeting strategies being explored in early phase and preclinical studies (**Figure 2-14**).[20, 121, 122] Given the association of EMT phenotype with response to PD-1 therapy in published transcriptomic datasets, we queried the expression of AXL in pretreatment melanoma specimens and correlated this to reported clinical response. Significantly, high AXL expression prior to therapy was associated with non-response to anti-PD-1 therapy (**Figure 2-16**).[123, 124] It has been reported that tumor AXL activity and stage correlates to levels of its serum detectable ligand, Gas6, and receptor cleavage product in oral squamous cell cancer.[125] In clinical samples, the immune cell-AXL relationship remains highly complex and poorly understood with several host factors, including age, gender, and obesity, influencing the inflammatory cascade and response to immunotherapeutics.[126-129] The use of AXL as a therapeutic biomarker remains undefined but may present an opportunity for precision tailoring of therapies and logical targeted combination strategies to mitigate resistance to modern immunotherapies. It will remain critical to define which AXL-expressing cells are at play in the progression of melanoma to further define AXL inhibition strategies as specific to aggressive, resistant melanoma or as a broad strategy to target immunosuppressive tumor environments.

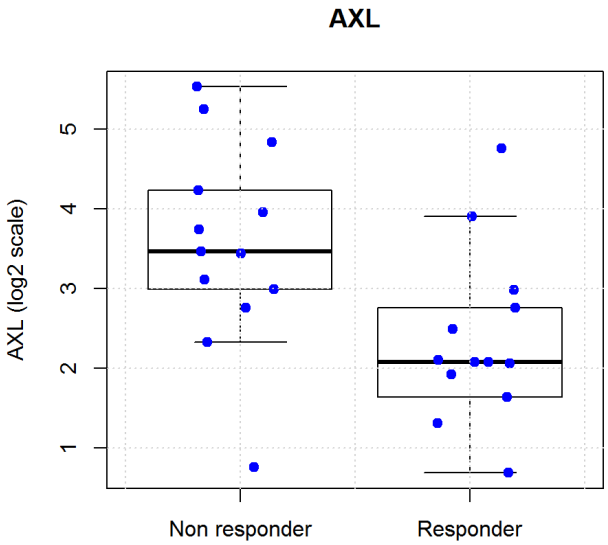

Figure 2-16. AXL expression is associated with PD-1 therapy nonresponse. Pretreatment biopsies of Stage IV melanoma patients treated with pembrolizumab reveal signatures of mesenchymal programming in tumor cells are associated with poorer response to anti-PD-1 therapy. AXL TK was found to be significant in this signature (p=0.02).[123,124]

Chapter 3 Methodology

1. Human Studies

Study Approval

The study protocol was approved by the Institutional Review Board (IRB) of UC Davis (approval no: 1529612) and the study was conducted in compliance with Good Clinical Practice (GCP), as described in the ICH Harmonised Tripartite Guidelines for GCP 1996, US 21 Code of Federal Regulations dealing with clinical studies, and the Declaration of Helsinki, concerning medical research in humans. Patients were enrolled after obtaining informed, written consent for participation in UCDCCSO304/NCT02211131, including written consent for photographic image usage and publication. A record of these consents has been retained per cancer center policy.

Trial Design

After IRB approval, patients were recruited from the UC Davis Comprehensive Cancer Center (UCDCCC). Inclusion criteria included: treatment-naive adults older than 18 years of age, with cutaneous melanoma greater than 2.0 mm in depth with residual tumor not eligible for systemic therapy, and life expectancies of over 3 months. Any patients who received previous TVEC treatment, had additional malignancies or severe comorbidities, had regional or systemic metastasis, or were currently enrolled in another clinical trial were excluded. All injections were performed in the outpatient setting. Standard TVEC dosing was determined based on lesion size. A loading dose of TVEC (10^6 PFU/mL) was given 3 weeks prior to initiation of the treatment dose (10^8 PFU/mL). Three treatment doses were given prior to surgical removal. The treatment doses were administered on days 1, 21, 35, and 49 for all patients. On day 56, a wide local excision was performed with sentinel lymph node biopsy (SLNB). Sex as a variable was recorded in the study design; however, at the time of study closure only one eligible female had presented for evaluation

and was eligible for enrollment. Therefore, sex as a variable is not reported in the results of the study.

Antibodies and Reagents

The monoclonal antibodies mouse anti-PD-1 and rabbit anti-PD-L1 were purchased from Abcam (catalogue numbers ab52587 and ab205921, respectively). AffiniPure $F(ab')_2$ fragment donkey anti-mouse IgG (H+L) and peroxidase AffiniPure $F(ab')_2$ fragment donkey anti-rabbit IgG (H+L) were purchased from Jackson Immuno Research (catalogue numbers 715-006-150 and 711-036-152, respectively). Pierce endogenous peroxidase suppressor, tyramide signal amplification (TSA) SuperBoost kit, and Prolong Glass antifade mount were purchased from Thermo Fisher Scientific (catalogue numbers 35000, B40925, and P36980, respectively). Atto 488 NHS ester, bovine serum albumin (BSA) and rhodamine B, were purchased from Sigma Aldrich (catalogue numbers A2153-100G and 234141-10G, respectively).

Two-site Assay for PD-1/PD-L1

(**Supplementary Figure. S3.1**) The tissue microarrays (TMAs) were constructed in collaboration with BioIVT. Tissue sections were reviewed under dermatopathological guidance for the selection of appropriate regions for sampling. Core samples (2 mm) were obtained from formalin-fixed paraffin-embedded (FFPE) blocks of the tumor core, tumor:normal skin interface, post-therapy tumor bed, and DSLN. TMAs underwent an antigen retrieval process using the Envision Flex retrieval solution, pH 9. The Dako PT-Link system was utilized, for which the slides were heated to 95°C for 20 minutes. Using a PAP pen, an aqueous-repelling border was outlined around each tissue fragment. Pierce endogenous peroxidase suppressor was then applied to each specimen, and the slides were left to incubate for 30 minutes at 21°C room in a humid-controlled environment. The samples underwent two washes with phosphate-buffered saline (PBS) before being incubated for an hour at room temperature with 3% BSA (10 mg/ml). The donor-only slides

were incubated with anti-PD-1 (at a dilution of 1:100). The donor-acceptor slides were treated with the following primary antibodies: anti-PD-1 (1:100) and anti-PD-L1 (1:500). Primary antibodies were incubated overnight at 4°C. Samples were washed with 0.02% PBS-tween (PBST). The samples were then treated with secondary F(ab')2 fragments. F(ab')2- Atto 488 (at a dilution of 1:100) was introduced to the donor-only slides. The donor-acceptor slides received both F(ab')2-Atto 488 (1:100) and F(ab')2- horseradish peroxidase (HRP) (1:200). These samples were incubated for 2 hours in the dark at room temperature in a humidified container. After the incubation period, slides were washed with 0.02% PBST. The donor-only slides were mounted with 1 drop of Prolong Glass antifade mount. The donor-acceptor slides were subjected to TSA. The purpose of TSA is to amplify the acceptor labeling, which increases the signal-to-noise ratio and enhances the resonance energy transfer. This procedure is described in detail in Veeriah *et al.* (2014)[130] and Magraner Sanchez *et al.* (2020).[76] The antibodies were labeled with species-specific F(ab')2 fragments which were conjugated to Atto 488 (donor chromophore, used to label the receptor primary antibody) or HRP (used to label the ligand primary antibody). TSA was used to conjugate the acceptor chromophore (Alexa 594) to the HRP labeling the ligand.

Time-Resolved Immune Förster-Resonance-Energy Transfer (iFRET) Determined by Frequency-Domain FLIM.

The quantitative molecular imaging platform utilizes a custom-made semi-automated frequency-domain Fluorescence Lifetime Imaging (FLIM). The first slide (donor only) was excited by a modulated (40 MHz) diode 473 nm laser, and the lifetime of the donor alone was recorded. The second slide was excited by the diode modulated 473 nm laser and lifetime of the donor in the presence of the acceptor was recorded. The reduction of donor lifetime (caused by resonance energy transfer) due to the presence of the acceptor reports on distances of 1-10 nm and therefore acts as a "chemical ruler" enabling to quantify receptor-ligand interactions. We identified the coinciding regions where both the donor and acceptor were observed. A total of 10 to 20 regions

of interest (ROIs) were selected within these coinciding regions. Subsequently, the lifetimes, along with their corresponding standard deviations (SD), were automatically obtained and exported to an Excel spreadsheet.

Photophysical parameters for quantification of protein interactive states.

We automatically calculate lifetime image of the donor in the presence of an acceptor (τ_{DA}) and a lifetime image of the donor (τ_D), followed by calculation of reduction of τ_{DA} compared to τ_D, which is reflected in a parameter called FRET-efficiency (*Ef*):

Ef = [1 − <τ_{DA}>/<τ_D>]x100 Eq-1

FRET-efficiency was calculated as an average for each coincident region. Ef is directly related to the distance between the donor and acceptor fluorophores (Atto 488 and Alexa 594) (Eq-2), where r is the distance between Atto 488 and Alexa 594 in these experiments. 'R0' the Förster radius in this case is 5.83 nm and it is the distance whereby the transfer efficiency is 50%.

Ef=R06R06+r6 Eq-2

r= 6R06*(1-Ef)Ef Eq-3

Mass Cytometry

Peripheral blood mononuclear cells (PBMCs) were thawed and pre-warmed in RPMI media containing 1:10,000 Benzonase (25 U/mL final concentration) and resuspended in 1 mL of CyFACS buffer (PBS with 0.1% bovine serum albumin (BSA), 2 mM Ethylenediaminetetraacetic acid (EDTA) and 0.05% Na azide). One million viable cells were added to each well of a 96-well plate, followed by titrated antibody cocktail containing metal-chelating polymer-labeled antibodies. Cells were normalized using CYTOF Software v.7.0.8493 EQ-P13H2302_ver2. Raw data eliminated bead only reads to identify live, intact single cells. Gating was then conducted

according to **Table 3-3** to identify the total number of cells per population. The frequency of each individual cell population was defined by the total cells or by total cell population by sample, as described in Table 3.. All live, intact, single cells were subjected to t-distributed stochastic neighbor embedding (tSNE) for dimensionality reduction using FlowJo V10.9.0.[131, 132] Dimensionality reduced cells were used to represent gated cell populations.

Table 3-3. Flow cytometry gating strategy

Phenotypic Characterization		Treatment Groups (% & Standard Deviation [SD])						
Immune Cell Subset	**Phenotype**	**Control**	**Pre-Treatment (n=3)**	**SD**	**During Treatment (n=3)**	**SD**	**Post-Treatment (n=2)**	**SD**
CD8 T Cell	**CD3+ CD8+ CD4-**	**10%**	**10%**	**0.04**	**11%**	**0.01**	**9.0%**	**0.04**
Naïve CD8	CCR7 +/- CD45RA+	71%	56%	0.08	49%	0.02	45%	0.06
Central Memory CD8	CCR7- CD45RA-	6.2%	10%	0.06	5.3%	0.02	3.9%	0.00
Effector Memory CD8	CCR7+ CD45RA+	23%	34%	0.03	45%	0.04	51%	0.06
HLADR+	HLADR+	6.3%	5.6%	0.06	2.1%	0.00	1.7%	0.00
CD57+	CD57+	40%	30%	0.14	44%	0.13	43%	0.27
ICOS+	ICOS+	1.2%	0.6%	0.01	0.1%	0.00	0.2%	0.00
PD-1+	PD-1+	3.3%	1.1%	0.01	0.3%	0.00	0.2%	0.00
CD4 T Cell	**CD3+ CD8- CD4+**	**19%**	**26%**	**0.13**	**22%**	**0.13**	**18%**	**0.03**
Naïve CD4	CCR7 +/- CD45RA+	33%	55%	0.13	37%	0.17	39%	0.28
Central Memory CD4	CCR7- CD45RA-	36%	27%	0.11	29%	0.09	19%	0.15
Effector Memory CD4	CCR7+ CD45RA+	30%	17%	0.07	34%	0.11	41%	0.13
HLADR+	HLADR+	16%	3.6%	0.02	3.3%	0.02	2.0%	0.02
CD57+	CD57+	1.9%	3.0%	0.01	7.4%	0.07	5.8%	0.05
ICOS+	ICOS+	10%	1.2%	0.01	0.8%	0.00	0.8%	0.01
PD-1+	PD-1+	5%	0.3%	0.00	0.5%	0.00	0.2%	0.00
T Reg	CD25+ CD127-	16%	4.4%	0.04	2.7%	0.02	0.8%	0.00
T Reg CD161+	CD161+	0.5%	0.1%	0.00	0.0%	0.00	0.1%	0.00
T Reg CD39+	CD39+	4.4%	1.1%	0.02	0.7%	0.01	0.1%	0.00
T Reg CD45RA+	CD45RA+	2.4%	0.4%	0.00	0.1%	0.00	0.2%	0.00
MDSCs	**CD3-CD19-CD20-CD56-CD16-HLADR-CD11b+CD33+**	**0.8%**	**0.3%**	**0.00**	**0.4%**	**0.00**	**0.1%**	**0.00**
DCs		**3%**	**3%**	**0.01**	**5%**	**0.03**	**3%**	**0.00**
mDCS	CD3-CD19-CD20-CD11b+CD33-CD14-CD56-CD16-CD11c+CD123-	58%	86%	0.10	94%	0.05	95%	0.02
pDCS	CD3-CD19-CD20-CD11b+CD33-CD14-CD56-CD16-CD11c-CD123+	42%	13.5%	0.10	6.4%	0.05	5.3%	0.02
NK	**CD3-CD19-CD20-CD56+CD16+**	**6%**	**6%**	**0.07**	**1.2%**	**0.01**	**0.4%**	**0.00**
NK Mature	CD27+CD16+	36%	3.3%	0.03	2.1%	0.02	2.3%	0.03
NK Immature	CD27-CD16+	64%	97%	0.03	98%	0.02	98%	0.03
NKT	**CD3+ CD19-CD20-CD56+CD16+**	**1%**	**0.1%**	**0.00**	**0.1%**	**0.00**	**0.0%**	**0.00**
NKT Mature	CD27+CD16+	39%	36.3%	0.21	27.5%	0.18	0.0%	0.00
NKT Immature	CD27-CD16+	61%	63.7%	0.21	72.5%	0.18	100.0%	0.00
B Cells	**CD3-CD19+CD20+**	**8.7%**	**7.7%**	**0.06**	**4.0%**	**0.02**	**1.2%**	**0.01**
B Plasma Cells	CD38+CD27+	7.1%	1.5%	0.01	1.9%	0.01	1.5%	0.02
B Memory Cells	CD38-CD27+	7.7%	16%	0.04	16%	0.02	12%	0.08
B Regulatory Cells	CD38+CD27+CD24+	4.8%	1.2%	0.01	1.0%	0.01	1.2%	0.02
Monocytes	**CD3-CD19-CD20-CD11b+CD33+CD14+**	**39.4%**	**15.9%**	**0.10**	**16%**	**0.06**	**2.2%**	**0.01**
Classical	CD14+CD16-	93%	94%	0.02	94%	0.05	69%	0.41
Intermediate	CD14+CD16+	3.4%	3.1%	0.01	2.3%	0.02	1.8%	0.01
Alternative	CD14-CD16+	4%	3%	0.02	4%	0.03	29%	0.39
Unlabeled	**None**	**12.5%**	**30.6%**	**0.02**	**40.1%**	**0.14**	**66.4%**	**0.00**
Total Gated Cells		**88%**	**69%**	**0.02**	**60%**	**0.14**	**34%**	**0.00**
Total Live Cells		**170,356**	**44,487**	**25,001**	**33,621**	**17,004**	**23,389**	**1,964**

Luminex

Patient serum samples were sampled at Day 1, 21, and 56 of therapy. Standard Luminex Immunoassay was performed per Stanford Human Immune Monitoring Core protocol using standard assay materials, with kits purchased from EMD Millipore Corporation and run according to the manufacturer's recommendations with modifications described as follows: The H48 kits

include one panel: Milliplex HCYTA-60K-PX48. The assay setup adhered to the recommended protocol, which included samples preparation in which samples were diluted 3-fold in a 96-well plate, while (plasma) supernatant samples were ran undiluted. The samples were incubated overnight at 4°C with shaking. Cold and room temperature incubation steps were performed on an orbital shaker at 500-600 rpm. After incubation, plates were washed twice with wash buffer using a BioTek ELx405 washer (BioTek Instruments). After a one-hour incubation at room temperature with a biotinylated detection antibody, streptavidin-PE was added and incubated for 30 minutes with shaking. Plates were then washed as described above, and Wash Buffer was added to the wells for reading in the Luminex FlexMap3D Instrument, ensuring a lower bound of 50 beads per sample per cytokine. Each sample was measured in duplicate. Custom Assay Chex control beads (Radix BioSolutions) were added to all wells. GraphPad Prism was used to examine data and variances were evaluated by one-way ANOVA.

Single Cell Sequencing

Data Extraction: We collected five single-cell RNA sequencing (scRNA-seq) datasets and two bulk RNA sequencing datasets for humans from publicly available repositories, including Gene Expression Omnibus (GEO), Single Cell Portal, and The Cancer Genome Atlas (TCGA). For the 10X Genomics data, raw sequencing files were obtained using SRA-Toolkit (v3.0.2) via the fastq-dump utility. After obtaining the raw sequencing data, gene expression (GEX) matrices were generated through a comprehensive pipeline. First, the data were demultiplexed to separate individual cell barcodes from sequencing reads. Next, barcode processing was performed to filter out low-quality or ambiguous barcodes, ensuring accurate assignment of reads to specific cells. The processed reads were then aligned to the human reference genome Hg38 using a highly optimized alignment algorithm. Finally, gene quantification was carried out, whereby aligned reads were counted to generate a matrix of gene expression levels across all cells. All steps in this pipeline were performed using the 10X Genomics CellRanger software (v7.1.0). For datasets

generated using the SMART-Seq2 protocol, GEX matrices were directly downloaded from the Gene Expression Omnibus (GEO) and Single Cell Portal repositories.

Single-cell RNA Data Filtering and Normalization

To enhance the accuracy of gene expression estimates, we utilized the `remove-background` function in CellBender (version 0.3.0) for each sample. CellBender utilizes a deep learning-based approach to model and remove technical artifacts, such as background noise and ambient RNA, which can contaminate single-cell RNA sequencing data. By estimating the true biological signal from the raw gene-by-cell count data, CellBender generates ambient-corrected count matrices that provide a more accurate reflection of the cellular transcriptome.

These corrected matrices were then imported into R (version 4.2.2) and converted into Seurat objects using Seurat (version 4.9.9.9086). We applied stringent cell selection criteria to ensure data quality: cells were retained if they exhibited less than 10% or up to 20% mitochondrial reads, expressed between 3,500 and 7,500 genes and had unique molecular identifier (UMI) counts ranging from 500 to 60,000. Next, doublet cells were identified using Scrublet (version 0.2.3), which computes doublet scores based on the expected doublet rate, preset at 10%. Cells flagged as doublets by Scrublet with the default parameters were excluded from further analysis. For datasets generated using the SMART-Seq2 protocol, we incorporated pre-filtered datasets sourced from public repositories, including GEO and Single Cell Portal.

After data filtering, the gene-by-cell expression matrices were merged using the `merge` function. We then proceeded with pre-processing using SCTransform (version 0.4.0), which incorporates a variance-stabilizing transformation (VST) method. SCTransform replaces conventional normalization and scaling procedures with a regularized negative binomial regression model, effectively controlling for technical noise. This method adjusts gene expression measurements by modeling unwanted variation and emphasizing biological variability.

Unsupervised dimensional reduction and clustering

For dimensionality reduction, Principal Component Analysis (PCA) was conducted. PCA reduces the dimensionality of the data by transforming the original variables into a new set of variables, which are linear combinations of the original variables. These new variables, called Principal Components (PCs), are ordered so that the first few retain most of the variation present in the original variables.

Upon completion of PCA, the datasets were prepared for integration using Harmony, applied through the `RunHarmony` function with specified covariates: project, sequencing techniques, tissues, and donors. Harmony leverages a model-based approach to adjust the principal components across different datasets, mitigating the impact of batch effects and other technical discrepancies. This step ensures that the integrated data are aligned in a shared dimensional space that more accurately reflects the underlying biological heterogeneity.

Following the successful integration of datasets, we employed Uniform Manifold Approximation and Projection (UMAP) for further dimension reduction. We used the top 30 corrected principal components derived from Harmony. UMAP operates on a manifold learning technique that maps high-dimensional data into a more manageable two-dimensional space, facilitating the visualization and interpretation of complex data structures and relationships.

Clustering and identification of marker genes

To determine the optimal number of clusters across the entire cell population, we utilized the `estimate_k` function from scCCESS (version 0.3.3), configuring the criteria method to use NMI criterion and selecting the k-means algorithm. We set the ensemble size to 10 to ensure robustness by averaging results across multiple initializations. Once the optimal cluster number was identified, we applied it in the `ensemble_cluster` function, again using the k-means algorithm, to partition the cells into distinct clusters based on their gene expression profiles.

Subsequently, we focused on the myeloid cell population. The clustering process was repeated specifically for these cells. We began with the `estimate_k` function, using the same parameters as those applied to the whole cell population. We then utilized `ensemble_cluster` with the k-means algorithm and the newly determined optimal number of clusters to better capture the unique expression patterns of the myeloid cells. This independent analysis resulted in a different optimal number of clusters, reflecting the distinct biological characteristics of the myeloid cells.

Next, we identified significant marker genes for each myeloid cell subset using the `FindMarkers` function in Seurat. We employed the MAST method for statistical testing, which is well-suited for single-cell RNA-seq data, particularly in handling sparsity and zero-inflation. To ensure robustness in the marker identification process, we set the minimum percentage (min.pct) of cell expressing a gene to 10%, meaning that a gene had to be expressed in at least 10% of cells in either of the groups being compared. Additionally, we applied the logarithmic fold change threshold (logfc.threshold) of 0.1, focusing on genes that exhibited at least a modest difference in expression levels. These criteria allowed us to identify marker genes that are both statistically significant and biologically relevant for each subset of myeloid cells.

Individual datasets were also analyzed using in-house software (Maverakis Lab, https:shiny.physioseq.net) for analysis and graphic display.

Statistical Analysis

To evaluate FRET-efficiencies in two distinct experimental configurations (PD-1/PD-L1), box and whisker plots were employed to visually represent the data from each sample independently. This approach aimed to facilitate obtaining the graphs and comparison of FRET efficiency distributions among patient samples. Following this, the Mann-Whitney U test was utilized to statistically analyze and compare the FRET efficiencies between pre-treatment and post-treatment samples. A p-value of <0.05 was considered statistically significant.

2. *In Vivo* Experiments

Animal Studies

All animals were housed in a pathogen-free facility with 24-hour access to food and water. Experiments were approved by, and conducted in accordance with, an IACUC approved protocol at UC Davis for initial therapeutic studies with warfarin, cabozantinib, and bemcentinib. Bemcentinib studies were repeated for a total of three independent experiments to serve as controls for the myeloid depletion models, with the second two studies performed at Stanford University. Four- to six-week-old female C57/Bl6 mice were obtained from an on-campus supplier. A total of 1×10^6 YUMM1.7, YUMMeR1.7, and B16F10 melanoma cells, were injected orthotopically as described.[133] Mice were randomized to receive 0.5 mg/L (500 nM) once tumors were measured at caliper volume of 100mm3 and water was replenished every 3 days. Mice treated were treated were treated with bemcentinb (50 mg/kg) or cabozantinib (30 mg/kg), or Invivomab anti-PD-1 (1 mg/kg) or combination as described. Targeted therapies were administered daily by oral gavage and immunotherapy by intraperitoneal injection 3x/week. Therapy was administered for 14-21 days until control tumors reached 1,500 mm^3.

Luminex Assay

Mouse serum samples were collected on day 18, at time of sacrifice. Mouse 48-plex Procarta kits (EPX480-20834-901) were purchased from Thermo-Fisher/Life Technologies and used according to the manufacturer's recommendations with modifications as described. In brief, beads were added to a 96-well plate and washed in a BioTek ELx405 washer. Samples were added to the plate containing the mixed antibody-linked beads and incubated overnight at 4°C with shaking. Cold (4℃) and room temperature incubation steps were performed on an orbital shaker at 500-600 rpm. Following the overnight incubation, plates were washed in a BioTek ELx405 washer and biotinylated detection antibody was added for 60 minutes at room

temperature with shaking. The plate was washed, and streptavidin-PE was added for 30 minutes at room temperature, anfter which the plate was washed and reading buffer was added to the wells. Each sample was measured in duplicate. Plates were read using a Luminex 200 or a FM3D FlexMap instrument with a lower bound of 50 beads per sample per cytokine. Custom Assay Chex control beads (Radix BioSolutions)were added to all wells. GraphPad Prism was used to examine data and variances were evaluated by one-way ANOVA.

Flow cytometry

Single-cell suspensions were prepared from tumor samples and stained with fluorescently-labeled antibodies according to the manufacturer's instructions. Cell sorting/flow cytometry analysis for this project was performed on instruments at the Stanford Shared FACS Facility with appropriate gating strategy to identify specific cell populations. Data analysis was performed using FlowJo software (Tree Star, Ashland, OR) to quantify and analyze cell populations.

3. ***In Vitro* Experiments**

In Vitro Migration Assay

Raw M0 macrophages or THP-1 M0 macrophages were utilized for migration assays with Yumm1.7 and SK-MEL24 cell lines, respectively. To induce THP-1 cell differentiation into M0 macrophages, cells were incubated with phorbol myristate acetate for 24 hours. M0 macrophages were then either polarized into M1 or M2 macrophages using 100 ng/mL of lipopolysaccharide (LPS) or 20 ng/mL of IL-4 and IL-13, respectively. The macrophages were differentiated in RPMI media with 1% FBS and were incubated with their respective M1- or M2-inducing agents for 24-48 hours. Once macrophage differentiation occurred, conditioned media was harvested. One million cells of SK-MEL24 and Yumm1.7 were cultured in RPMI media with 10% FBS in each well of 6-well cell culture plates until they reached at least 70% confluency. After confluency was

reached, media from each well was aspirated and in all wells except 4 per cell line, RPMI media with 1% FBS was added. In the 4 wells without RPMI, M1-conditioned media was added to half of the wells, and M2-conditioned media was added to the remaining wells. Next, Gas6 was added to one unconditioned media well per cell line and one M1-conditioned media well per cell line at a concentration of 25 μg/mL. Bemcentinib was added to one unconditioned media well per cell line and one M2-conditioned media well per cell line at a concentration of 0.5 mM. After all wells had their desired treatments and conditioned medias, a cell culture wound closure assay protocol was performed.[134] Images were then taken using a Zeiss Axio Observer fluorescent microscope for each well and were designated as time 0 images. The cell culture plates were then placed in an incubator and images were taken for Yumm1.7 cells at the 8- and 24-hour timepoints at the same location. SK-Mel-24 cell line images were taken at the 24- and 32-hour timepoints due to their slower proliferation rate at baseline. After all images were acquired, they were compiled and analyzed with ImageJ using the measuring tool to determine the width of the wound at 5 points along the wound. The wound closure for each condition was then plotted using Graphpad software. To standardize between different initial wound widths, we determined the percentage of wound closure by assessing the difference between the initial and final widths as a percentage of the initial width.

Efferocytosis Assay.

M1 and M2 macrophages were derived from Raw mouse macrophages through differentiation protocols utilized in our other *in vitro* assays. M1 macrophages were activated with 100 ng/mL LPS for 24 hours, while M2 macrophages were polarized with 20 ng/mL of IL-4 and IL-13 for 24 hours. The macrophages were then labeled with Cytotel blue dye (Efferocytosis kit Cayman Chemicals). Yumm 1.7 melanoma cells were cultured in RPMI supplemented with 10% FBS. Apoptotic Yumm 1.7 cells were induced by treating cells with 5 μM staurosporine for 6 hours, after which cells were labeled with CFSE green-fluorescent dye (Efferocytosis kit Cayman

chemicals). Co-culture experiments were performed in duplicate with each experiment initiated by seeding 1x10^6 macrophages per well in 5 wells of 6-well plates: one M0, two M1, and two M2 wells. This was followed by the addition of labeled apoptotic cells at a ratio of 5:1 (apoptotic cells:macrophages). At this step, we added drugs of interest, including bemcentinib (0.5 μM) and Gas6 (100 ng/ml), to one M2 macrophage and one M1 macrophage condition, respectively. After a 2-hour incubation at 37°C, the co-culture samples were fixed for immunofluorescence staining using CD86 for M1 or CD206 for M2 macrophage phenotypes. Flow cytometry analysis was employed to quantify efferocytosis, measuring the percentage of macrophages that had engulfed apoptotic cells through the colocalization of Cytotel blue and CFSE dyes.

Phagocytosis Assay

Phagocytosis was performed in M0, M1, and M2-differentiated macrophages cells using the same differentiation protocol and treatment as described for the efferocytosis experiment. Initially, we seeded the raw cells in a 6-well plate and allowed them to grow overnight. The following day, macrophages were polarized by exposing them to RPMI-1640 culture media with 1% FBS. Specifically, M1 macrophages were polarized with 100 ng/mL LPS from Escherichia coli, O111:B4 (Sigma Aldrich), while M2 macrophages were polarized with 20 ng/mL of mouse IL-4 and IL-13 recombinant protein (PeproTech®, Gibco, Thermofisher) for 24 hours. After the 24-hour polarization period, we set up treatment conditions in three control wells for M0, M1, and M2 macrophage conditions individually. For M2, we included bemcentinib (0.5 μM) and Gas6 (100 ng/mL) treatments, and for M1, we used bemcentinib (0.5 μM) and Gas6 (100 ng/mL) separately. Following the 24-hour treatment, we removed the culture media, washed the cells, and resuspended them in cold PBS. We employed the Phagocytosis Assay Kit (Green Zymosan - ab234053, Abcam) containing Green Zymosan slurry. To each well, 5 μL of Zymosan slurry was added, and the plate was placed back in the incubator protected from light for 4 hours. After the incubation period, media was removed and cells were washed twice with 100 μL of ice-cold Assay

Buffer containing the effector of interest. Cells were then suspended in 200 µL of ice-cold Assay Buffer. To accurately measure *in vitro* phagocytosis, we used a fluorescence plate reader (Agilent) with FL-600 settings for Excitation filter at 485/20 and Emission Filter at 530/25, scanning all experimental and control wells.

Flow Cytometry

Single-cell suspensions were prepared from tumor samples and stained with fluorescently-labeled antibodies according to the manufacturer's instructions. Cell sorting/flow cytometry analysis for this project was performed on instruments in the Stanford Shared FACS Facility (RRID: SCR_017788) with appropriate gating strategy to identify specific cell populations. Data analysis was performed using FlowJo software (Tree Star) to quantify and analyze cell populations. The list of antibodies and kits used includes the following: Zombie Violet™ Fixable Viability Kit, PE/Cyanine7 anti-mouse CD3, PE anti-mouse CD4, FITC anti-mouse CD8a, PE anti-mouse CD68 Antibody, Brilliant Violet 650™ anti-mouse CD86, Brilliant Violet 785™ anti-mouse CD206 (MMR), PE/Cyanine7 anti-mouse CD163 Antibody, FITC anti-mouse F4/80 Antibody, Brilliant Violet 570™ anti-mouse/human CD11b, Brilliant Violet 750™ anti-mouse CD11c, Alexa Fluor® 700 anti-mouse CD68, PE anti-mouse CD279 (PD-1), and PE/Cyanine7 anti-mouse CD274 (B7-H1, PD-L1) were purchase from BioLegend (BioLegend Way, San Diego, CA 92121 United States) and antigen-presenting cell (APC)/AXL Monoclonal Antibody (MAXL8DS) from eBioscience™, Thermofisher.

T Cell Activation Assay

In the first step of our experimental protocol, we differentiated Raw mouse macrophages into either M1 or M2 subtypes using 100 ng/ml of LPS or 20 ng/ml of IL-4 and IL-13, respectively. These macrophages were allowed to differentiate for 24 hours incubated at 37℃. On the next day, we initiated the apoptosis of YUMM 1.7 mouse melanoma cells using staurosporine at 1 uM

for 8 hours. At the conclusion of the apoptosis session, these YUMM 1.7 cells were added to the differentiated macrophages at a concentration of 3 x 10^5 cells per well and were incubated overnight. In parallel, we collected two spleens from healthy euthanized mice. The spleens were processed into single cells, and T cells were isolated using the Dynabeads Untouched Mouse T Cell kit (Invitrogen). After isolation, the T cells were labeled with carboxyfluorescein succinimidyl ester (CFSE) and were incubated at 37℃ in a flask with RPMI media and 10% FBS to expand them overnight. After 24hr incubation, T cells were prepared for cell-cell interaction with macrophages, and a triple coculture system was employed involving T cells, macrophages, and their apoptotic tumor cells. The final step of the experiment involved the analysis of T cells and macrophages by flow cytometry. For CFSE-labeled T cells, markers such as CD3, CD4, CD8, PD-1, and AXL were assessed, while macrophages were evaluated for Live/Dead, PD-L1, CD68, CD86, and AXL by flow cytometry as described for tumor studies.

Statistical Analysis

The data were examined using GraphPad software (GraphPad Prism 10 for Windows; GraphPad Software; www.graphpad.com). Findings are presented as mean ± standard error of the mean (SEM) or SD. Statistical analysis involved t-tests or ANOVA, with significance determined at $p < 0.05$.

Chapter 4: Functional Analysis of Neoaduvant Oncolytic Virus

A pilot Phase II study (**Figure 4-1A**) was designed to explore the use of the OV TVEC[135, 136], to stimulate an immune response prior to standard surgery with intent to perform in-depth biomarker interrogation of pre- and post-treatment specimens. A novel interactive state iFRET assay was utilized to contextualize and delineate TVEC responders from those without benefit, who may be better served by upfront surgery or ICB.[137] It was hypothesized that patient-specific variations of the innate immune system might impact the heterogeneity of response observed with TVEC, as prior reports in both OV and ICB under-investigated these contributions to checkpoint engagement.[3]

1. Trial Design and Clinical Analysis

Patients with primary melanoma of at least 2 mm thickness, without clinical evidence of nodal involvement, and residual lesion *in situ* were enrolled in our open-label Phase II study between June 2020 and July 2022. Patients were treated with four injections, starting with a 10^6 loading dose and followed by three doses of 10^8 PFU/mL of TVEC per standard dosing guidelines (Study Schematic is provided in **Figure 4-1A**). Of note, given the very small size of presenting lesions, the maximum administered dose was 0.5 mL. Standard wide local excision and SLNB were performed at 1 week following the final injection. Primary endpoints of the study were safety and feasibility of approach and determination of pathologic complete response rate, which remains unknown at this short time course of 7 weeks, compared to standard time to response in previously reported studies of 12 weeks – 4 months.

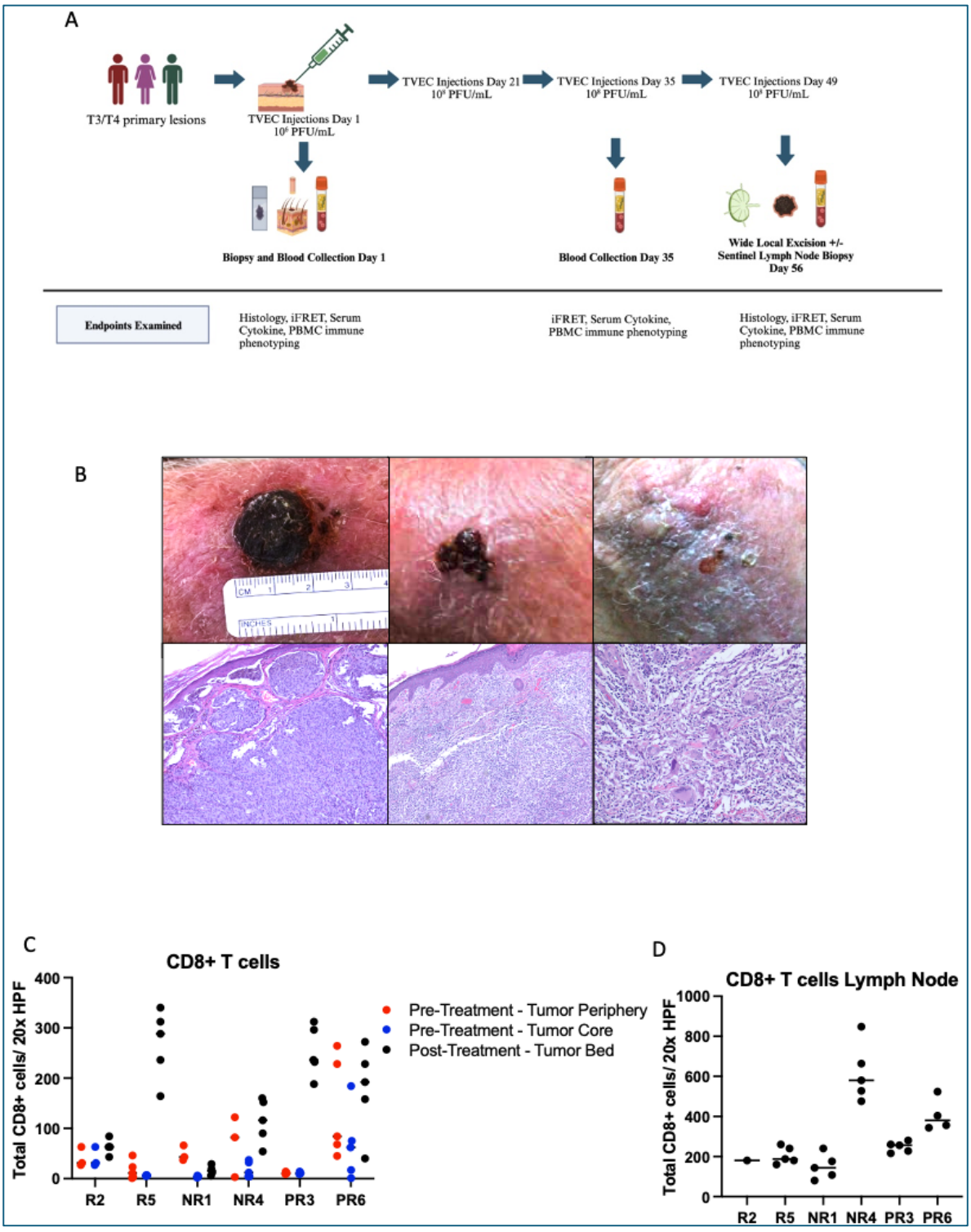

Figure 4-1. Trial Design and clinical analysis. A) TVEC was injected neoadjuvantly for six weeks prior to standard wide local excision and SLNB. PBMCs and serum specimens were collected on days 1, 35, and 56 and analyzed by CYTOF immune-phenotyping and Luminex immunoassay. Tissue was collected pretreatment and at time of definitive surgery for wide local excision and SLN biopsy. B) Clinical response and inflammatory infiltrate demonstrating resolution of tumor with robust lymphocyte and melanophage infiltrate. C) $CD8^+$ T cell infiltrate at baseline at tumor: skin interface, tumor core and at post-treatment surgical resection of the tumor bed. D) $CD8^+$ T cells within SLN shown as number of cells per 20x HPF.

Secondary endpoints included sentinel lymph node positivity and exploratory analysis of biomarkers predictive of response to intralesional therapy. Due to time frame of study opening, trial accrual was significantly dampened by coronavirus disease 2019 (COVID-19)-related closures. As a result, data of six patients completing therapy and surgical resection are presented. Clinicopathologic characteristics of each individual patient are shown in **Table 4-1**. Primary tumor assessment, based on the American Joint Committee on Cancer, Eighth edition, was >2.0 to 4.0 mm (pT3, 66.6%) or >4.0 mm (pT4, 33.3%).[138] Five patients were male (83.3%) and the average age was 64 years (range 51-76).

Table 4.1. Clinicopathologic features

Patient	1	2	3	4	5	6
Age (Years)	76	62	51	61	72	64
Sex	Male	Female	Male	Male	Male	Male
Site	Extremity	Extremity	Trunk	Extremity	Extremity	Trunk
Type	Acral	Acral	Nodular	Acral	Nodular	Nodular
Breslow depth	5.1	4.7	2.5	>2	2.1	3.4
T stage	T4b	T4b	T3a	T3b	T3b	pT3a
Ulceration	Yes	Yes	No	Yes	Yes	No
LVI	No	No	No	No	N/A	No
Mitotic Index	10	2	7	6	4	1-2
SLN (predicted)	54%	60%	18%	37%	12%	19%
SLN	-	-	-	+, IHC only	-	-
Recurrence	No	No	No	Yes, 18 months	No	No
Adverse Events, Grade*	1	1	1	1	1	1
Surgical Complication	No	No	No	No	No	No
Systemic Therapy	No	No	No	Adjuvant	No	No

Table 4.1. Clinicopathologic features						
Patient	1	2	3	4	5	6
Age (Years)	76	62	51	61	72	64
Sex	Male	Female	Male	Male	Male	Male
Response	NR	CR	PR	NR	CR	PR
Residual disease	IHC only	IHC only, <10%	Gross	IHC only	N	Gross
Inflammation score	1+	2+	3+	1+	3+	2+
Other				PD-L1 1%		

*IHC: immunohistochemistry; LVI: lymphovascular invasion; NA: not able to be determined; PD-L1: programmed cell death ligand 1; SLN: sentinel lymph node: Unk: unknown. Pathologic response: residual disease determined by IHC only, *Grade 1 events included: Flu-like, pyrexia, fatigue, chills, headache, arthralgia, myalgia, injection site reaction/pain for 24-48 hours.*

Intralesional injection was well tolerated with all patients experiencing adverse events (AE) limited to Grade 1, including injection site pain, fever, myalgia, or nausea, which resolved at 48 hours post-injection. All patients completed the therapy as planned and underwent standard of care surgery with no experienced perioperative complications.

Pathologic examination revealed positive SLNB in 1 of 6 patients (16.6%) by IHC examination only and with evidence of regression and fibrosis. Predicted risk of SLNB positivity was calculated using the Melanoma Risk Assessment Tool and averaged 33% (range 12-60%) [139] Importantly, there was an over-representation of acral disease, a difficult to treat phenotype, in our cohort at 50%. Median follow-up time was 18 months (range 6 to 26 months). Only the patient with positive SLN was treated with adjuvant ICB and developed distant metastatic disease at 18 months post-surgery with continued progression events on ICB rechallenge. No other patients have experienced relapse to date. For primary endpoint of major/complete pathologic

response (pCR), 2 of 6 patients (33.3%) demonstrated pCR with an inflammatory score of 3+ (**Figure 4-1B**). Two patients demonstrated partial response (PR) with 2+ inflammatory scoring and evidence of residual gross tumor on wide local excision and possible evidence of fibrosis indicative of SLN regression or treatment effect. The remaining patients (33.3%) were classified as non-responders with 1+ inflammatory scoring and presence of residual tumor on IHC, inclusive of positive SLN disease.

2. Shifts in the TiME

Few biomarkers of response have been explored in this setting, with a large heterogeneity in correlation to predicted response. Moreover, preclinical studies indicate that profiles predictive of response to oncolytic viral therapies may significantly differ from those associated with response to ICB.[66]

We aimed to perform extensive tissue and circulating immune characterization before and after therapy using both reported clinical markers, CD8 and PD-L1, as well as novel functional assessments of immune receptor engagement using iFRET, cytometry by time of flight (CyTOF) characterization of PBMC immune phenotypes, and the Luminex Immunoassay. $CD8^+$ T cells were measured by IHC in five HPF and compared between the tumor core, periphery, and at the biopsy site in post-treatment specimens. Patient 1, a non-responder, was noted to have decreases in the $CD8^+$ T cell infiltrate at the post-treatment assessment, while all other patients demonstrated an expected increase in the $CD8^+$ T cell count with wide distribution in counts per 20x HPF (**Figure 4-1C**). $CD8^+$ T cell counts were similarly assessed in SLNB with the highest infiltrate observed in the positive SLN ($p<0.0001$)(**Figure 4-1D**).

3. iFRET Functional Immune Engagement

iFRET was used to quantitatively assess PD-1/PD-L1 interaction in the TiME in serial sections obtained from tumor beds before and after therapy using two-site amplified time-resolved

FRET assay, as described in Methods. The interaction of a donor Atto 488-conjugated secondary antibody to a primary anti-PD-1 antibody and the acceptor Alexa Fluor 594-conjugated secondary antibody to a primary anti-PD-L1 antibody leads to a decrease in the lifetime of the donor, which, when detected with a higher efficiency, indicates a more robust PD-1 and PD-L1 interaction (**Figure 4-2A**). In iFRET, the minimum distance between two fluorophores is 5.83 nm, a distance associated with the maximum energy transfer efficiency of 50%, known as the Förster radius. FRET efficiency values are calculated where τ_D and τ_{DA} are the donor lifetimes in the absence and presence of the acceptor, respectively[76]. A transfer efficiency of 4% or lower is representative of no interaction. A true 0 value measurement is reflective of the absence of PD-L1 labeling. Conventionally, response to TVEC is associated with increased $CD8^+$ T cell infiltrate and PD-L1 upregulation[8]. We explored the impact of these changes on regulatory immune checkpoint functional engagement and the contribution of the pre-existing immunosuppressive myeloid milieu on response to OV.

In our population, there were distinct shifts in PD-1/PD-L1 engagement before and after TVEC therapy detected by iFRET (**Figure 4-2B**). Among complete responders, Patients 2 and 5, a significant increase was observed from 0% to 12.95% and from 4.41% to 17.56 %, respectively. In contrast, no PD-1/PD-L1 engagement, pre- or post-therapy, was observed in Patient 4, who had confirmed metastatic disease. Amongst partial responders, FRET value changes were variable with increases shown in patients with a high post-treatment inflammatory score, such as Patient 3, portending a high post-treatment inflammatory score. While decreases or no change was observed in patients with no histologic response to therapy. Patient 6 demonstrated a high FRET efficiency at baseline, a partial clinical response to therapy with a 2+ inflammatory score and histologically present residual disease, and a decrease in PD-L1 expression to nearly zero post-TVEC therapy.

FRET efficiency values both pre- and post-TVEC did not directly correlate to underlying PD-L1 expression in the tumor bed (**Figure 4-2C, D**). Distribution of PD-L1 intensity correlated to

expression levels, measured pre- and post-TVEC, revealed wide heterogeneity of expression throughout the tumor bed in patients with either aa complete response or residual gross tumor (**Figure 4-2D**). Representative FRET acquisitions are shown, highlighting changes in PD-L1 expression and PD-L1 donor:PD-1 acceptor interaction (**Figure 4-2E,**). While very recent publications have explored the interpretation of FRET values on this axis in the setting of immunotherapies, none have explored both pre- and post-treatment matched values, nor described the relevance of this functional receptor engagement in the draining lymph node. In our cohort, wide heterogeneity in FRET efficiency was also observed in both responders and non-responders but not explained by an increase in PD-L1 expression alone (**Figure 4-2D).**

4. <u>Immune Monitoring</u>

On-treatment shifts in immune cell populations and circulating cytokines were assessed by CYTOF analysis of cryopreserved PBMC or plasma Luminex, measured at baseline presentation, at 3 weeks post-induction dose (immediately prior to the first 10^8 dose), and at the time of surgical resection. Further, samples obtained from healthy controls were included for baseline population characterization. The gating strategy is shown in **Table 3-1**. Baseline immune cell characterization revealed differences in pre-treatment myeloid and T cell distribution (**Figure 4-3A**). An alternative gating strategy was used to explore and define the significant shift in post-treatment unlabeled populations, highly suggestive that these cells most closely represented an increase in immature dendritic cells; however, this could not be definitively confirmed within our immune marker phenotypes. While reports of population shifts at these early time points (3 weeks, 7 weeks) are limited, they indicate that, given the nature and time course of anti-viral immunity, these early time points demonstrate an overall degree of inflammatory response and cellular mobilization.[140]

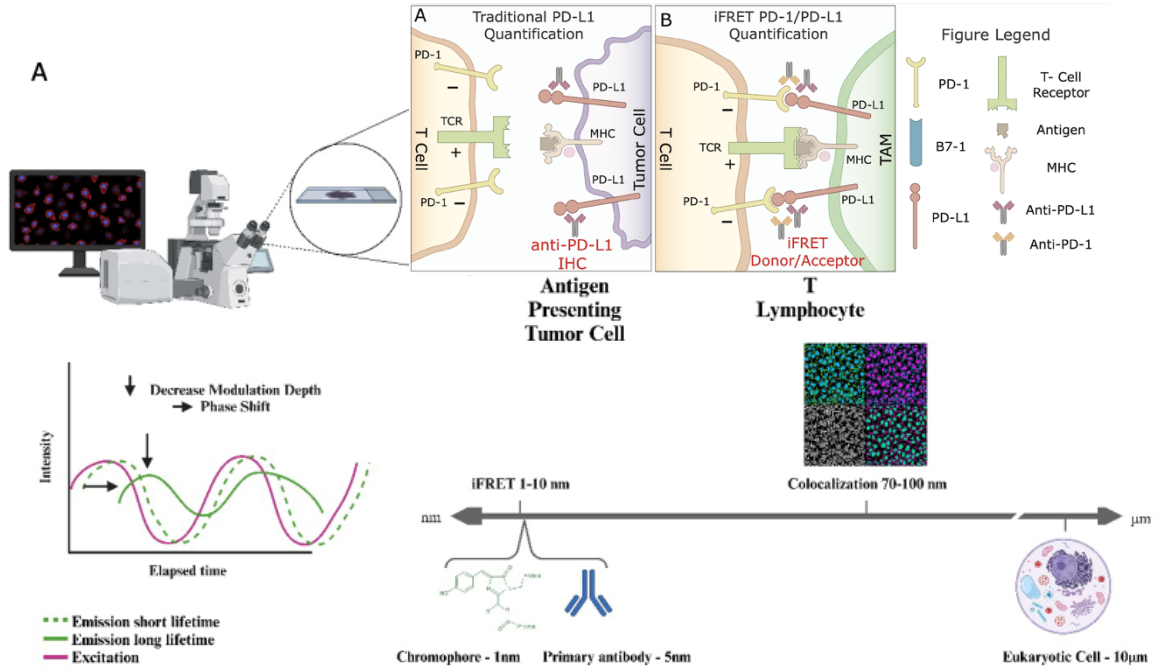
A
Traditional PD-L1 Quantification
PD-1
PD-L1
TCR
MHC
T Cell
Tumor Cell
anti-PD-L1 IHC
Antigen Presenting Tumor Cell
B
iFRET PD-1/PD-L1 Quantification
TAM
iFRET Donor/Acceptor
T Lymphocyte
Figure Legend
T- Cell Receptor
Antigen
MHC
B7-1
Anti-PD-L1
Anti-PD-1
Decrease Modulation Depth
Phase Shift
Intensity
Elapsed time
Emission short lifetime
Emission long lifetime
Excitation
iFRET 1-10 nm
Colocalization 70-100 nm
nm
µm
Chromophore - 1nm
Primary antibody - 5nm
Eukaryotic Cell - 10µm

B

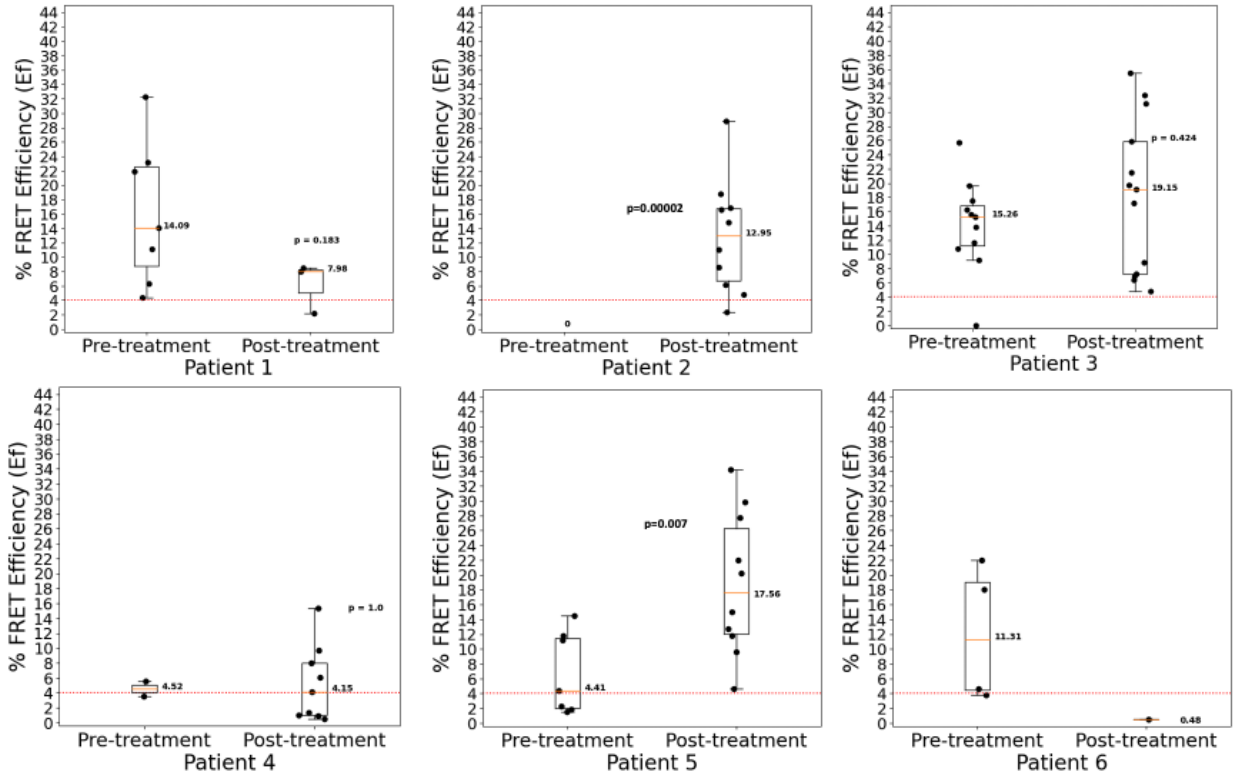
% FRET Efficiency (Ef)
Pre-treatment
Post-treatment
Patient 1
14.09
p = 0.183
7.98
Patient 2
p=0.00002
0
12.95
Patient 3
15.26
p = 0.424
19.15
Patient 4
4.52
p = 1.0
4.15
Patient 5
p=0.007
4.41
17.56
Patient 6
11.31
0.48

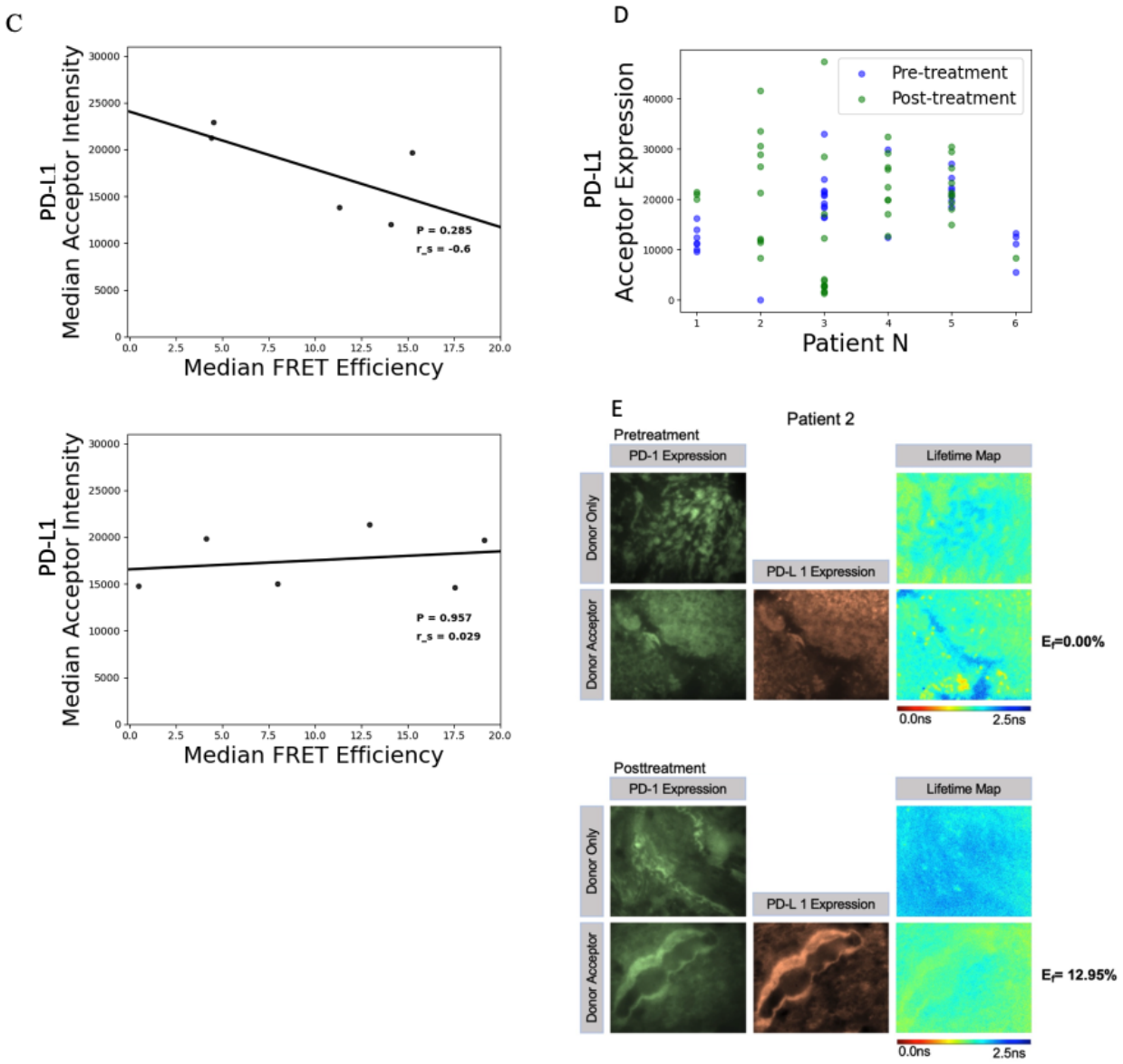

Figure 4-2. iFRET functional receptor analysis corresponds to treatment response, not PD-L1 expression A) iFRET schematic B) iFRET before and after TVEC treatment. Patients 2 and 5, complete responders, demonstrate low PD-L1/PD-1 engagement prior to therapy with strong engagement post-treatment. Patients 1 and 6 demonstrate strong engagement pre-therapy, diminished post-therapy. Patient 4, metastatic, with low engagement before and after therapy. C) PD-L1 ligand expression does not correlate to iFRET intensity D) PD-L1/PD-1 receptor expression changes before and after therapy. E) Representative acquisition images for Patient 2.

Overall, $CD8^+$ T cells in circulation minimally changed on therapy and a moderate overall decrease in $CD4^+$ T cells was observed (**Figure 4-3B**). Monocyte populations overall significantly decreased at 7 weeks; however, the monocyte phenotype revealed a decrease in classically activated monocytes with an increase in alternatively activated monocytes (**Figure 4-3C**). A transient peak in total DCs was observed after the first TVEC dose but returned to near baseline values at the post-treatment time points, and subset analysis detected increases in the population derived from myeloid DCs (mDCs) with corresponding decreases in circulating plasmacytoid DCs (pDCs) (**Figure 4-3D**). Both B cell and NK cell populations varied widely at baseline but demonstrated decreases throughout the first seven weeks of therapy (**Figure 4-3E, F**).

Figure 3.

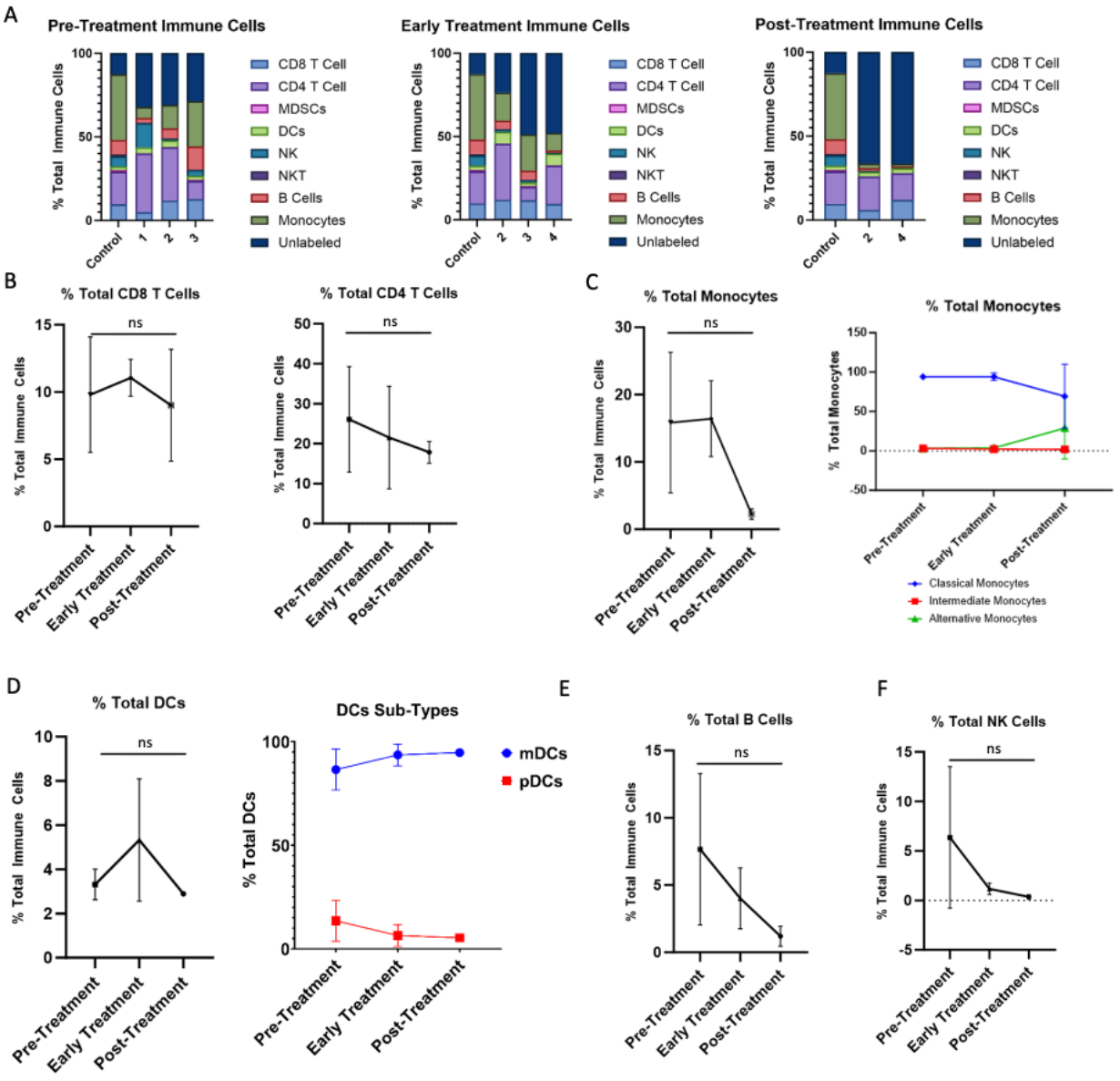

Figure 4-3 Total immune population changes over treatment course. A) Systemic immune shifts with TVEC therapy over 6 weeks therapy, early-on treatment collection was performed at 3 weeks post-loading dose, prior to first therapeutic dose. Post-treatment collection was performed at 7 weeks, at time at day of wide local excision and SLNB. Non-melanoma patient control and individual patient samples shown. B) $CD8^+$, $CD4^+$ T cell total population shifts C) Monocyte total population and subset shifts D) DCs and subsets E, F) Decrease in total B cells and NK cells.

5. Variability in Innate Systemic Response

Given the overall wide distribution of total population values in our study and previous reports, we aimed to dissect the variability in response between patients contributing to this heterogeneity as well as relative immune shifts per patient.[16, 141] Initial unique differences were most apparent in the myeloid and innate immune populations compared to healthy control (**Figure 4-4A,B**) and subsequent on-treatment population changes were divergent between responder and metastatic/non-metastatic non-responders (**Figure 4-4C**). Interestingly, Patient 2 was a responder with a starting PD-L1 score of 0/0% FRET, demonstrated a significant skew toward a classically-activated monocyte profile (88-90%) with decreases in alternatively-activated monocytes on therapy (0%, from 1% at baseline). Contrastingly, metastatic or non-responders presented with a similar starting profile (94% classically-activated) but heavily shifted toward an immunosuppressive profile on therapy with a decrease in classically-activated monocytes (55% post-treatment) and an increase in alternatively-activated monocytes (**Figure 4-4D**). Baseline myeloid-derived suppressor cells (MDSCs) also demonstrated wide distribution in starting values (34-53%) with a peak at early-therapy measurement followed by a subsequent drop, similar to the overall monocyte trends. However, individual patient trends demonstrated extremely low starting values for responder compared to metastatic, non-responder patients (**Figure 4-4F**).

Tissue level macrophage changes were subsequently evaluated to determine the relationship of the change in circulating myeloid phenotype to TAM infiltration and lymph node characterization. Complete and major responders demonstrated a significant skew toward starting with a M1-dominant TAM profile and significantly increased TAM recruitment at post-treatment assessment (**Figure 4-4E**). NK cell trends were also examined but no large variations in total populations or subset investigation of maturation and activation were detected. Divergences in NK cell response to therapy were only observed at the pre-treatment to early-on treatment shift with an increase in NK cells observed in the responding patient (1.1 to 1.5%) with

a subsequent decrease by 7 weeks (0.5%) in range with overall patient shifts (6% to 1.2% to 0.4%, all patients) (**Not shown)**).

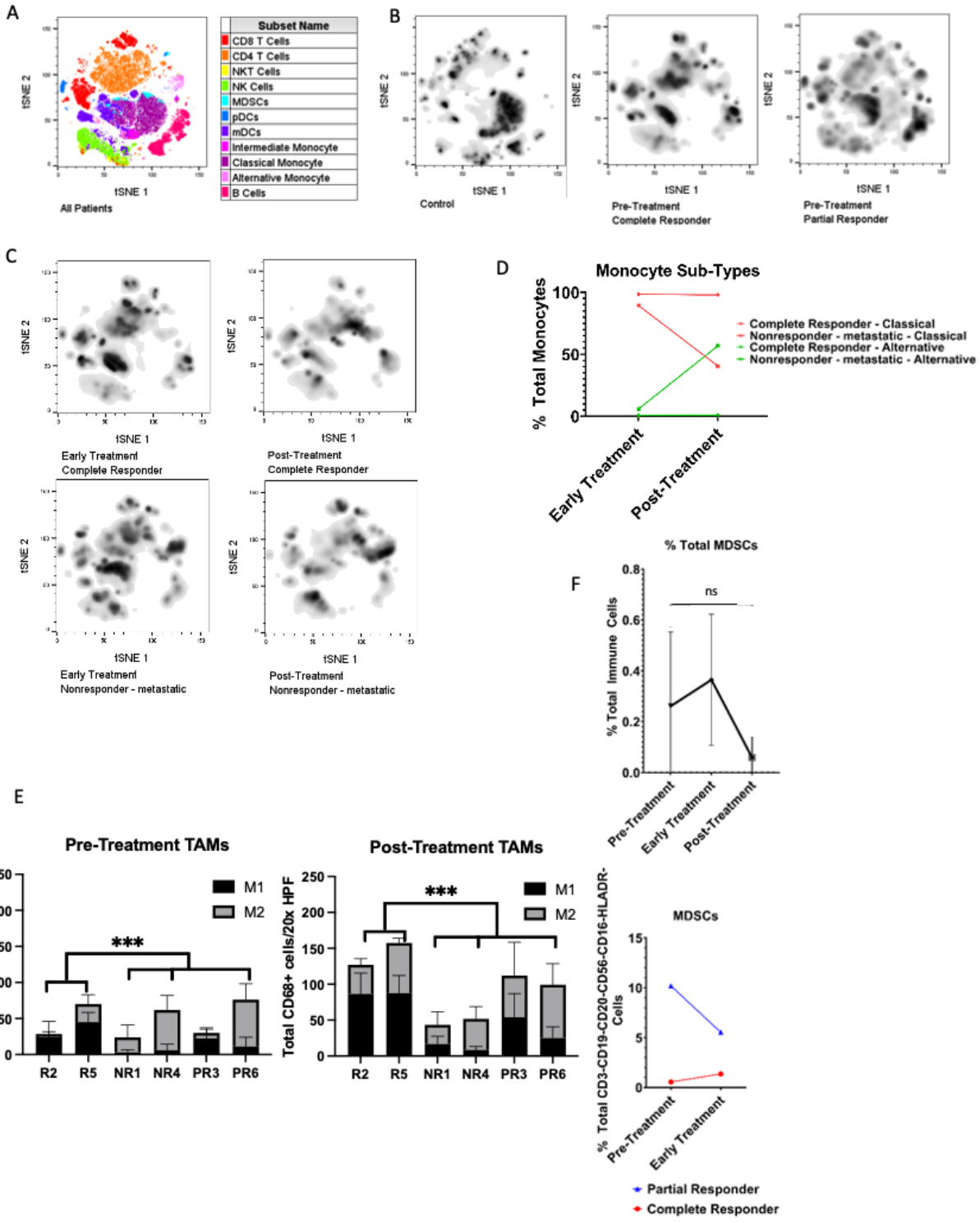

G

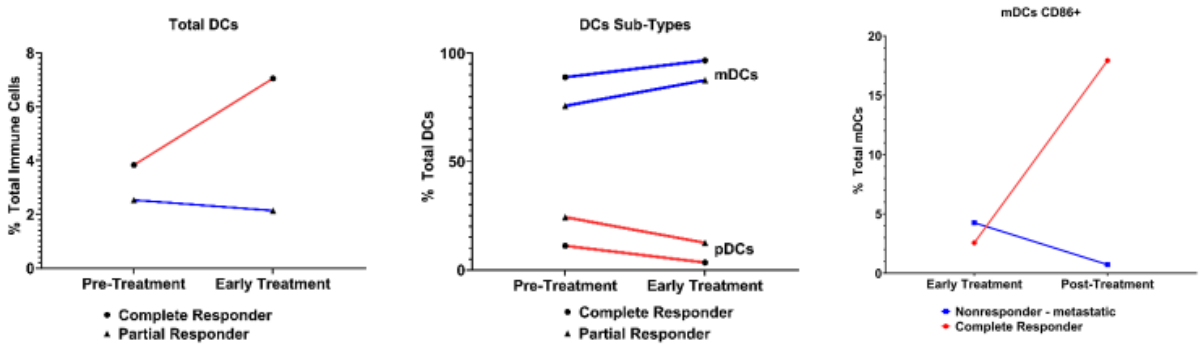

Figure 4-4 Immune cell subset shifts with TVEC therapy differ amongst responders, non-responders, and metastatic disease. A) tSNE representation of circulating immune cell phenotypes with (B) Pre-treatment baseline cell population differences in control and patients with melanoma, and C) Differences in shifts in responder vs. partial responder or metastatic (non-responder) early on-treatment time point, and at post-treatment time of surgery. D) Classically and alternatively activated monocytes demonstrate uniquely variable and opposing shifts after treatment. E) TAM phenotype significantly differs in complete responder Patients 2 and 5 versus non-responder with greater M1 infiltrate and increased macrophage recruitment in post-treatment specimen. F) MDSC populations decrease on therapy in overall population with directional differences observed by response. G) Total DC changes are not reflected in conventional plasmacytoid or myeloid populations, with differences observed in activated DC population.

Chapter 5: Macrophage-Dependent Synergy of AXL Tyrosine Kinase Inhibition with Anti-PD-1 Therapy

AXL has emerged as a molecular target of interest due to its involvement in both malignant behavior by tumor cells and its critical role in immune regulation. However, understanding of its role and potential therapeutic impact in melanoma remains poorly understood. AXL expression has been associated with resistance to targeted therapies and immunotherapies, making it a potential target for novel treatment strategies. However, the prevalence and activity of AXL is variable between cancer types and may also be stage-dependent or tissue-specific. In particular, AXL is conventionally associated with regulatory immune function, and M2-like behavior is conventionally attributed to AXL-expressing macrophages. Reciprocally, AXL inhibition in many tumor models is associated with macrophage depletion and polarization toward M1-like behavior. However, the evolution of single-cell sequencing has demonstrated that the binary classification of M1/M2 type macrophages is highly limited with many M1-like and M2-like markers expressed in transitional states with highly plastic functions. Moreover, as a promiscuous molecule in the TiME, effects of AXL inhibition in tumors as well as its utilization as a biomarker for therapeutic selection are challenged. Here, the role of AXL specifically in immunotherapy-resistant melanoma and TAM function was explored in an effort to contextualize rationale for targeting AXL to rescue ICB-refractory melanoma. First, the current clinical landscape of AXL in melanoma was explored in an effort to better define the prevalence and biology of AXL in patients with melanoma given the mixed results of clinical trials assessing AXL inhibition. Second, ICB-resistant melanoma cell models were used to characterize various aspects of AXL function, including phagocytosis, efferocytosis, cytokine expression, PD-L1:PD-1 modulation, and tumor behavior.

1. The Clinical Landscape of AXL Expression in Melanoma

Warfarin has been shown to reduce cancer risk via vitamin K-related AXL TK inhibition. Although AXL has been implicated in disease progression and therapy resistance in preclinical

models, there are no clinical studies evaluating the impact of warfarin on melanoma prognosis. To evaluate the relationship between warfarin and survival in melanoma, a retrospective population-based cohort study of patients with melanoma aged ≥65 years diagnosed between 2009-2013 was conducted from the Surveillance, Epidemiology, and End Results-Medicare database. Patients were grouped according to warfarin therapy 6 months prior to and after melanoma diagnosis. Univariable and multivariable Cox proportional hazards models were used to compare OS and melanoma-specific survival (MSS) between groups. Overall, 10,778 patients with invasive melanoma were included. Of these, 13.2% were prescribed warfarin, with atrial fibrillation being the most common indication (74.1%) (**Table 5-1**).[142] Warfarin prescription was associated with older age, male sex, and a greater number of comorbidities (all p<0.001). Patients prescribed warfarin more frequently presented with ulceration, T3 and T4 disease, and Stage II disease (all p<0.05). In order to control for comorbid indications requiring anticoagulation treatment that may negatively impact predicted survival, patients maintained on prophylactic anticoagulation for atrial fibrillation were examined as a controlled cohort. Warfarin prescription was associated with longer MSS and OS in multivariable models (MSS adjusted hazard ratio [aHR] 0.72, 95% CI 0.54-0.96, p=0.02; OS aHR 0.88, 95% CI 0.79-0.99, p=0.04) (**Figure 5-1**).[142] These findings highlight the potential for vitamin K-related pathways to impact cancer-specific activity.

Table 5-1. Baseline demographics of patients with melanoma relative to warfarin usage[142]

	Warfarin prescription N=1418		**No warfarin prescription** N=9360		
Demographics	N	(%)	N	(%)	P value
Age (mean, SD)	78.8	(7.2)	76.2	(7.6)	<0.01
Sex					
Female	422	(29.8%)	3770	(40.3%)	<0.01
Male	996	(70.2%)	5590	(59.7%)	
Race					
White	1377	(97.1%)	8927	(95.4%)	<0.01
Other*	41	(2.9%)	433	(4.6%)	

Charleson Comorbidity Index (mean, SD)	1.9	(1.9)	1.1	(1.5)	<0.01
Atrial fibrillation	1051	(74.1%)	824	(8.8%)	<0.01
Pulmonary embolism	90	(6.3%)	30	(0.3%)	<0.01
Deep vein thrombosis	126	(8.9%)	51	(0.5%)	<0.01

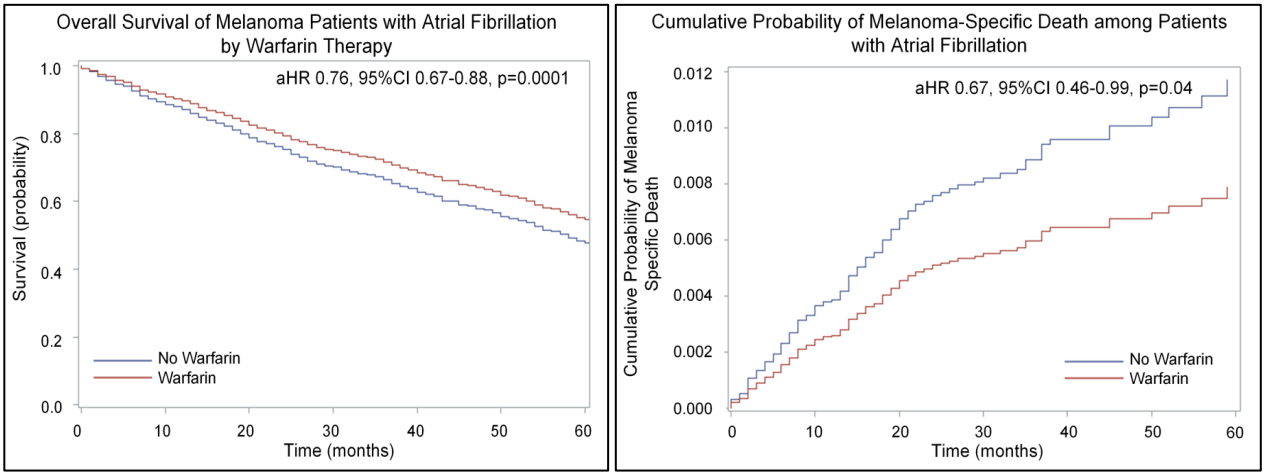

Figure 5-1. The clinical landscape of AXL in melanoma. A) Warfarin, inhibitor of vitamin-K dependent proteins, such as the AXL ligand Gas 6, is associated with improved melanoma-specific survival. B) Melanoma-specific death is reduced in the setting of warfarin usage.[142]

Next, the association of AXL TK with melanoma survival was examined using the The Cancer Genome Atlas (TCGA)- skin cutaneous melanoma (SKCM) dataset, we found compelling evidence of a significant relationship between AXL expression levels and patient survival outcomes. Kaplan-Meier survival curves were stratified by mean AXL expression, with higher AXL expression correlating with improved OS (**Figure 5-2A**). Overall, AXL expression in this dataset trended in line with changes in inflammatory markers, such as PD-L1 and macrophage-specific proteins, as opposed to T cell signatures or tumor-specific markers (**Supplement X**). Patients with melanoma seen at the UC Davis Comprehensive Cancer Center were screened for circulating levels of soluble AXL (sAXL), as elevated circulation of the cleaved portion of the receptor has been reported to be a potential biomarker of advanced disease in other tumor types (**Figure 5-2B**). Elevated sAXL significantly correlated to advanced disease stage with the highest levels observed in patients with Stage IV disease. These findings

suggest that AXL in melanoma may be somewhat paradoxical with AXL expression being favorably representative of robust inflammatory response in tumors or PD-1 resistant, mesenchymal or immunosuppressed tumor types, complicating its potential as a stand-alone biomarker.

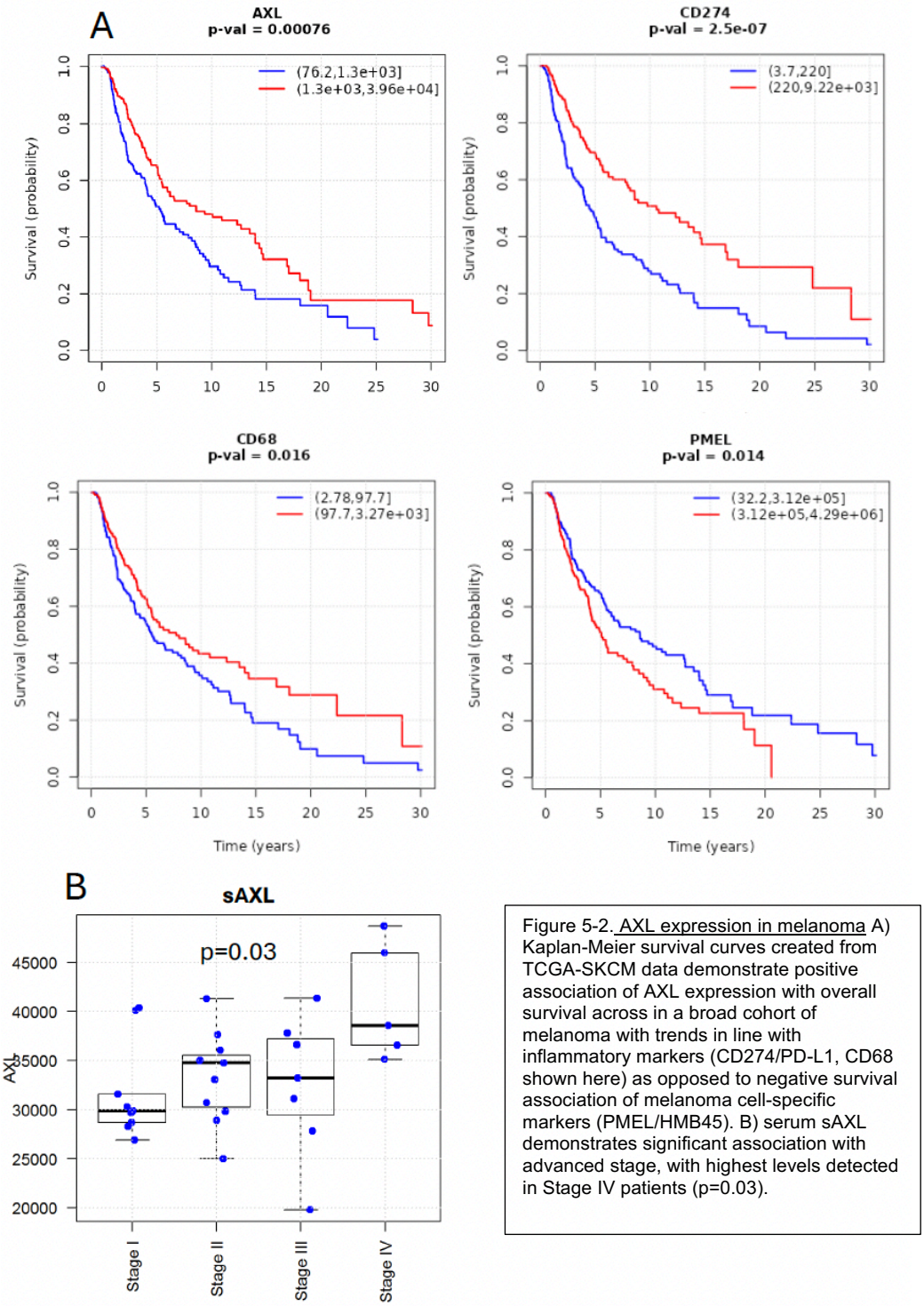

Figure 5-2. AXL expression in melanoma A) Kaplan-Meier survival curves created from TCGA-SKCM data demonstrate positive association of AXL expression with overall survival across in a broad cohort of melanoma with trends in line with inflammatory markers (CD274/PD-L1, CD68 shown here) as opposed to negative survival association of melanoma cell-specific markers (PMEL/HMB45). B) serum sAXL demonstrates significant association with advanced stage, with highest levels detected in Stage IV patients (p=0.03).

Available single cell data sets (GSE115978, GSM6022254) were then examined for contextualization of cell type-specific AXL expression in melanoma in therapeutically challenging tumor types (e.g. melanoma brain metastases (MBM) and PD-1-resistant melanoma) (**Figure 5-2B**). Previously reports from Jerby *et al*. (GSE115978) data demonstrated AXL expression in tumor cells to be associated with mesenchymal programming and anti-PD-1 resistance.[123] However, in both tumor types, AXL was only expressed in a small subset of tumor cells with the predominant AXL expression found in TAMs. However, TAM and immune profiles in relationship to PD-1 resistance were not previously reported. Multiple immune cell types demonstrated AXL expression in the TiME, such as DCs and NK cells. Interestingly, it was observed that AXL was strongly expressed in a subset of $CD4^+$ T cells, which has not been previously reported, but was consistently present in all examined datasets (**Figure 5-3A, B**).

Among TAMs, AXL expression was found to be equally present in M1-like (CD80/86+, TNF^+, MHC class II) and M2-like macrophages ($CD206^+$/$MRC1^+$, $CD163^+$, $IL\text{-}10^+$, $VEGF^+$). Importantly, the predominant expression of PD-L1 in melanoma tumors was also by TAMs, opposed to tumor cells. However, AXL expression was significantly linked to PD-L1 expression across cell types (**Figure 5-4A**). To interrogate this ambiguity further, all available peer-reviewed single cell datasets in melanoma were synthesized using Harmony to interrogate the relevance of AXL-related protein expression across the diverse biogeographic landscape in melanoma in an effort to distinguish the predominantly conserved macrophage types by function in relationship to AXL expression. The extended reporting of this work is ongoing in analysis; however, the broader dataset validated our findings in PD-1-resistant melanoma and MBM that AXL^+ tumor cells remained a very small subset of disease, with macrophages and cancer-associated fibroblasts (CAFs) representing the major sources of AXL activity in the TiME (**Figure 5-4B**). GAS6 ligand, conventionally thought to be the dominant activating ligand of AXL, was also identified throughout TiME cells in TAMs, CAFs, endothelial cells, and B cells but, surprisingly, virtually none was detected among tumor cells. Alternatively, there is emerging evidence that prior

descriptions of other class ligands being limited in relevance of AXL activity may have significantly underappreciated the potential of PROS1-AXL associated signaling. Here, PROS1 was found to be an abundant protein in tumor and stromal cells and examination of cell chat features is ongoing to discern inflow and outflow amongst cells expressing these features. We hypothesize that further clinical development of AXL inhibitors may require deeper classification of AXL activity, including co-receptor and co-ligand complexing, in the TiME to understand if targeting of macrophage-driven AXL activity represents a rational combination strategy, agnostic of tumor cell activity, or if anti-PD-1 resistance is driven by the aggressive tumor behaviors associated with AXL activation in tumor cells.

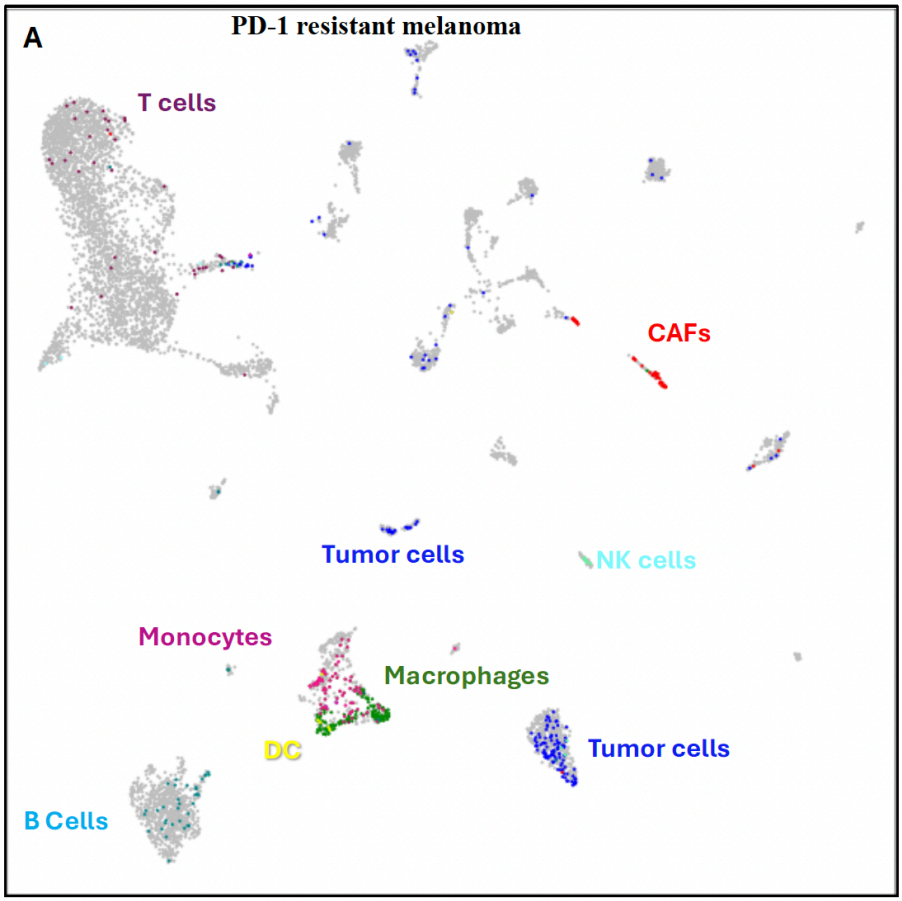

Cell Type	AXL+	AXL-
Tumor	112	1906
Macrophage	181	239
Dendritic Cell	23	95
NK	1	29
CAF	59	47
CD8	41	1718
CD4	27	829

B AXL family receptors and ligands in Brain TiME

Melanoma TiME Gene Expression By Cell Type	Cell Count	AXL	Gas6	MERTK	PROS1	TYRO3	PDCD1	CD274
Melanoma	2770	0.11	0.07	0.31	0.08	0.27	0	0
T Cells	236	0.06	0.02	0.1	0.03	0	1.24	0.08
Macrophages	2483	2.07	1.29	4.49	0.2	0.01	0.02	0.06
Dendritic Cells	118	0.98	0.97	1.95	0.18	0	0.03	0.23
PD1 Expressing Cells	148	0.55	0.29	1	0.08	0.02	2.44	0.08
PDL1 Expressing Cells	221	1.24	0.5	1.77	0.07	0.06	0.06	1.16

Figure 5-3. AXL expression and cellular association in advanced melanoma A) Single cell sequencing of anti-PD-1 refractory melanoma, Uniform Manifold Approximation and Projection (UMAP) and quantification of AXL positivity (expression >1) by cell type demonstrates predominant expression in the TiME by TAMs with <10% of tumor cells demonstrating significant AXL expression. B) single cell sequencing of untreated melanoma brain metastases shows AXL family receptors, ligand and PD-1/PD-L1 expression by cell type with high AXL TAM expression and by PD-L1 expressing cells

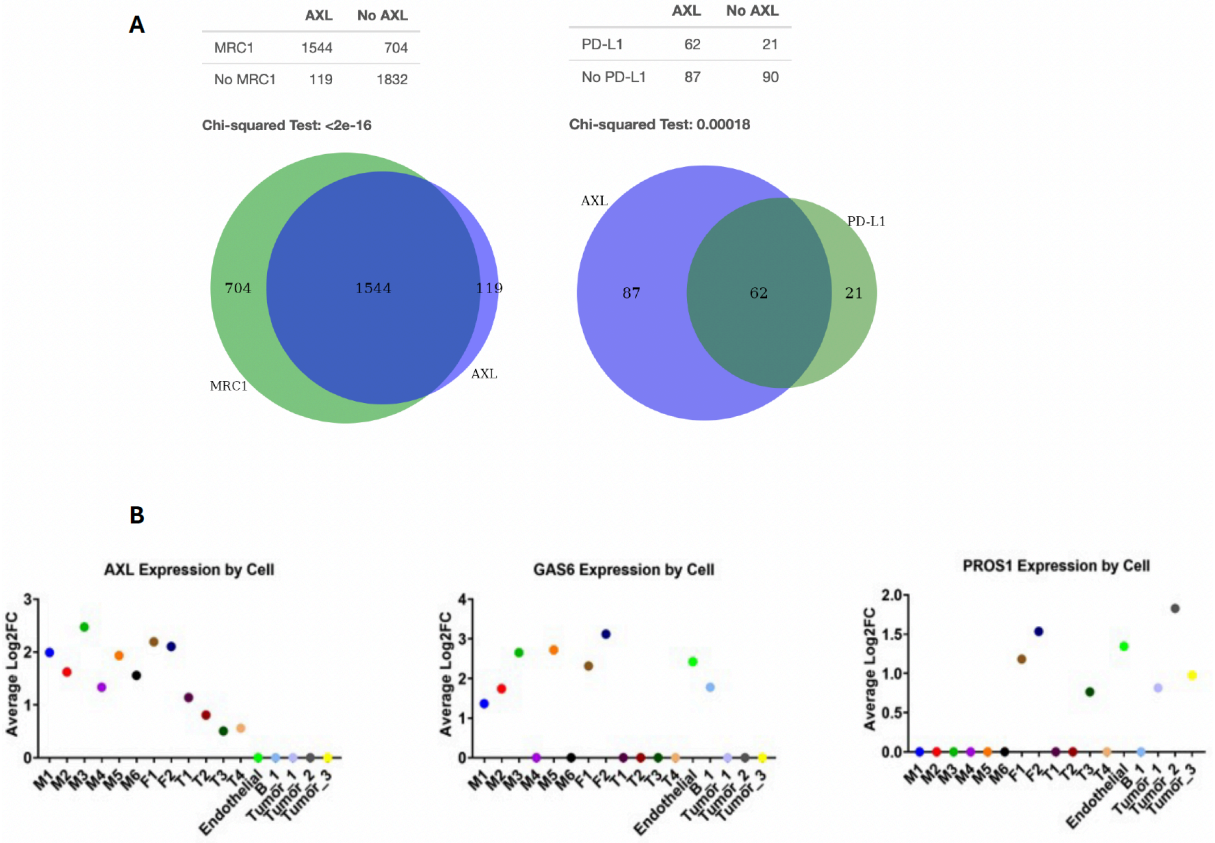

Figure 5-4. Diversity of AXL family receptor and ligands expression in the melanoma TiME A) Single cell interrogation of macrophage polarization reveals equal AXL expression by M1-like and M2-like TAMs in the TiME (MRC1/CD206 M2-like expression shown) and significant correlation to PD-L1 expression. B) Cluster analysis from combined datasets across melanoma biogeography confirms predominant AXL source in macrophages and fibroblasts, previously unreported expression by $CD4^{+}$ T cells, and presence of alternative ligand, PROS1, on tumor cells.

2. AXL Inhibition in Models of Anti-PD-1-Resistant Melanoma

Melanoma models known to be resistant to PD-1 therapy, YUMM1.7 and B16F10 mouse melanoma lines, and the anti-PD-1-sensitive cell line YUMMer1.7 were screened for AXL expression by western blot and tested *in vitro* for AXL functional activity. YUMM1.7, B16F10, and B16F10-LN6 demonstrated high AXL expression, while YUMMer1.7 lines expressed minimal AXL levels (**Figure 5-5A**). AXL activation was measured by p-AXL expression and demonstrated minimal increases in basal p-AXL levels with addition of GAS6. However, p-AXL levels were diminished in the setting of warfarin exposure (**Figure 5-5B**). Direct impact of AXL inhibition on tumor cell behavior *in vitro* was measured by migration assay, given the association of AXL in

melanoma and other cancer cells with mesenchymal features, such as motility and invasive capacity. Migration was significantly increased with GAS6 incubation, which was inhibited when combined with warfarin (**Figure 5-5C**).

In vivo testing was then performed using the syngeneic C57/Bl6 subcutaneous mouse model with multiple strategies of AXL inhibition to examine the impact of ligand targeting with warfarin versus receptor inhibition with the AXL-specific small molecule inhibitor, bemcentinib, or multi-TKI (AXL, VEGF, X) cabozantanib as single agents or in combination with invivomab anti-PD-1 therapy. Given prior reports of biphasic AXL expression in tumor initiation versus tumor invasion and metastasis, warfarin was administered either prior to tumor inoculation or after establishment of tumors and continued for 21 days. There were no differences in tumor sizes between the treatment groups, with similar sizes observed throughout the treatment course. At the time of sacrifice, both warfarin-treated groups demonstrated significant reduction in tumor burden compared to control mice (**Figure 5-5D, E).**

Next, B16F10, and YUMMer1.7 cells were implanted subcutaneously to examine survival impact of warfarin therapy and to explore host versus tumor cell-specific impacts of AXL inhibition. Final tumor weights were not significantly different between treatment arms in B16F10, however, survival was modestly, but significantly, extended for warfarin-treated animals ($p=0.04$)(data not shown). However, YUMMer1.7 cells, an established immunotherapy-sensitive and AXL^- cell line, demonstrated natural regression at approximately day 14 after initial establishment of 50 mm^3 tumors in most animals (n=14/20). At Day 100 post-injection, only 1/20 animals demonstrated measurable tumor, consistent with other reports that YUMMer1.7 can be highly variable with some models indicating complete tumor regression, such as ours (data not shown).

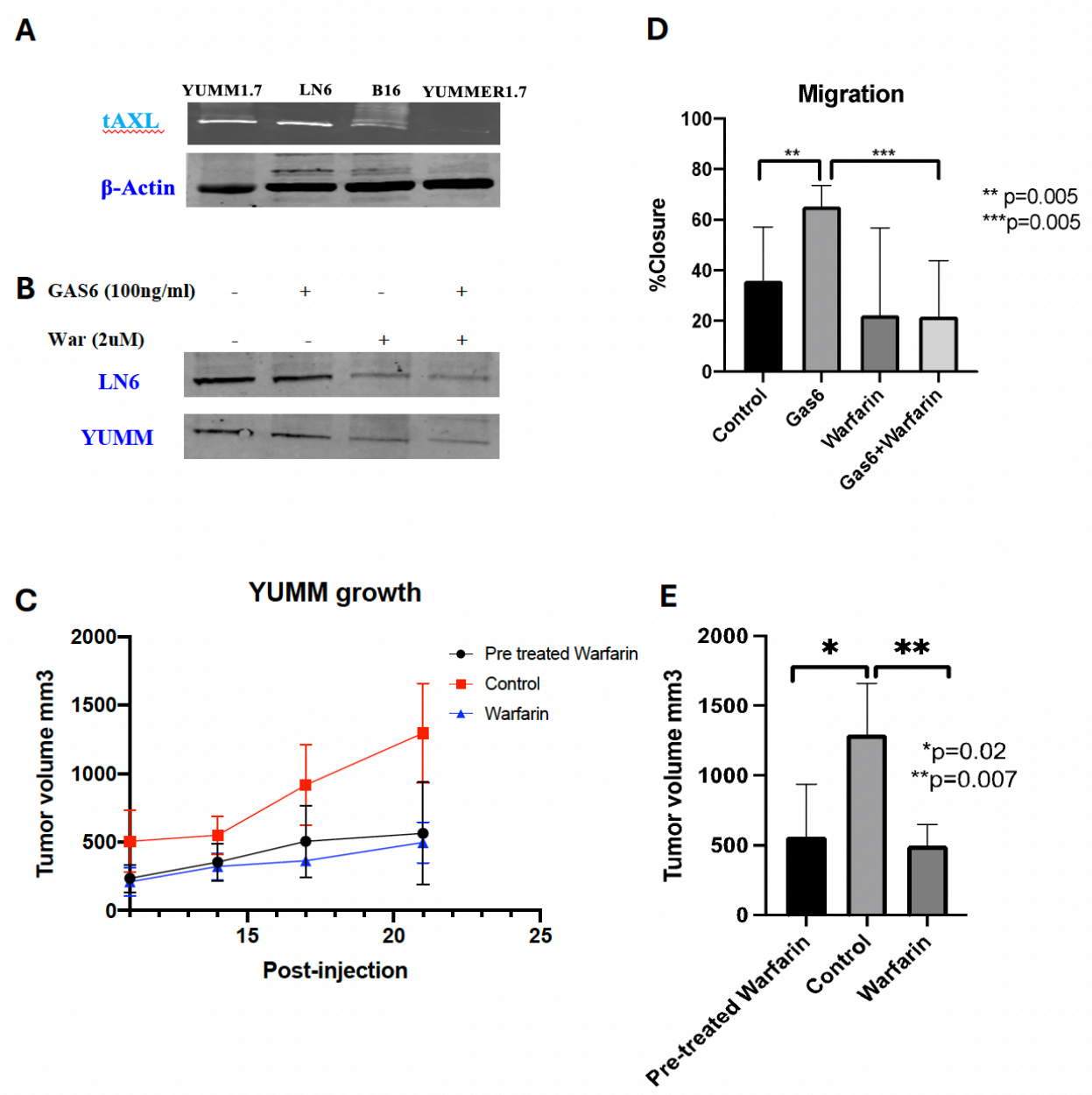

Figure 5-5. AXL targeting in anti-PD-1-resistant melanoma. A) Melanoma cell lines were screened for baseline AXL expression *in vitro*, revealing higher expression in anti-PD-1-resistant models with B) inhibition of p-AXL with warfarin exposure *in vitro*. C) Migration of YUMM1.7 cells was significantly stimulated by GAS6 (p=0.02) and inhibited by warfarin 2 μM (p=0.007). D) Mice (n=6/group) were pretreated with warfarin for 7 days prior to subcutaneous injection of YUMM1.7 tumor cells versus randomized to therapy with warfarin (500 nM supplied in drinking water) after establishment of tumors (>150 mm^3). No differences in tumor size were observed between warfarin administration before or after tumor establishment with both treatment groups demonstrating significant tumor growth reduction ($p<0.05$).

3. AXL Inhibition Augments Anti-PD-1 Therapy

Multiple strategies of AXL inhibition were tested in the YUMM1.7 syngeneic mouse model as single agent, or in combination with anti-PD-1 therapy using warfarin (500 nM), bemcentinib (50 mg/kg), and cabozantinib (30 mg/kg) (**Figure 5-6A**). YUMM1.7 tumors were not significantly controlled by anti-PD-1 therapy, consistent with prior reports. Warfarin and cabozantinib, as single agents, significantly reduced tumor size compared to control ($p<0.05$); however, reduction in tumor size for bemcentinib alone was not significant (**Figure 5-6B,C**). Combination therapy with AXL and PD-1 inhibition yielded the smallest tumors. However, when compared to either single agent AXL inhibitor or anti-PD-1 therapy, only warfarin-treated tumors or bemcentinib combination with anti-PD-1 therapy demonstrated significant reduction compared to anti-PD-1 monotherapy ($p<0.05$) (**Figure 5-6B**). There was no observed difference between combination therapy vs warfarin single agent therapy.

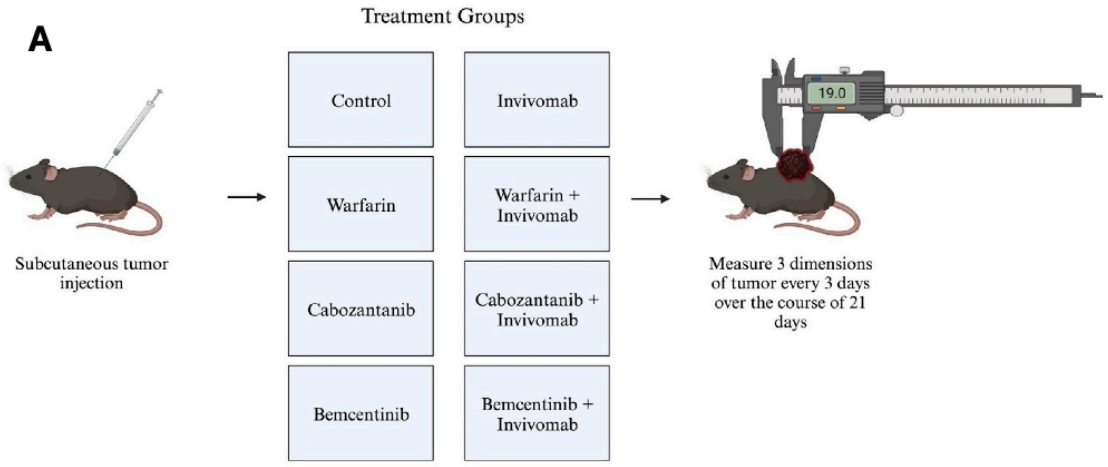

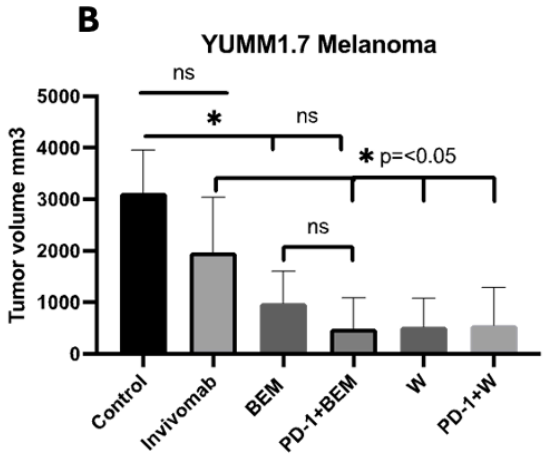

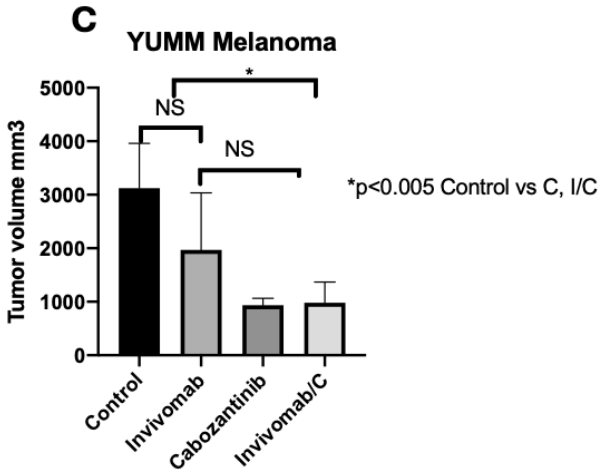

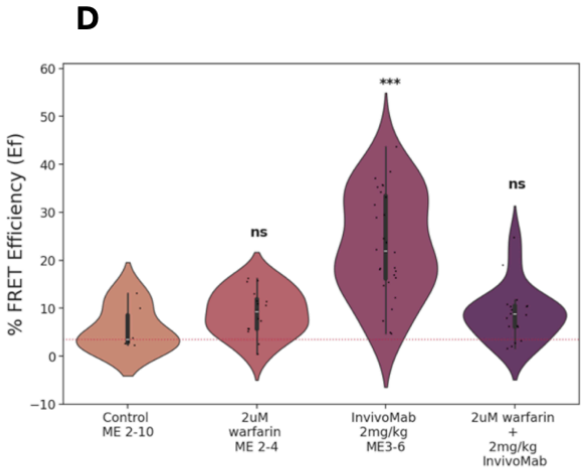

P (Control ME 2-10/ warfarin ME 2-4) = 0.15
P (Control ME 2-10/ InvivoMab ME3-6) = 1e-04
P (Control ME 2-10/ Warfarin +Invivomab) = 0.31

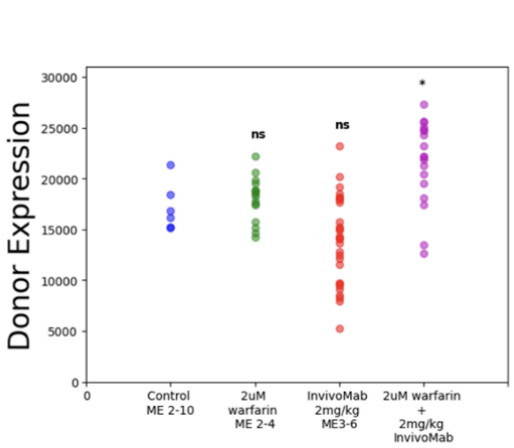

p (Control ME 2-10/ warfarin ME 2-4) = 0.449
p (Control ME 2-10/ InvivoMab ME3-6) = 0.053
p(Control ME 2-10/InvivoMab ME3-6+Warfarin +Invivomab) = 0.018

Figure 5-6. AXL inhibition synergizes with anti-PD-1 therapy A) Schematic of mouse model of anti-PD-1-resistant melanoma and therapeutic groups, n=5/group. Warfarin and bemcentinib treatment groups were performed in triplicate. B) AXL-targeted strategies were effective as single agent therapy and in combination with PD-1 therapy ($p<0.05$). C) AXL-inhibiting multi-TKI cabozantinib demonstrated similar tumor control as single agent and in combination. D, E) PD-L1:PD-1 checkpoint interactive state, measured by mean iFRET efficiency in YUMM1.7 melanoma tumors, demonstrates dynamic shift in PD-L1:PD-1 engagement in the setting of warfarin therapy with highest iFRET values observed with anti-PD-1 therapy ($p<0.001$). PD-L1 donor protein was significantly increased in combination anti-PD-1 and warfarin treatment; however, the iFRET value confirmed this increased expression was minimally interactive, with iFRET efficiency values remaining low ($p=0.018$)

We next aimed to determine the functional interactive state of immune checkpoint ligand:receptor engagement by measuring iFRET efficiency across the PD-L1:PD-1 complex. Control tumors demonstrated minimal regions of functional interaction (median iFRET efficiency <4%), whereas warfarin monotherapy groups demonstrated median efficiency of 10%. Anti-PD-1-treated tumors demonstrated the highest iFRET values, with a significant increase at a median of 21% ($p<0.001$). Combination therapy-treated tumors demonstrated iFRET efficiency values similar to single agent warfarin, with significant changes to the receptor interactive state in the presence of dual agent therapy versus single agent anti-PD-1 (**Figure 5-6D**). By contrast, PD-L1 (iFRET donor protein), was not significantly altered among groups, with the highest median values detected in combination-treated tumors. This aligns with prior reports that PD-L1 expression does not directly correlate with measurements of interactive state and dual agent therapy impacts ligand:receptor binding and function without significant, direct changes to ligand expression in the TiME (**Figure 5-6E**).

4. TiME Shifts with AXL and PD-1 Inhibition

Tumors from mouse treatment models were examined by flow cytometry for T cell populations (CD4, CD8), AXL expression, and myeloid constitution ($F480^+$ TAMs, M1-like phenotype, M2-like, AXL^+TAMs, and DCs). Overall, tumors demonstrated heterogeneity in populations within groups and no significant differences were observed in total T cell ($CD3^+$) or $CD8^+$ and $CD4^+$ T cells (**Figure 5-7A**). Given that aberrant T cell differentiation within tumors and tertiary lymphoid structures has been reported, we also examined double positive and double negative populations

and did not find any significant differences (not shown). AXL^+ cells represented a small population of total tumor cells with a small decrease in the AXL^+ population in the group treated with combination warfarin therapy versus those treated with anti-PD-1 monotherapy only (p=0.05) (**Figure 5-7B**). $F4/80^+$ TAMs were overall reduced in all treatment groups, but not significant compared to control (p=0.06). Unlike reports in previous preclinical models, the TAM profile was not significantly altered, and we observed no differences in M1-like ($F4/80^+CD86^+$), M2-like ($F4/80^+CD206^+$), or AXL^+ TAMs ($F4/80^+AXL^+$) (**Figure 5-7C**).

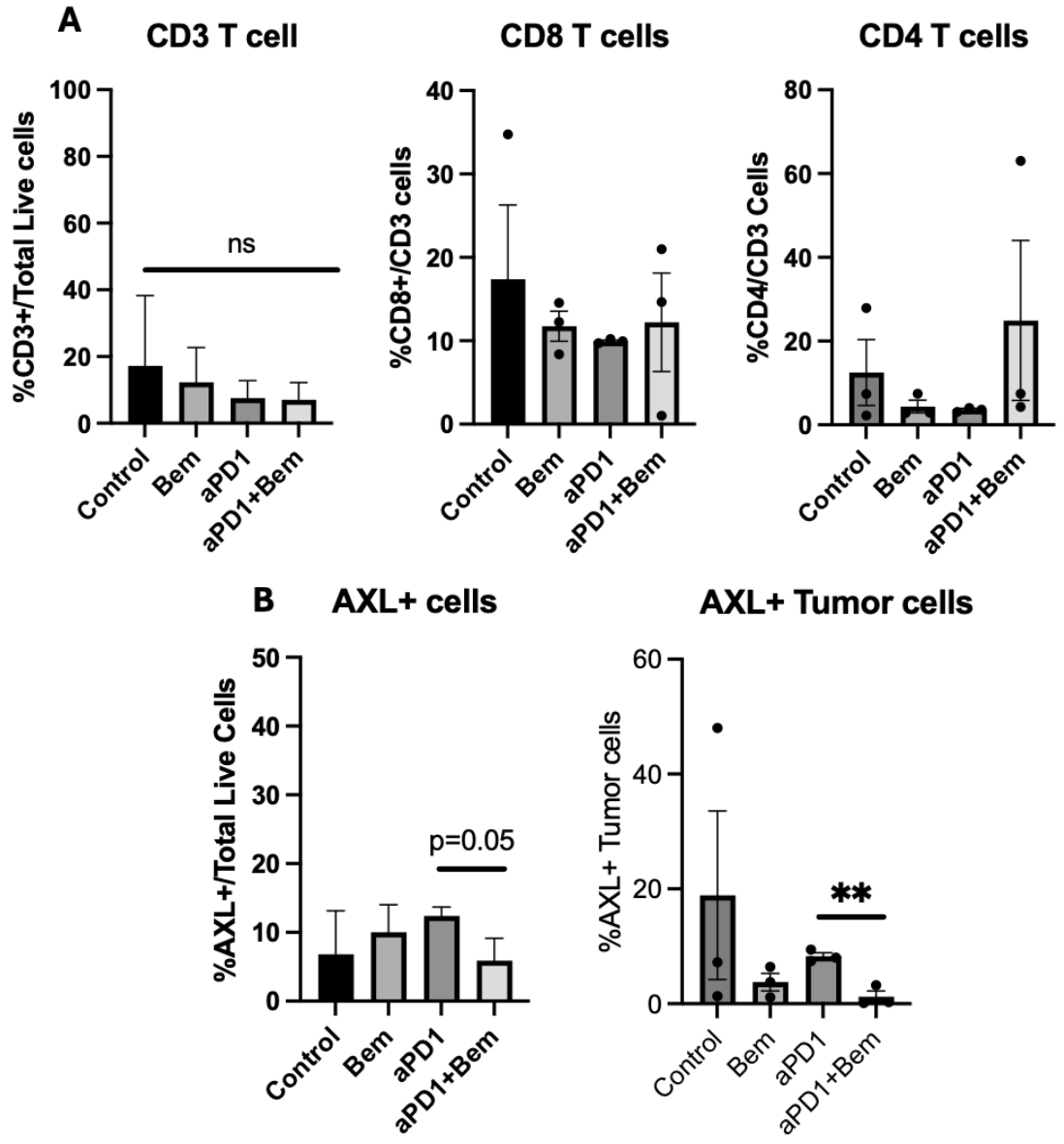

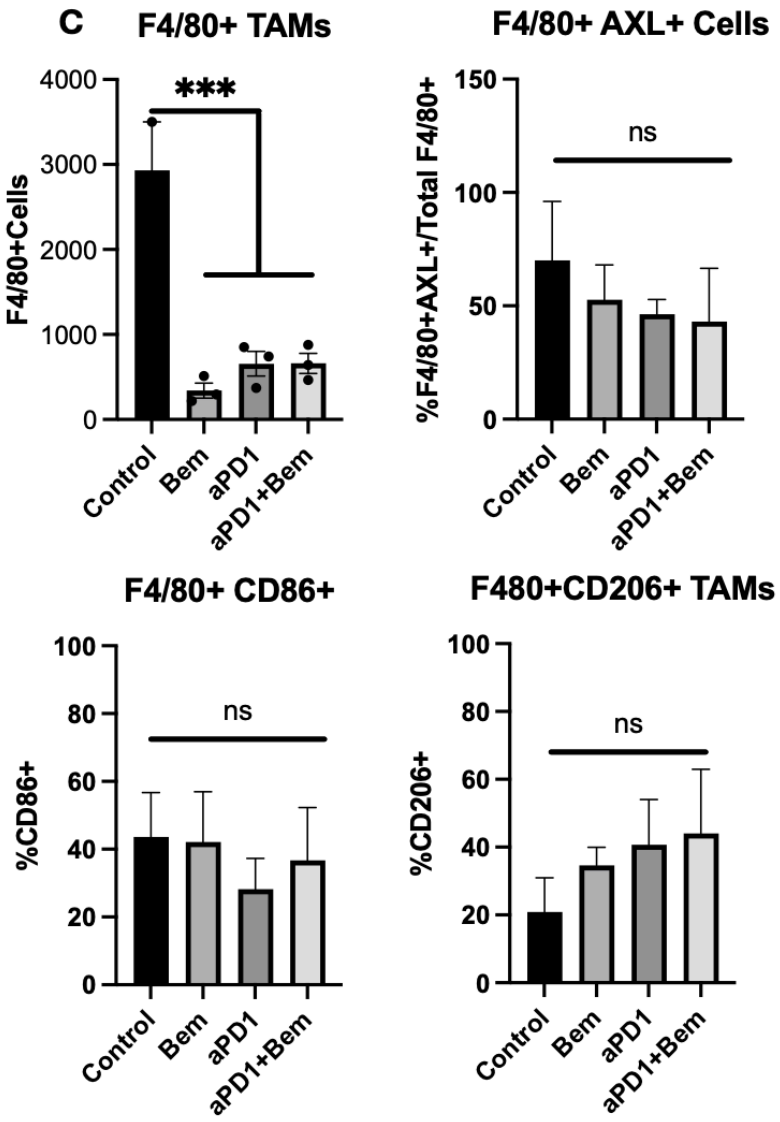

Figure 5-7. TiME shifts with AXL and PD-1 inhibition A) No significant differences were observed among treatment in total CD3 T cells, $CD8^+CD3^+$ T cells, or $CD4^+CD3^+$ T cells following administration of bemcentinib (Bem), aPD1 (anti-PD-1 Invivomab), or combination therapy Bem+aPD1. B) Diminished AXL^+ cell population was observed with combination therapy only in terms of both a decreased total AXL^+ cell population ($p=0.05$) and AXL^+ tumor cells ($p<0.01$). C) Global TAM depletion was observed in all treatment groups; however, AXL^+ TAMs ($F4/80^+$ cells) were not significantly altered. Overall differences in M1-like or M2-like phenotype among therapeutic groups were not significantly different or changed from control populations among the residual TAM population.

5. Selective Depletion of TAMs Impacts Anti-AXL-mediated Inhibition of Tumor Growth

It has been suggested that the preexisting immunosuppressive tumor profile may impact response to anti-PD-1 therapy and that a metronomic approach to therapy to correct the microenvironment

may sensitize to anti-PD-1 therapy. To determine the impact of TAM-targeting on response to anti-PD-1 therapy and AXL-related macrophage-specific activity in the TiME, we employed two models of macrophage depletion. First, anti-CSF1R targeting antibodies were administered prior to tumor inoculation to examine pan-myeloid depletion of bone marrow-derived macrophages (BMDM) followed by an identical therapeutic approach as described for control becentinib experiments. Second, growing evidence suggests that TAMs may initially heavily represent tissue-resident phenotypes that are capable of self-replenishing with BMDM that skew predominantly toward the M2 phenotype. As such, an F4/80-targeting antibody was utilized to deplete TAMs at the end-target tissue level prior to tumor injection (**Figure 5-8A**). CSF1R-depleted mice had significantly increased tumor growth at baseline compared to untreated mice (**Figure 5-8B**). There were no differences in tumor sizes between treatment groups in the setting of the CSF1R depletion strategy (**Figure 5-8B**). Due to the significantly increased growth in the setting of CSF1R depletion, animals required early sacrifice (Day 9 of therapy) and were not compared to final tumor weights of non-depleted animals. Alternatively, F4/80 depletion did not impact tumor sizes in mice in the control or anti-PD-1 monotherapy treatment groups. However, F4/80 depletion sensitized to bemcentinib monotherapy with a significant reduction in tumor growth compared to control ($p<0.01$). Further, there was a significant reduction in tumor growth in mice treated with combination therapy compared to anti-PD-1 monotherapy ($p<0.05$) **(Figure 5-8C**).

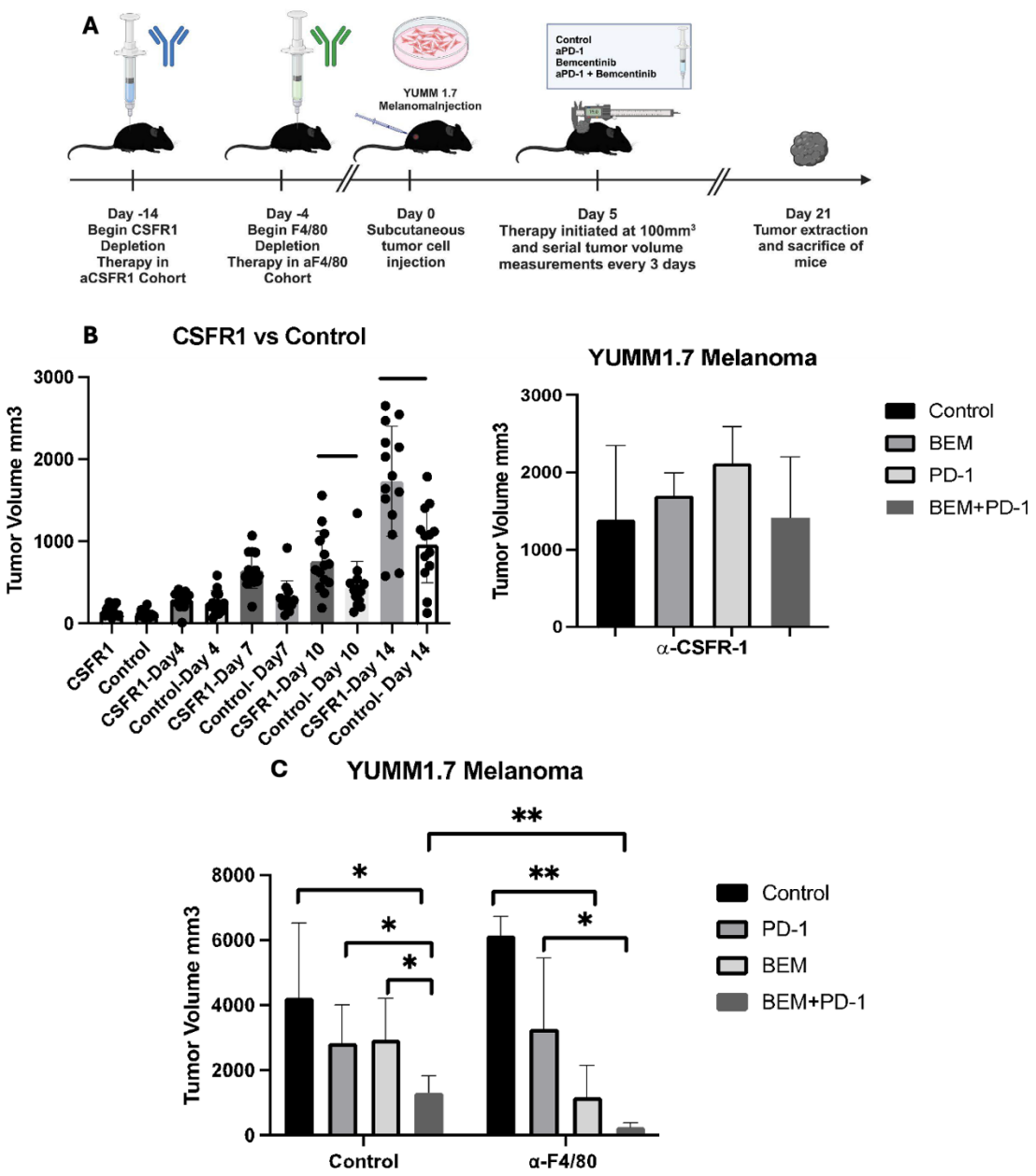

Figure 5-8. AXL and PD-1 targeting in multiple models of macrophage depletion A) Schematic of macrophage depletion approach. Anti-CSF-1R antibody administration began 2 weeks before tumor injection to suppress bone marrow-derived macrophage and myeloid cell development, ant-F/4-80 antibodies were administered 3 days prior to tumor injection for depletion of tissue-level TAMs. B) Accelerated tumor growth was observed in anti-CSF-1R (CSF1R) treated animals with significant size differences observed among control animals at day 10 and persisting at day of sacrifice ($p<0.05$). Final tumor volumes were not significantly different among therapy groups. C) F4/80 depletion, alternatively, increased the observed effect of inhibitors with sensitization to single agent bemcentinib ($p<0.01$ compared to control-therapy in F/480-depleted animals, with significant reduction in tumor size for combination therapy compared to anti-PD-1 monotherapy within F4/80 depleted cohort ($p<0.05$). Global TAM depletion was observed in all treatment groups: however, AXL^+ TAMS ($F4/80^+$ cells) were not significantly altered. Overall differences in M1-like or M2-like phenotype between therapeutic groups were not significantly different or changed from control populations among the residual TAM population. Tumor sizes for combination-treated animals in the F4/80-depletion model were significantly reduced compared to non-depleted control animals treated with combination therapy ($p<0.001$)

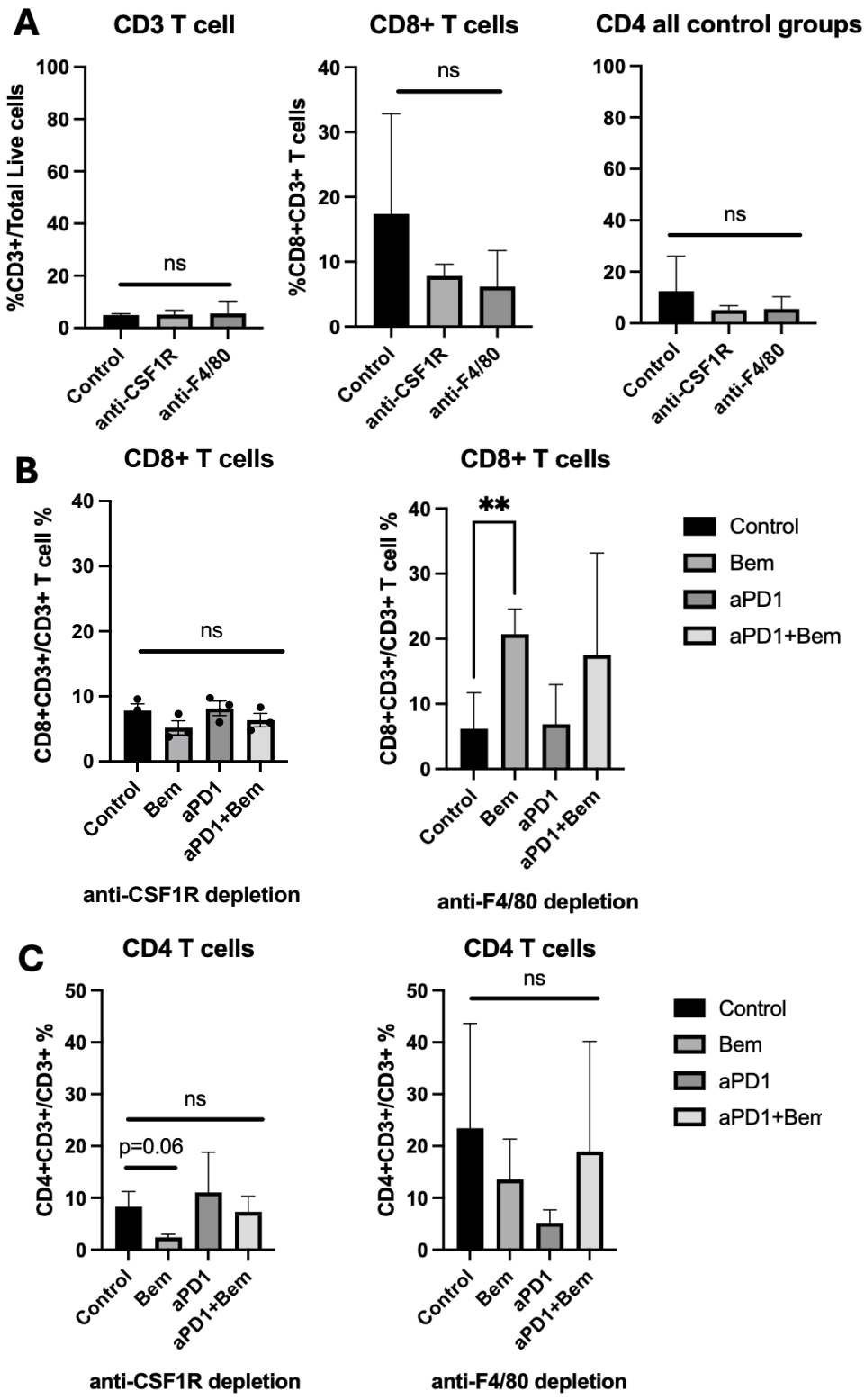
A
CD3 T cell
%CD3+/Total Live cells
ns
Control
anti-CSF1R
anti-F4/80
CD8+ T cells
%CD8+CD3+ T cells
ns
CD4 all control groups
ns
B
CD8+ T cells
CD8+CD3+/CD3+ T cell %
ns
anti-CSF1R depletion
CD8+ T cells
**
anti-F4/80 depletion
Control
Bem
aPD1
aPD1+Bem
C
CD4 T cells
CD4+CD3+/CD3+ %
ns
p=0.06
anti-CSF1R depletion
CD4 T cells
ns
anti-F4/80 depletion
Control
Bem
aPD1
aPD1+Bem

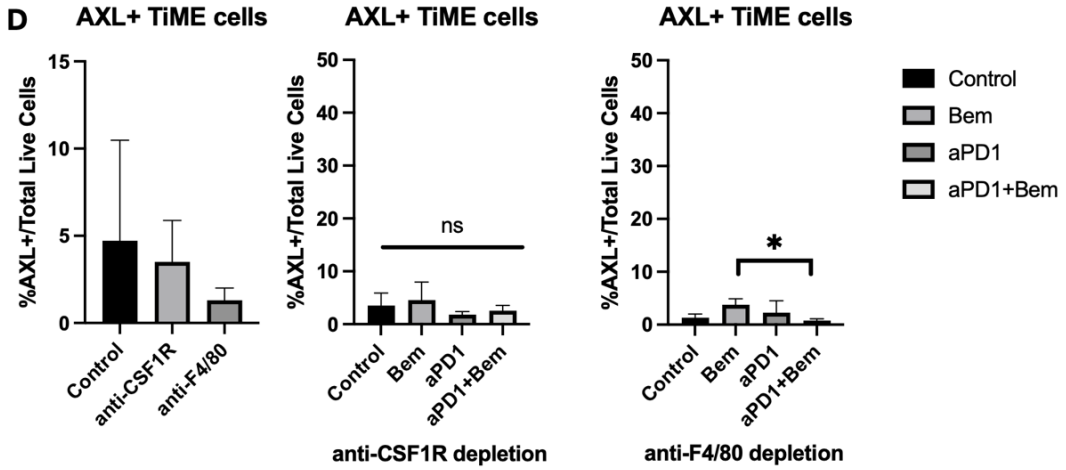

Figure 5-9. TiME alterations in response to macrophage depletion A) Baseline differences in T cell infiltrate were compared in control and treated animals among control, anti-CSF-1R, and anti-F4/80 depletion strategies. Observed reductions in $CD4^+$ or $CD8^+$ T cells in macrophage depletion models were not significant. B) $CD8^+$ and C) $CD4^+$ T cell infiltrate was compared among therapeutic groups. Only bemcentinib (Bem) monotherapy significantly increased $CD8^+$ T cell infiltrate ($p<0.01$ vs. control) in F4/80-depleted animals with a trend toward decreased $CD4^+$ T cell counts in CSF-1R-depleted animals, which was below statistical significance ($p=0.06$). D) Total AXL-expressing cells in the TiME were not significantly different after macrophage depletion strategies, although reduced numbers were observed in F4/80-treated animals. There were no differences in AXL^+ cell presence in therapy groups within the anti-CSF-1R-treated cohort. In F4/80-depleted animals, there was a significant reduction of AXL^+ cells in the combination therapy group compared to Bem monotherapy treatment ($p<0.05$)

6. TiME Impact of Myeloid Cell Depletion

Tumor flow cytometry was performed as previously described, first establishing baseline changes in T cell infiltrate with myelodepletion strategies. Overall, no significant differences in T cell populations were observed among all control-therapy animals (**Figure 5-9A**). The $CD8^+$ T cell infiltrate was not significantly changed among all therapy groups in CSF1R-antibody-treated animals; however, there was an increase in the $CD8^+$ T cell infiltrate for bemcentinib-treated animals in the setting of F4/80 depletion (**Figure 5-9B**). There were no significant differences in the $CD4^+$ T cell infiltrate for either depletion strategy. Notably, a baseline decrease of AXL^+ cells was observed in the setting of F4/80 depletion; however, this finding was below statistical significance (**Figure 5-9C**). Synergy was observed with combination therapy in the context of anti-F4/80 treatment only with the combination of anti-PD-1 and bemcentinib demonstrating a significant reduction in AXL^+ cells compared to bemcentinib monotherapy ($p<0.001$) (**Figure 5-9D**).

7. AXL expression and activity related to macrophage polarization

M1-like and M2-like differentiation was induced in M0 Raw macrophages using established protocols (**Figure 5-10A**). Baseline polarization with LPS stimulation (M1-like) versus IL-4 and IL-13 activation (M2-like) was established by $CD86^+$ or $CD206^+$ expression on differentiated macrophages (**Figure 5-10A**). Notably, despite frequent characterization of AXL^+ macrophage expression categorizing as M2-like macrophages, in this model LPS stimulation strongly induced AXL expression, consistent with inflammation-driven activation of AXL, whereas M2 macrophages were not significantly AXL-positive at baseline (**Figure 5-10B**). *In vivo* inhibition strategies of bemcentinib, and combination therapy were initiated after 24 hours of exposure to differentiation media as well as stimulation with Gas6 ligand with or without bemcentinib (**Figure 5-11D**). No differences in AXL expression were observed in M0 macrophages treated with Gas6 stimulation or bemcentinib inhibition without the presence of differentiation media cytokines. M1-like macrophages did not demonstrate significant differences in AXL expression among treatment groups or with additional Gas6 stimulation. However, the greatest reduction in expression was observed for combination therapy with bemcentinib and anti-PD-1 ($p=0.066$) (**Figure 5-11B**). No significant differences in AXL expression were observed in M2-like conditions.

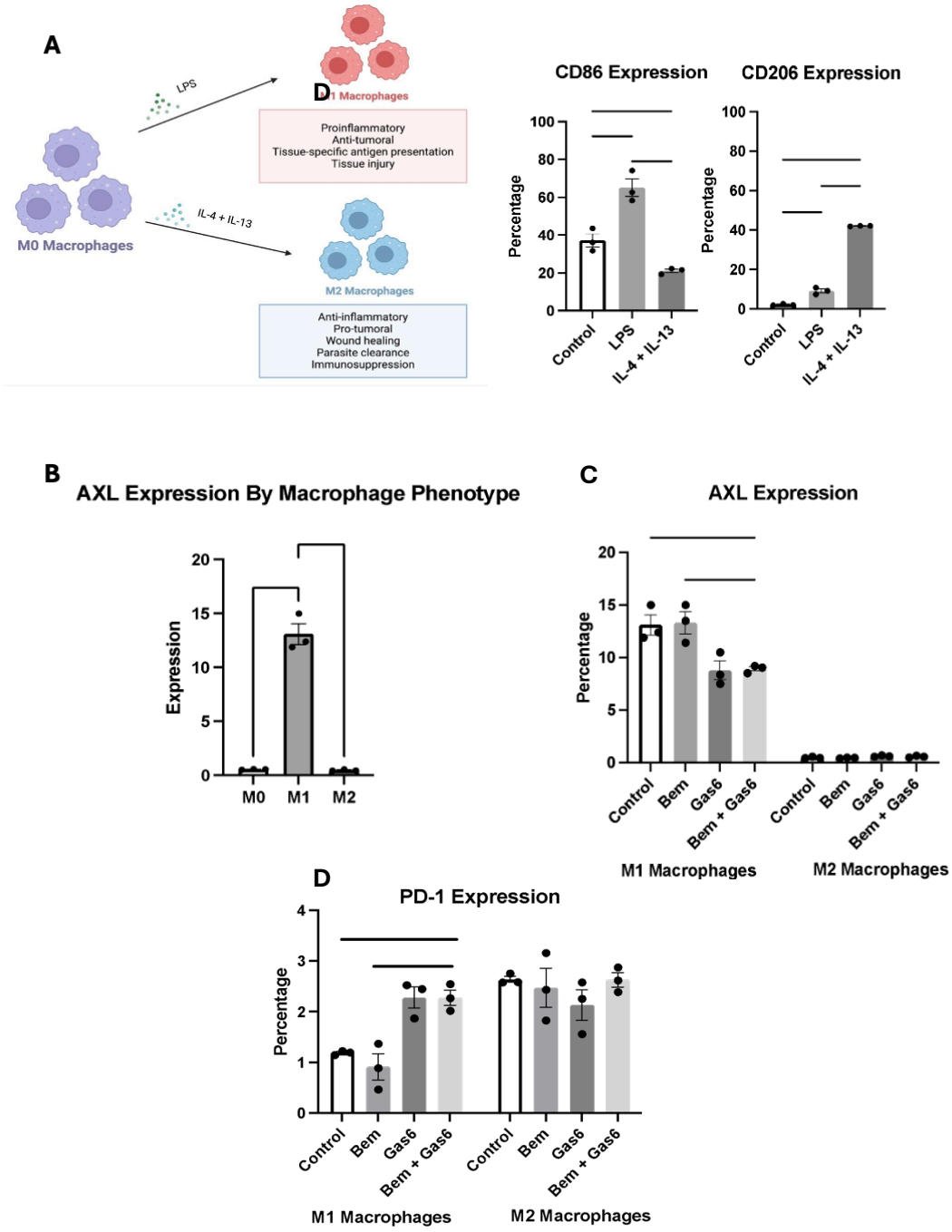

Figure 5-10. *In vitro* macrophage differentiation and AXL expression A) Schematic of differentiation protocol. M0 RAW3.7 Macrophages were treated with either LPS or IL-4 + IL-13 for 24 hours and measured for CD86 (M1-like) or CD206 (M2-like) to confirm shifts in polarization B) Baseline AXL expression was measured post-differentiation. LPS stimulation significantly drove AXL expression in M1-like macrophages whereas, in this model, AXL expression was not strongly induced in M2-like macrophages. C) Stimulation with Gas6 or inhibition with bemcentinib was tested post-differentiation to determine the relationship of AXL to cellular plasticity of differentiated macrophages. AXL inhibition with bemcentinib did not alter AXL expression; however, AXL expression was suppressed with Gas6 incubation of M1-like macrophages and was not reversed by bemcentinib ($p<0.05$). No changes were observed among M2-like macrophages. D) PD-1 expression increased with Gas6 stimulation in M1-like macrophages which was not reversed by bemcentinib ($p<0.05$). No changes in PD-1 expression were observed in M2 macrophages.

8. AXL-related Checkpoint Expression is Context-dependent

Next, changes in polarity markers with therapeutic inhibition post-differentiation was examined in an effort to determine the plasticity of macrophages and the capacity of AXL inhibition to "reprogram" M1-like or M2-like features. Overall, no statistically significant differences were measured in unactivated M0 macrophages with exposure to Gas6 or bemcentinib for AXL expression, macrophage phenotype markers, or PD-1/PD-L1 in the absence of prior stimulation via differentiation protocol (**Figure 5-11A)**. Differentiation experiments were then repeated with the addition of PD-1 inhibition, with or without bemcentinib, to examine the synergistic impact of AXL inhibition.

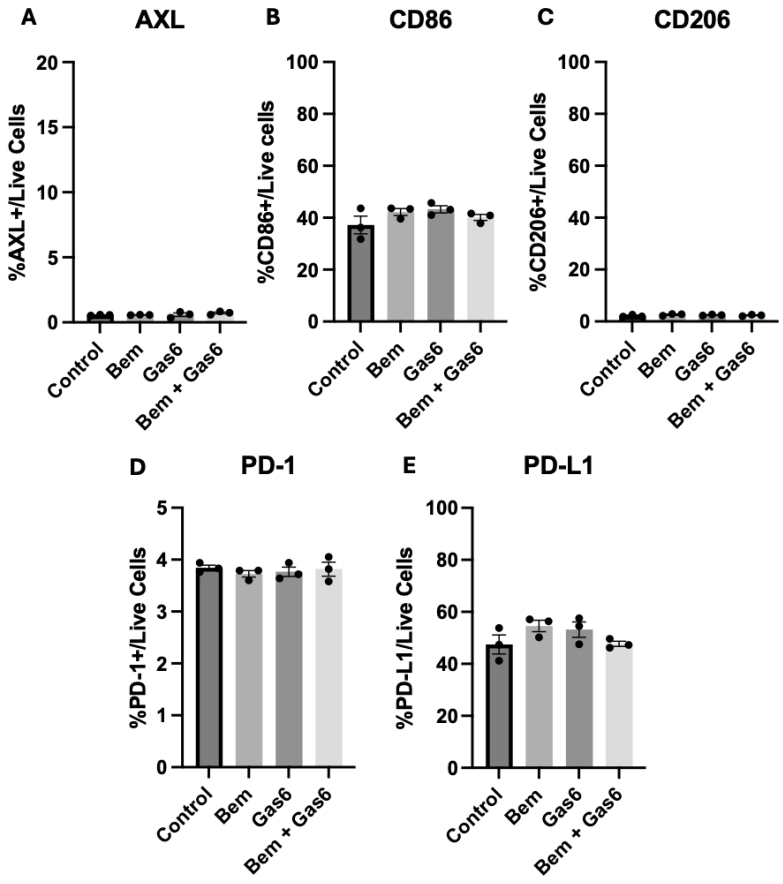

Figure 5-11. Direct influence of AXL inhibition and Gas6 activation on macrophage polarity M0 Raw3.7 macrophages were incubated with Gas6 (100 ng/ml serum-free media), bemcentinib, or their combination, to determine the stimulatory capacity of AXL activation by Gas6 to influence polarization. A-E) No significant differences in macrophage phenotype or checkpoint expression were observed between groups in the absence of cytokine activation with differentiation media as described (Figure 5-10)

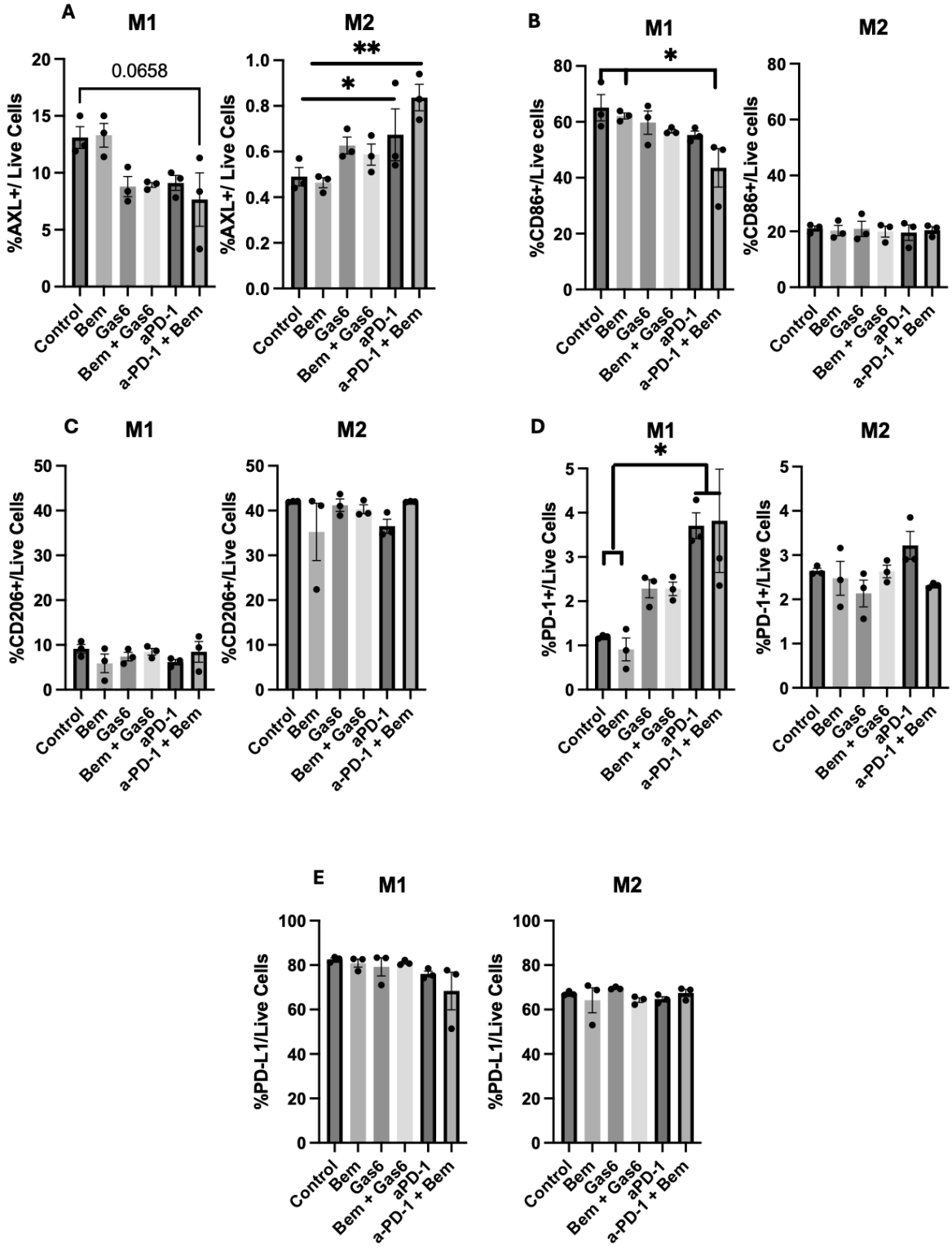
A
M1
M2
0.0658
**
*
%AXL+/ Live Cells
B
%CD86+/Live cells
C
%CD206+/Live Cells
D
%PD-1+/Live Cells
E
%PD-L1/Live Cells
Control
Bem
Gas6
Bem + Gas6
aPD-1
a-PD-1 + Bem

Figure 5-12. Shifts in macrophage phenotype and checkpoint expression with AXL and PD-1 inhibition M0 Raw3.7 macrophages differentiated as described in Figure 5-9 and then exposed to bemcentinib (Bem), Gas6 (100ng/ml), anti-PD-1 antibody, and combination strategies as listed for 12 hours to examine signaling differences in M1- versus M2-like macrophages, to determine stimulatory capacity of AXL activation by Gas6 to influence polarization. A) AXL expression decreased with the combination of anti-PD-1 + Bem but did not reach statistical significance (vs. control, $p=0.0658$). AXL expression was significantly increased after combination therapy in M2-like macrophages ($p<0.05$) but not after monotherapy. B,C) Phenotypic markers CD86 and CD206 were not significantly different between treatment groups. D, E) Checkpoint molecules PD-L1 and PD-1 reflected changes to PD-1 expression only in M1-like macrophages for anti-PD-1-treated groups. There were no significant differences in the presence of AXL inhibition or Gas6.

AXL expression in M1-like macrophages was unchanged with bemcentinib exposure alone and decreases observed with gas6 exposure, single-agent PD-1 inhibition, or combination therapy, however none of these trends met statistical significance ($p=0.0658$ for combination therapy). Changes in CD86 expression were observed only combination therapy treatment of M1-like macrophages ($p<0.05$ vs Control, Bemcentinib) with no change in M2-like macrophages for either CD86 or CD206 (**Figure 11B,C**). Increased PD-1 expression was observed in M1-like macrophages with gas6 exposure that was not rescued by bemcentinib. Further increase in PD-1 expression was observed with anti-PD-1 treatment in this group ($p<0.01$ vs control, bemcentinib) but without change in combination therapy (**Figure 11D**). No changes in PD-L1 expression were measured in M1-like or M2-like macrophages in this model (**Figure 11E**).

9. AXL-related Macrophage Function

Figure 5-13. Impact of AXL inhibition and macrophage phenotype on phagocytosis and efferocytosis. M0 Raw3.7 macrophages differentiated as described in Figure 5-9 and then exposed to bemcentinib (Bem), Gas6 (100ng/ml) to determine AXL-dependent phagocytic function. A) Schematic of efferocytosis assay in which Yumm1.7 melanoma cells are incubated with apoptosis inducer staurosporine prior to co-culture with differentiated macrophages, labeled with CFSE. B) Flow cytometry was performed to assess % efferocytosis in co-culture system, C) Histogram representation of replicate experiments demonstrates increased efficiency for M1-like macrophages over M0 ($p<0.05$) or M2 ($p<0.01$) with no differences in the presence of gas6 or AXL inhibition. D) Phagocytosis, performed with bacterial bait, yielded similar results.

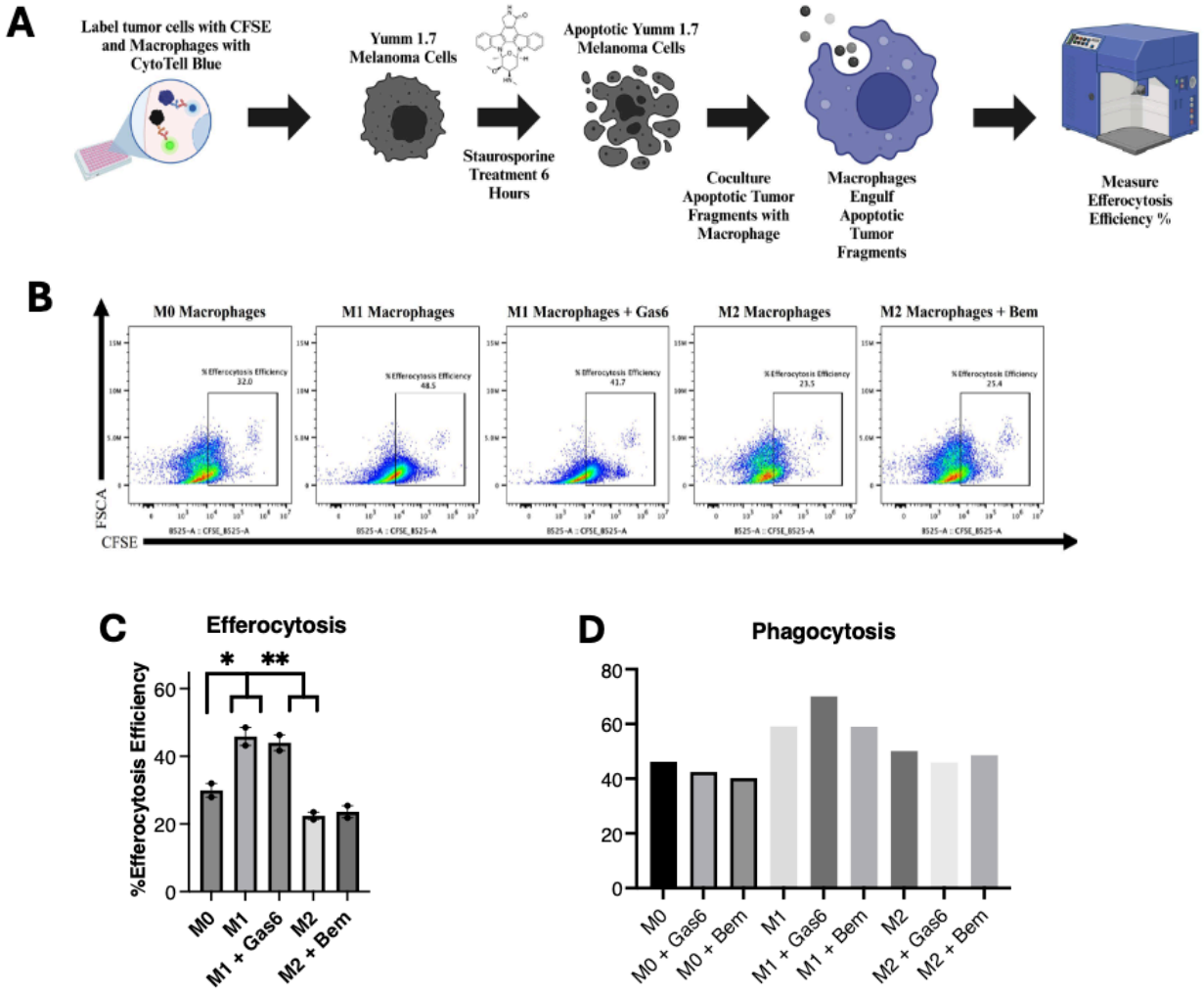

AXL function is implicated as critical to efferocytic function over other AXL-family receptors, in part due to co-ligand functions of gas6 and phosphatidyl serine. As such, efferocytosis assay was performed (**Figure 5-13A**) using apoptotic YUMM 1.7 cells as macrophage bait and measured by flow cytometry (**Figure 5-13B**). Overall, significant changes in efferocytosis efficiency were only attributable to macrophage phenotype with M1-like macrophages demonstrating significantly higher efferocytosis than M2-like macrophages with no differences observed with additional gas6 stimulation of M1-like macrophages or AXL inhibition in M2-like macrophages (**Figure 5-13C**). Given the observation that M1-like macrophages had higher efficiency over M2-like macrophages, which are the conventional actors in efferocytosis processes in situ, phagocytosis was evaluated

for comparison using bacterial bait to discern if apoptotic-driven signaling altered this function behavior. Due to concern that incomplete apoptosis of bait, resulting in live AXL+ tumor cells, could impact responses to AXL inhibition, experiments were repeated in YUMMer1.7 cells. Results were unchanged (not shown). Here, phagocytosis results were similar with increased phagocytosis in M1-like macrophages but no observable differences for addition of gas6 stimulation or bemcentinib inhibition (**Figure 5-13D**).

10. Environmental context impacts AXL and PD-1 synergistic function

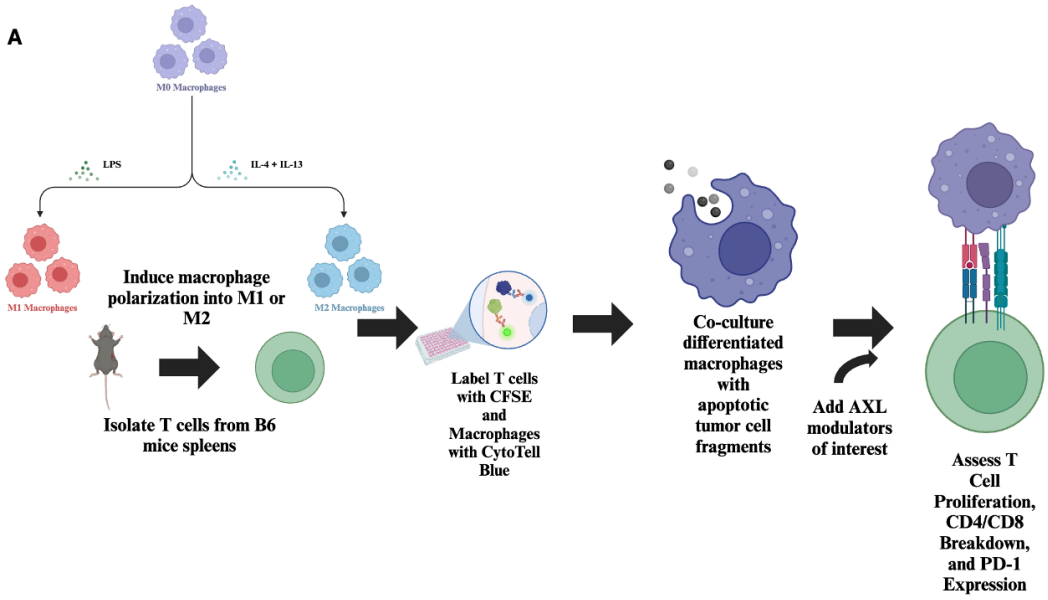

Figure 5-14. Impact of AXL inhibition and macrophage phenotype on T cell proliferation. M0 Raw3.7 macrophages differentiated as described in Figure 5-9 and then exposed to bemcentinib (Bem) with or without Gas6, and with or without anti-PD-1 as in Figure 5-13. A) Schematic of T cell co-culture in which macrophages are incubated with naïve T cells from mouse splenocytes after co-culture with tumor-bait. B) Flow cytometry was performed to measure live T cells. C) Histogram representation of replicate experiments demonstrates no significant shifts in CD4 population/normalized to live CD3 cells. D, E) Combination PD-1 inhibition and AXL inhibition resulted in increased CD8 population with significant reversal of gas6-induced suppression of T cell proliferation with Bem in M2-like culture conditions with increase PD-1+CD8+ T cells after exposure to Gas6+Bemcentinib. F) Differences in co-stimulation by macrophage-secreted factors were examined by performing T cell incubation with or without the presence of treated-macrophage conditioned media, indicating divergences in AXL and gas6-related signaling depending

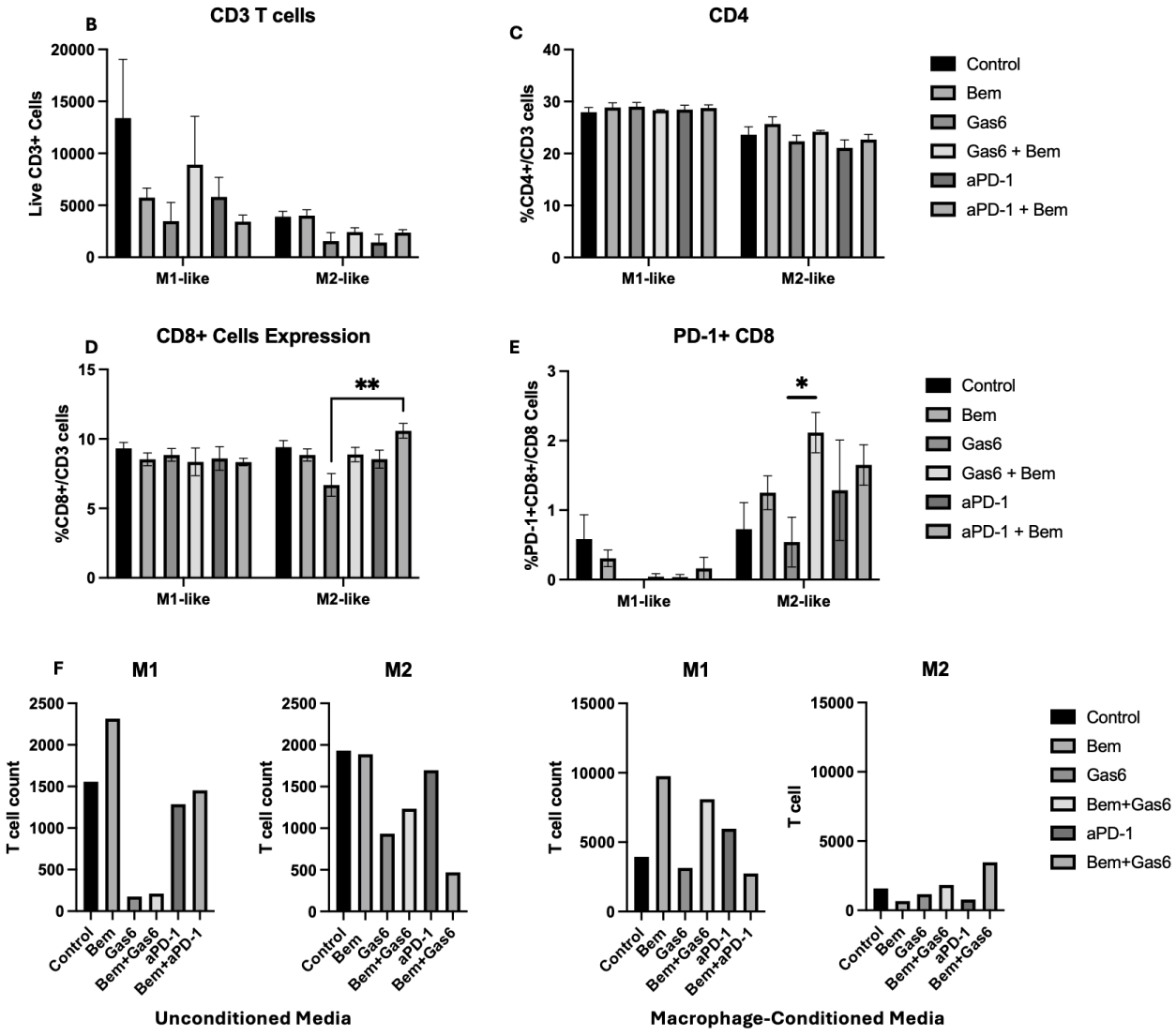

Antigen presentation by macrophages and impact on T cell proliferation was examined by continuation of efferocytosis assay design with a third step of co-incubation of naïve T cells with bait-exposed macrophages (**Figure 5-14A**). Overall, T cell proliferation was widely suppressed across M2-like co-culture conditions with significant suppression of M1-like associated T cell expansion in the presence of gas6 or anti-PD-1 (**Figure 5-14B**). Here, bemcentinib co-incubation reversed the effects of gas6; however, the combination of anti-PD-1 plus bemcentinib did not reverse anti-PD-1 effect. No differences were observed for CD4 T cell differentiation; however, in

M2-like macrophage conditions, the combination of anti-PD-1 and bemcentinib significantly increased CD8 T cell population ($p<0.05$) (**Figure 5-14C, D**). Finally, to examine contributions of co-stimulatory secreted factors, assay was repeated with exchange of macrophage-conditioned media for unconditioned media at the point of macrophage-T cell co-culture. Results are undergoing final evaluation and replication; however, initial results suggest divergences in direct macrophage-T cell interactions across the gas6-AXL axis.

11. AXL-inhibition induces changes in the secretome

Recognizing the differences in downstream functions of antigen presentation and T cell activation in the absence of conditioned media, macrophage-secreted factors were analyzed in vitro from conditioned media sampled prior to T-cell introduction in co-culture. Similar analytes were then measured from in vivo mouse models. In M1-like macrophages, AXL inhibition suppressed inflammatory, and compensatory regulatory, signaling (IL-6, IL-2, IL-10 shown) while increases in inflammatory signaling with gas6 exposure were more pronounced (**Figure 5-15A**). The ability of bemcentinib to inhibit gas6-related stimulation was evident in IL-10 secretion but not IL-6 for M1-macrophages, whereas M2-like macrophages showed bemcentinib inhibition of gas6-related secretion in both cytokines. Differences between combination inhibition with anti-PD-1 and bemcentinib versus pd-1 alone were present only in M2-like macrophages with an increase in inflammatory signaling and dampening of regulatory signaling for combination group. In vivo, synergistic impact was observed with increase in these same analytes in combination therapy groups over anti-PD-1 monotherapy (**Figure 5-15B**). Interestingly, this represented a reversal in pattern from AXL monotherapy with dampening of inflammatory signaling for bemcentinib monotherapy and significant increase in combination therapy. Final analysis of 48-cytokine panel is ongoing to define the impact in related chemokine, cytokine, and metabolic signaling pathways. Overall heatmap of per mouse patterns is shown (**Figure 5-15C**).

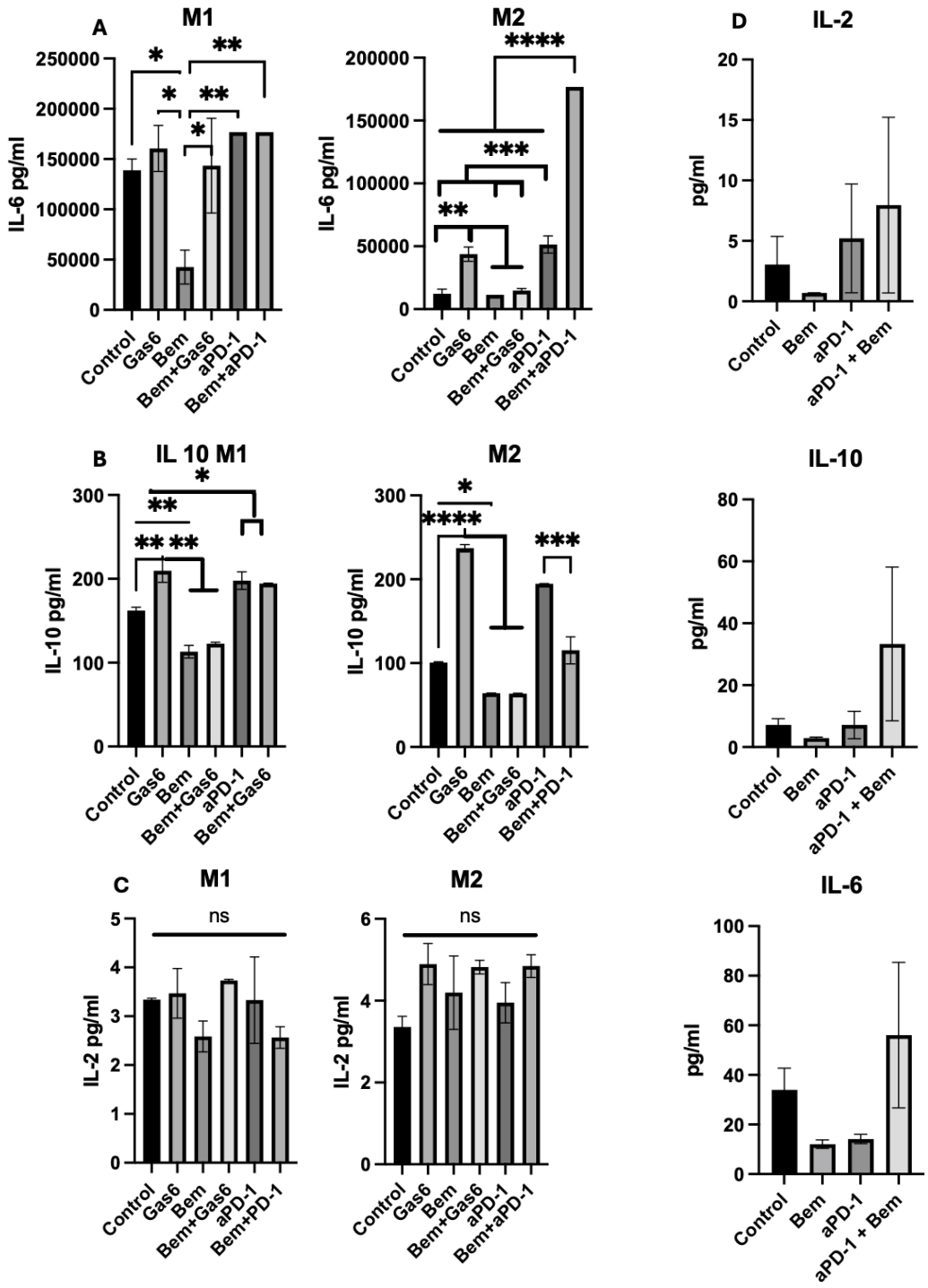
A
M1
IL-6 pg/ml
250000
200000
150000
100000
50000
0
Control
Gas6
Bem
Bem+Gas6
aPD-1
Bem+aPD-1
M2
IL-6 pg/ml
200000
150000
100000
50000
0
****
***
**
D
IL-2
pg/ml
20
15
10
5
0
Control
Bem
aPD-1
aPD-1 + Bem
B
IL 10 M1
IL-10 pg/ml
300
200
100
0
Control
Gas6
Bem
Bem+Gas6
aPD-1
Bem+Gas6
M2
IL-10 pg/ml
300
200
100
0
****
***
Control
Gas6
Bem
Bem+Gas6
aPD-1
Bem+PD-1
IL-10
pg/ml
80
60
40
20
0
Control
Bem
aPD-1
aPD-1 + Bem
C
M1
IL-2 pg/ml
5
4
3
2
1
0
ns
Control
Gas6
Bem
Bem+Gas6
aPD-1
Bem+PD-1
M2
IL-2 pg/ml
6
4
2
0
ns
Control
Gas6
Bem
Bem+Gas6
aPD-1
Bem+aPD-1
IL-6
pg/ml
100
80
60
40
20
0
Control
Bem
aPD-1
aPD-1 + Bem

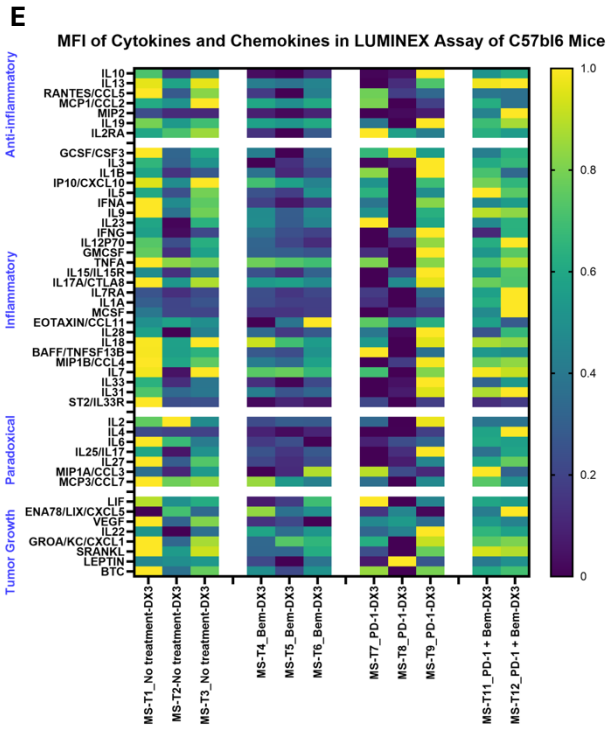

Figure 5-15. Impact of AXL inhibition on the microenvironmental secretome. Conditioned media from experiments performed in Figure 5-14 was evaluated by ELISA using Luminex ImmunoAssay. A, B, C) Gas6-related increases in IL-10 were significantly amplified in M2 conditions with the most significant increases in IL-6 observed in M2 macrophages treated with combination bemcentinib (Bem) and anti-PD-1. Overall conditional changes in IL-2 were negligible. D) *In vivo* cytokine measurements demonstrated significant differences for combination Bem and anti-PD-1 ($p<0.05$ compared to monotherapy). E) Heatmap of all cytokines measured in vivo demonstrates shifts in pro- versus anti-inflammatory profiles in

Chapter 6: Discussion

Precision medicine is the gold standard we strive to achieve to tailor therapy to individual patients, maximizing the effect while minimizing toxicities. Modern cancer treatments that harness the power of the patient's own immune system have dramatically impacted survival for certain patients. However, we currently do not have consistent, predictive markers to identify which patients will be responders versus those with severe AEs. Tumor profiling efforts do not consistently correlate with response to therapies, severely limiting precision application and underscoring the need for improved biomarker tools. Ideal platforms provide 1) high distinguishability, 2) single to subcellular resolution, and 3) high throughput, low-cost preparation. Currently, there are no precise genomic- or protein-based tools in routine clinical use and there is an urgent need to develop usable strategies to mitigate risk in the very poor outcomes for immunotherapy-resistant tumors.

Many techniques have evolved to improve the granularity of oncology research with this aim in mind; however, few capture whether proteins and genes are in an activated state. As such, most retrospectively identified potential targets, such as PD-L1 score, IFNγ signature, or Gene Expression Profiling, have not yet demonstrated strong predictive value for prospective therapeutic selection. In part, this may be a failure of static capture at non-normalized time points in the highly dynamic and heterogenous TiME, as well as failure to integrate post-translational modification data that can dramatically alter the function of oncogenic genes and proteins. Here, the use of a novel technical approach using iFRET was used to resolve the collective impact of these variables as a representative function of tumor activity beyond expression levels. One clear advantage of this approach is the ability to interrogate FFPE tissues at an expense comparable to routine IHC, such that validation of the interpretation of this novel output could broadly expand our ability to interrogate the absolute wealth of archived tissue in melanoma, where small tumor sizes and need for fixation for clinical diagnostics may otherwise prevent wide use of techniques

better suited for fresh processing or modern spatial transcriptomic techniques that would be considerably cost-prohibitive for routine incorporation to clinical trial designs.

There exists considerable interest in the field for defining the role of neoadjuvant therapy, including better predictive metrics, as evidenced by the multitude of studies both reported and ongoing in this space. Most studies of neoadjuvant therapy applied to surgically resectable disease have explored stage III/IV disease and, while efficacious, the extrapolation to earlier stage disease has been limited due to the measurable AEs without clear predictive risk/benefit stratification. Here, analysis of both circulating immune cells and tumor-infiltrating immune cells indicated that, amongst responders, shifts in immune populations can be brisk and identified early while on therapy. However, the exact markers determined to be of significance and interpretation of measurement have varied widely across reports. In general, therapy responses have been associated with influx of lymphocytes, inflammatory signature, and mobilization of memory T cells. Building upon prior evidence that intralesional OV can similarly stimulate inflammation and provoke a reinvigorated response to ICB, several studies have explored this approach both in combination with ICB or after ICB failure, yet utilization of single agent regional approaches, particularly in the neoadjuvant context, have been limited.

In this novel study of neoadjuvant OV for high-risk melanoma, pilot data showed promising early signal of both the efficacy of regionally applied therapies to generate systemic responses responsible for durable disease control and a significantly lower AE profile compared to systemic therapy. This design was based upon the hypothesis that patient-specific variations in the innate immune system might impact the heterogeneity of response observed with OV, as prior reports in both OV and ICB under-investigated these contributions to checkpoint engagement and OV response. Here, pre-surgical utilization of intralesional OV therapy with TVEC prior to standard wide local excision and SLNB was a feasible approach in primary melanoma and stimulated significant immune reaction in both local skin and regional draining lymph nodes over a six-week course of therapy. The rationale for the neoadjuvant approach relies on the increased potential

for stimulation of tumor-specific immune responses when tumors remain *in* situ. Importantly, pathologic complete response has become a surrogate marker for recurrence-free and disease-free survival but, with continued follow-up, even partial responders show superior clinical outcomes compared to nonresponders.[7, 143, 144] Response stratification is expected to allow for de-escalation of both surgery and systemic adjuvant therapy as well as exploration of rational alternative approaches for early rescue of poor responders. From a translational perspective, this approach also allows us to dynamically dissect tumor biology before and after therapy to define the unique heterogeneity amongst melanoma tumors responsible for therapeutic successes or failures.

In this 6-week study design, there were no progression events, and all patients successfully completed therapy without complication. Continued longer-term follow-up and expanded patient enrollment will be necessary to contextualize the relevance and durability of complete or partial response in this patient cohort with earlier stage disease. Nearest to this study design are reports from a team at the University Medical Center in Amsterdam, who explored a single preoperative, regional injection of CpG-B or CTLA-4 inhibitors following wide local excision but prior to SLNB.[141, 145, 146] These studies were inclusive of even earlier stage I and II disease and report positive findings in the primary endpoint of SLN burden reduction. Ultimately, this endpoint may be more biologically relevant in the design of regional and neoadjuvant studies. Evidence of a systemic response to address metastatic disease builds upon the rationale that the regional stimulation of tumor-draining lymph nodes can mitigate antigen tolerance or attack is critical for cancer control.

Traditional assessments, e.g. PD-L1 expression and T cell phenotyping, were *not* illustrative of response trends, consistent with the failure of prior studies to identify biomarkers capable of stratifying patients appropriate for this type of therapy and the failure of combination TVEC with ICB in the Phase III setting.[70] Contrastingly, this data demonstrated that TAM phenotype at pre-treatment baseline, as well as shifts with treatment response, significantly

correlated with OV response**.** This finding, combined with results demonstrating a high interactive checkpoint state in complete responders, in which PD-L1 expression is not contributed by tumor cells critically underscores the role of PD-L1: PD-1 engagement across a multitude of cellular actors in the TiME beyond tumor cells. Instead, it was demonstrated that geographic functionality of checkpoints is widely variable and iFRET improves the fidelity of determining activity at play over protein expression alone. For the first time, the contribution of non-tumor, innate immune cells to PD-L1:PD-1 engagement was identified, showing high interaction after complete tumor resolution with responses correlating to TAM presence and phenotype over T cell infiltrate. The role of these cells in checkpoint responses has not been fully defined to date. This study demonstrates the very nuanced and broad inter-patient variability that has limited collective elucidation of strong biomarkers across the field.

A very recent exploration of iFRET in patients with NSCLC treated with immunotherapy described a multi-tiered stratification by combined PD-L1 expression and iFRET engagement across PD-L1/PD-1 based on findings that patients with low PD-L1/high FRET-type tumors have superior survival, while high PD-L1/low FRET-type tumors may be associated with worse survival.[77] Importantly, this study did not account for cellular infiltrate and the engagement of checkpoint receptors across other cell types, which may shed critically needed insight on the interpretation of this assay. The need for additional companion diagnostics is most highlighted by the high FRET-efficiency values found in this current study's post-treatment major- or complete-responders without viable tumor cells and the unexpected previous findings of the inverse correlation of total $CD8^+$ T cell infiltrate to FRET efficiency.[78] Within this patient cohort, the overall paradigm of high iFRET-efficiency in post-treatment tissue representing favorable clinical outcomes held true. However, surprisingly, in both a non-responder (Patient 1) and a partial responder with gross residual disease (Patient 6), iFRET- efficiency decreased despite stable or increased PD-L1 expression. In complete responders, TVEC therapy powerfully shifted FRET engagement from starting at very low values with Patient 2 having a low PD-L1/low FRET-type

and Patient 5 having high PD-L1/low FRET-type at pre-treatment baseline. Yet, all major or complete responders demonstrated high PD-L1/high FRET at post-treatment measurement. Towards the goal of a strong pre-treatment predictive metric, iFRET remains an important companion piece of the very complex TiME puzzle that will be explored further in follow-up studies.

The impact of the innate immune response in contributing to therapies aimed at generating systemic, adaptive immune responses have been globally undercharacterized. Previous tissue studies of pre- and post-intralesional OV therapy failed to fully characterize the subset myeloid shifts that are not necessarily apparent in the overall population characterization. There is an overall paucity of reporting myeloid responses to date and these emerging studies importantly share the finding reported here that responses by APCs may substantially influence the ability to engage and modify the adaptive immune responses associated with durable control.[147, 148] Important to the rational design and application of next-generation intra-lesional therapies is that many of the agents employed to stimulate stronger immune responses, such as the GM-CSF delivered by TVEC, have detailed pre-clinical evidence of existing as an oncogenic rheostat that can result in expansion of the regulatory immune machinery with repeated exposure. This double-edge sword results in a bidirectional response with some tumor cells, particularly in melanoma, being directly stimulated by the cytokine, counterintuitive to the conventional understanding of its mechanism.[97, 149] Future studies should aim to specifically incorporate longitudinal sampling of tumors given early signal in this dataset that the pre-existing immune milieu at the time of initial treatment *and* differences in post-therapy states may reflect these different patient biologies to predict long-term outcomes.

Despite the provocative findings of this data, there are limitations to address. First, overall patient numbers are low in this study for definitive conclusion and will require significant validation studies. Clinical trial accrual was severely hindered due to the overlapping timeline of the clinical trial study with the emergence of the COVID-19 pandemic. The study design was powered for 60

patients in order to evaluate a primary endpoint of pathologic complete response in treated tissue. Thus, initial delays in study onboarding, halting of patient accrual, and patient declination of frequent visits for therapy were all unfortunately impactful events in meeting accrual goals. Additionally, the surprising findings of a decrease in interactive state in select patients or no change in a patient with metastatic disease suggest that, at this time, median iFRET efficiency cannot yet be employed as a predictive biomarker as a stand-alone test. Unique to this data, the interrogation of the downstream impact of OV on the regional lymphatic basin has not been previously reported given the predominant application of intralesional therapies in the metastatic or refractory disease, where SLN are not typically sampled. This, in particular, may be critical to design improved, next-generation regional therapies that can maximize systemic response and the biology of abscopal response.

In follow-up studies with patient expansion, it will be important to stratify upfront profiles for precision approach detailing patients likely to benefit from upfront OV versus surgery versus upfront ICB by elaborating the clinical utility of emerging functional assays, such as iFRET, in concurrence with conventional immunoassays. This data suggests that interrogation at this level provides a highly granular companion diagnostic with greater sensitivity than proteomics alone but will importantly need definition of the specific cellular players for adequate interpretation. A final analysis of associated spatial transcriptomic changes is planned to provide in-depth insight into the cellular location of targets of interest to further contextualize the functionality of these targets in both the pre-treatment and post-treatment setting, as well as expanded profiling of innate immune components to importantly include more granular classification of a broader diversity of immune cells in this setting.

To further define the importance of TAMs in immunotherapy responses, the complex role of AXL tyrosine kinase was investigated in melanoma in reflection to its growing application in clinical scenarios and known effect on macrophage depletion and polarization in many tumor models. By reactivation of MAPK signaling, AXL TK has been a focus of acquired resistance to

molecular targeted therapies, such as BRAF inhibition.[150] However, its role in circumventing immunotherapeutic strategies is poorly understood. In clinical samples, the immune cell-AXL relationship remains highly complex and poorly understood with several host factors, including age, gender, and obesity, influencing the inflammatory cascade and response to immunotherapeutics.[127, 151, 152] Effort was first made to resolve available clinical data for the relevance of AXL expression in a diverse clinical population with melanoma, including primary disease, metastatic disease, and immunotherapy-refractory disease.

Utilizing the SKCM dataset from TCGA, AXL receptor-family and class ligand genes, as well as immune-related genes were assessed in association with survival outcomes. Unlike diseases, such as pancreatic adenocarcinoma, where AXL expression is overexpressed in a higher percentage of tumor cells and *negatively* correlates with survival[153, 154], in melanoma, AXL expression was linked to improved survival. It was observed that AXL expression aligned with other genes and clinical features associated with inflammatory signaling, such as PD-1 and a higher body mass index (BMI) (Appendix), where the positive association seems somewhat paradoxical but is generally thought to indicate better response to immunotherapies due to the increased inflammation.[155] Additionally, it has been shown that AXL activity in melanoma may be context dependent, with AXL and the melanocyte-inducing transcription factor (MITF) existing on a rheostat where MITF-subtypes are dominant in early melanoma and melanoma initiation and AXL expression increases with tumor progression.[156, 157] In particular, while AXL^+ cells may be a small percentage of primary melanoma, they represent a slow-cycling, highly invasive and drug-resistant subtype that is correlated with higher risk of metastases, particularly melanoma brain metastases.[158, 159] As such, AXL, and related gene expression was contextualized in available single cell sequencing datasets of PD-1-resistant melanoma and untreated melanoma brain metastases.

Taking this approach, it was importantly defined that AXL was expressed in a minority of tumor cells, with the overwhelming contribution of AXL expression in the TiME by TAMs.

Additional cell types with AXL expression were NK cells, B cells, stromal cells, neurons, and dendritic cells; however, the overall percentage of these cells in tumors was significantly lower than TAMs. Uniquely, it has not been previously described that AXL can be expressed by T cells. Additionally, it has been conventionally supported that ligand activation of AXL is fairly exclusively done by the Gas6 ligand, with the other class ligands, such as Pros1, predominantly interacting with other AXL-family receptors, such as MerTK.[118, 160] However, it is known that 1) AXL activation can happen through multiple promiscuous mechanisms, such as co-receptor dimerization with non-class receptors like VEGF, LRP, and EGFR, and 2) additional proteins, such as phosphatidyl serine, or PD-L1, function as co-ligands for AXL-related signaling.[18, 161-163] Further, the total ligand-receptor complex and conformational orientation highly contribute to the exact inflammatory versus regulatory function AXL may serve in a given cell or at a certain time point. Critical in this growing body of data is that the role of Pros1 may have been significantly under-characterized in controlled *in vitro* systems and that *in vivo,* Pros1 may have an important role in stimulating AXL activation in the setting of chronic inflammation that is not well understood.[164, 165] Here, it was shown that Gas6 signaling was high among immune cells but, similar to AXL, virtually none was expressed by tumor cells. By contrast, Pros1 expression was high in tumor cells, which may be an important finding to investigate in future studies to understand how tumor cells may influence AXL activity in surrounding immune neighborhoods.

Overall, in this clinical landscape it remained unclear what the potential impact of AXL inhibition in melanoma is, as it is possible that AXL inhibition may directly target a population of cells thought to be responsible for the most resistant and aggressive metastasis, as well as have potential to dramatically shift the TiME toward a more favorable tumor-killing immune state. The divergences in cellular expression, however, complicate understanding of its role as a biomarker of response in traditional IHC-based or bulk-tumor assessments that, similar to the described complexity of biomarkers in OV-response prediction, may change the overall effect of AXL inhibition in a highly-context dependent way. In particular, this could explain the mixed results

across multiple models assessing AXL inhibition as a means to improve tumor control. Here, it was rationalized that AXL inhibition may have potential to serve as a predominantly macrophage-targeting therapy with a significant role in immunosuppressive, PD-1-resistant tumor types somewhat agnostic to the potential direct tumor-killing impact.

We explored multiple syngeneic *in vivo* models using aggressive, PD-1-resistant cell lines and several strategies of AXL inhibition. While clinically relevant findings of improved melanoma outcomes with warfarin usage support those in pancreatic and colon cancer[166-168], the real-world usage of warfarin in patients with cancer has proven complicated with the potential for multiple comorbid states and usage of multiple other drugs potentially impacting warfarin metabolism and challenging regulation of anticoagulation, as such its modern usage has diminished significantly. It is notable that Gas6-related inhibition occurs in the nM range (as used here for cancer-therapeutic effect) vs. the approximately 2 μM range necessary for systemic anticoagulation and inhibition of other class ligands.[168] However, aims to exploit warfarin at a level subtherapeutic for anticoagulation may be challenged by the finding that Pros1 could have a significant role in oncogenesis and would potentially remain in play. Other AXL inhibition strategies, such as cabozantinib, are actively explored in the clinic, including in uveal melanoma, with approval being gained specifically in PD-1-refractory RCC.[169, 170] However, the AE profile can be limiting.[171] As such, bemcentinib was selected to further explore the direct impact of AXL inhibition in further studies.

AXL inhibition heavily influenced overall tumor cell makeup with an overall depletion of TAMs compared to control tumors. While capable of inhibiting tumor growth as a single agent, this result was inconsistently durable, and many tumors demonstrated late-stage escape. AXL inhibition synergized with PD-1 inhibition to provide significant tumor control in otherwise PD-1-resistant models. In the TiME, this was largely reflected by a shift in TAMs and without significant changes in T cell infiltrate. More important than quantifiable population shifts, however, was the finding that the strength of the PD-L1:PD-1 ligand:receptor interaction was altered by the

presence of AXL inhibition by warfarin. Not tested here, but of future importance, would be to follow-up investigation of these changes with bemcentinib to contextualize the role of AXL-receptor inhibition in this complex interaction versus vitamin K-dependent protein inhibition, and to further characterize the functional interactions both in relationship to potential co-ligand/receptor complexing as well as direct linkage to downstream phosphorylation and activation of the AXL receptor when this phenomenon is at play. However, here, it highlights the importance of interrogating functional states of molecules involved as this tumor property was significantly altered in AXL-treated groups, whereas other immune protein-expression interrogations were less revealing.

With the understanding that TAMs were the dominant AXL^+ cell type in the melanoma TiME, TAM depletion strategies were employed to further explore the role for targeting of the TiME prior to introduction of PD-1-targeting therapy and to explore the TAM context-dependent role of AXL inhibition. Here, it was demonstrated that the preexisting host milieu significantly contributed to immune recognition of tumor cells. It has been proposed that colony-stimulating factor 1 receptor (CSF-1R) inhibition alone could present a potential target for TAM-directed therapy.[73, 172, 173] This study highlights, again, the important context-dependent design of therapeutic investigations, as studies employing CSF-1R inhibition after tumor initiation have had more positive findings[174, 175] and, here, the depletion prior to tumor inoculation rapidly accelerated tumor growth. It is hypothesized that the loss of function in additional APCs and inflammatory M1s dampened overall immune recognition and control of tumor implants, but specifically there was no evidence of response to AXL or PD-1 inhibition in this setting. Alternatively, F4/80 inhibition was employed as a TAM-specific depletion approach that may have greater impact on M2-like TAM reduction without impacting bone marrow development of other myeloid cells.[176, 177] In this approach, the activity of AXL was enhanced, and the greatest tumor control was achieved in combination therapy with anti-PD-1. Analysis is continuing to fully categorize the altered myeloid milieu to give insight into the abundance and phenotype of the immune cell infiltrate from these

tumors that contributed to this finding. Future studies are also ongoing to further explore non-AXL expressing tumor lines or models reflective of earlier stage disease with less AXL-dependent activity; however, it was felt that this modeling was a critical first step to rationalize the continued development of AXL inhibition in the most aggressive and difficult-to-treat clinical scenarios.

Given the findings that immune complex interactive states were impacted by AXL inhibition and that alteration of the myeloid landscape changed the application of AXL-directed therapy, the direct impact on macrophage function was explored. In reflection of clinical single-cell sequencing findings that AXL has high expression in M1-like and M2-like macrophages, conditions of both were created *in vitro* to determine context-dependent functions. Interestingly, while AXL has been highly attributed to phagocytic and efferocytotic function with notably high AXL expression by efferosomes, this study found that those functions were largely attributable to macrophage cell-state with M1-like macrophages having significantly increased phagocytic capacity compared to M2-like macrophages and no significant differences were observed in this function with AXL activity. This may support alternative hypotheses that AXL activity may not directly impact phagocytic function but instead may be a secondary change signaling resolution of inflammatory insult or activation of cellular regulatory function to restore homeostasis.

Subsequently, given the high expression of AXL by both TAMs and DCs and the potential contribution to adaptive immune responses, AXL function in antigen presentation was explored in a co-culture design. Here, AXL inhibition was employed during incubation of macrophages with apoptotic tumor-bait prior to incubating tumor-exposed macrophages with naïve T cells. Overall, proliferative counts at 24 hours were not significantly changed amongst groups. While trends existed for M1-like exposed T cells to proliferate to a greater extent, as expected, and Gas6 exposure decreased T cell counts, no significant differences were measured amongst groups at 24 hours. Additional replicates and longer time points may be necessary to discern the relevance of these trends. Additional time points at 48 or 72 hours may also allow for quantifiable dilution of

CFSE to determine differences in T cell proliferation in this design versus the possibility of direct T cell attack contributing to the diminished T cell numbers in some treatment groups.

Similarly, differences in PD-1+CD8+ T cells were overall below significance amongst amongst groups. These cells represented a very small percentage of all T cells in this model (<3%). However, the findings that Gas6 combination with bemcentinib not only reversed Gas6 depression, but significantly increased PD-1 positive populations suggests that additional molecular actors, such as other AXL-family receptors capable of being stimulated by Gas6, may be critical to resolve. In particular, MerTK is not described here and it remains possible that canonical contribution of MerTK to phagocytic or antigen-presenting function may be increasingly activated by Gas6 in the setting of AXL inhibition. Additional ligands not measured include Pros1, which has historically been considered less relevant to AXL function. However, these studies suggest multiple divergences in which either Gas6 stimulation is not reversed by bemcentinib or AXL-inhibitory effects are not impacted by the presence of absence of Gas6. Combined with the demonstration here that Pros1, rather than Gas6, is heavily expressed on melanoma tumor cells, future studies will require examination of signaling across multiple family ligand-receptor pairs. Future work is underway to utilize the interactive dynamics of these pathways using iFRET efficiency measurements in coordination with downstream phosphorylation events in effort to demonstrate the impact of receptor-directed versus ligand-directed inhibition to resolve these questions.

Lastly, given the overall small differences in T cell proliferation in this multi-step co-culture design, the contribution of “Signal 3” was evaluated by repeating the design in the absence of the macrophage-conditioned media. As expected, proliferation was minimal in the absence of co-stimulatory factors secreted by macrophages. However, the complete reduction of T cell proliferation in the presence of Gas6 was notable. Again, this did not appear reversed by bemcentinib; whereas, bemcentinib treated groups otherwise had increased T cell counts,

suggesting potential unlinking of Gas6-AXL activity in this function. Addditional replicates and dedicated study design would be necessary to confirm the relevance of this observation.

Secreted factors in macrophage-conditioned media were evaluated by Luminex with multiple interesting findings. Final analysis is ongoing to categorize overall patterns of shifts in pathways associated with macrophage trafficking, T cell proliferation, inflammatory signaling, immunosuppression, and metabolism. Shown here, however, are the decreases in immunosuppressive signaling by IL-10 for bemcentinib treated groups by both M1-like and M2-like macrophages. Correspondingly, inflammatory signaling by IL-6 was increased in these groups. Importantly, in these studies, Gas6-mediated activity was consistently reversed by bemcentinib, suggesting that alternative AXL signaling or activation in T cell studies may be a function of direct cell:cell binding properties, such as co-receptor complexes and conformational changes, as the macrophage-secreted factors do not show differences, e.g. differences in Signal 3. Also important amongst multiple secreted factors (IL-6 shown) is the syngergy of anti-PD-1 therapy and bemcentinib to increase inflammatory signaling over either monotherapy. This finding was consistently replicated in in vivo analyte trends, however the wider variations for in vivo circulating cytokines resulted non-significant differences in these specific cytokines. Analysis of additional animals (n=3/5-6 measured here) may be needed and final analysis of the complete panel is to be reported. It is also critical to note that, in vitro, there were no differences in IL-2 measurements. The differences in in vitro secretory findings compared to in vivo suggest that additional cellular actors may facilitate these communications *and/or* 2D cellular communications may lack the functional complexity to completely resolve these relationships. Ultimately, the lack of wide variations in vitro or in vivo in T cell proliferation and infiltrate highlight the importance of the data contributed by iFRET efficiency and adds to the data in TVEC studies to suggest that functional analysis of this type may be critical to further define the true impact of these therapies where cell populations alone or proteomic data alone have failed to yield clear data to explain the collective improved responses in combination therapy treatment.

These studies have several limitations. First, the nature of mouse models for melanoma is highly complex with most mouse-derived models being heavily oncogenically driven and non-identical to the majority of cutaneous, UV-mutation driven melanoma.[178-181] The subcutaneous implant model is also not ideal for TiME reconstruction as the subcutaneous fat is necessarily a highly divergent environment from the highly immunogenic dermis.[182] Other groups have reported success with using the YUMMer1.7 model with intent to reflect a more immunogenic, PD-1 responsive melanoma model. However here, consistent with some reports, this proved to result in tumor rejection entirely, which interestingly immunized mice against later YUMM1.7 implantation (Appendix).[183] As such, our future mouse studies of melanoma metastases will include YUMM1.7 and B16F10 lines with AXL silencing to isolate the tumor-specific contribution of AXL function in these models. However, more important is to create human-faithful immune models and the forward focus of this work has been the development of patient-derived immune organoids from PD-1 refractory tumors.[184, 185] Additionally, multiple findings here raise implication of antigen presenting function being impacted in the presence of AXL inhibition, be it by secreted co-stimulation or direct antigen presenting cell : effector cell binding properties, both of which are suggested by this data. However, exploration of professional APCs, DCs, and other PD-L1 expressing immune cells was limited. For this study, the focus remained TAMs as the abundant cell type in tumors and with the understanding the APC-type and function may be significantly altered in the TiME, compared to normal immune processes in tumor-draining nodal tissue.[186, 187] AXL activation and function is certainly of relevance in these other cell types and spatial transcriptomic studies are currently underway to in follow up of these studies to further classify the greater immune milieu related to AXL expression and functional environmental changes in tumors. Overall, this data contributes important findings of context-specific AXL activity in melanoma that will require careful consideration in the broad clinical application of AXL inhibitors but presents important, rational foundation for the continued exploration of AXL inhibition in metastatic, immunosuppressive environments or immunotherapy-resistant clinical scenarios.

Chapter 7: Conclusion and Future Directions

The appropriate use of immunotherapy and *which* therapy remains highly debated in multiple stages of melanoma in balance of the overall risk to benefit of their use. Greater precision is needed both to predict patient responses and quantify those responses in post-treatment tissues. Expansion of tumor profiling studies, such as the studies presented here, will allow for de-escalation of both surgery and systemic adjuvant therapy as well as exploration of rational alternative approaches for early rescue of poor responders. From a translational perspective, dynamic dissection of tumor biology before and after therapy will be necessary to define the unique heterogeneity amongst melanoma tumors responsible for therapeutic successes or failures.

The clinical and translational work here offers significant contribution toward this aim as it marks the first exploration of intralesional oncolytic virus in Stage II disease prior to standard surgery. The pilot study revealed varying efficacy of TVEC but with promising results that advocate for further investigations using this approach. Future studies utilizing next-generation agents with improved abscopal response present an attractive option for neoadjuvant application and continuation of this trial design is underway. The positive risk-to-benefit profile of OV therapies emphasizes the necessity for additional exploration and implementation of neoadjuvant use of this treatment as a viable strategy for patients with high-risk primary disease. The integration of molecular and functional assays in the study yields a unique biomarker analysis that supports more precise and effective patient stratification for personalized therapeutic interventions. These findings underscore the essential requirement for comprehensive patient stratification to unravel the complexities of biomarker identification, crucial for advancing personalized treatment approaches.

Importantly, the data showcases a significant correlation between the TAM phenotype at pre-treatment baseline and the changes in these populations with treatment response. Critically, the results reveal a high interactive checkpoint state in complete responders post-treatment, where PD-L1 expression is unrelated to tumor cells, highlighting the pivotal role of PD-L1: PD-1 engagement across various other cellular components in the tumor microenvironment. These insights shed light on the microenvironmental factors influencing checkpoint function in tumors and reveal diverse trends, even within a small cohort. This finding underscores important gaps in knowledge, pointing to potentials for new therapeutic avenues, and emphasizing the need for translational research to comprehensively define innate immune profiles to improve immunotherapeutic approaches. The expansion of these initial findings may aid in identifying distinct patient profiles for tailored treatment selection, potentially guiding upfront therapy choices for those with a high interactive state towards options like ICB or potentially identify patients appropriate for surgery alone.

Towards the aim of novel biomarker discovery, several important variables were demonstrated in exploratory analysis here that highlight cellular and molecular actors at play in the divergence of patient responses. In particular, intra-tumoral functional shifts measured by iFRET and the diversity of innate immune responses significantly contributed to the contextualization of both OV and ICB in patient and mouse models. The need for additional companion diagnostics that can capture and layer this type of data will be necessary to contextualize exploding multi-omic interrogations. Given the finding of the importance of macrophage phenotype to tumor responses, it is expected that further characterization will highlight the importance of evolving the spatial interrogation of functional assays, such as iFRET, in partnership with modern proteomic and transcriptomic assays. Especially, previous studies attempting to dissect the relevance of the multi-functional TAMs may have been hindered in interpretation by the overly simplified nomenclatures used to date, such as M1 vs. M2 with the clear current understanding that macrophages exist and function on a much broader spectrum.

Toward this effort, we have expanded the characterization AXL expression in melanoma and the contribution of tumor associated macrophages to AXL functions. AXL remains a high-value target in the most aggressive melanoma tumor types and presents an attainable strategy to improve therapeutic responses in current melanoma treatment strategies. Further work will be necessary to explore the benefit of combination drug strategies versus metronomic therapeutic approaches for reprogramming the innate immune environment prior to arming T-cell based therapies. Current studies are ongoing to explore environment–specific impact of AXL-targeting, such as in melanoma brain metastases, which remain a clinically devastating scenario that is most often refractory to ICB. This work additionally involves direct-to-tumor drug designs using nano-delivery systems that are highly programmable and may serve as another steppingstone toward personalized drug regimens.

Biologically, much work is still to be done to dissect the intricacies of tumor-associated macrophages, particularly to define which functions of macrophages can be better exploited as therapeutic targets. In this context, much is left to resolve regarding the expression and role of AXL in monocyte development as well as the nature of AXL function tissue resident-macrophages versus recruited macrophages. Importantly, current efforts of this work in complex in vitro models, such as patient derived organoid-avatars, strongly suggests that 2D culture systems have failed to capture critically relevant biologies in patients where immunotherapy is concerned. Instead, multi-dimensional characterizations that also account for time and space, such as in 3D-organoids or before *and* after therapy will be necessary to understand the molecular crosstalk that contributes to complex tumor-immune interactions. Using these more complete models, conformational changes of co-receptor complexing, such as occurs with AXL and checkpoint ligand-receptor pairs, rapid acceleration of translational tumor studies into human-faithful models may be possible.

The major forward goal of this work is to improve the precision, quality, and accessibility of diagnostic and discovery tests and models that can incorporate a greater depth of these

variables. Novel data outputs, i.e. such as the quantitative FuncOmap designed by Prof. Larijani, have potential to resolve the functional states of regulatory signals, including checkpoints, with precision not previously possible. Work is currently underway to partner this technology with proteomic, genomic, and post-translational modification data that can be performed at very low cost. Collectively, the ability to assay tumor tissue in this way will deliver mechanistic insight not feasible by conventional methods and resolve the barriers that have persisted in appropriate biomarker discovery. Moreover, this data will also shed insight specifically into the rich innate immune milieu by offering deeply detailed descriptions of macrophage phenotype and resultant shifts in immunosuppressive versus inflammatory signaling that impact adaptive immune arming and, ultimately, responses to immunotherapy to improve outcomes for patients.

References

1. Erstad DJ, Witt RG, Wargo JA. Neoadjuvant therapy for melanoma: new and evolving concepts. Clin Adv Hematol Oncol. 2022;20(1):47-55.
2. Bello DM, Han G, Jackson L, Bulloch K, Ariyan S, Narayan D, et al. The Prognostic Significance of Sentinel Lymph Node Status for Patients with Thick Melanoma. Annals of Surgical Oncology. 2016;23(5):938-45.
3. Stege H, Haist M, Nikfarjam U, Schultheis M, Heinz J, Pemler S, et al. The Status of Adjuvant and Neoadjuvant Melanoma Therapy, New Developments and Upcoming Challenges. Targeted Oncology. 2021;16(5):537-52.
4. Larijani B, Miles J, Ward SG, Parker PJ. Quantification of biomarker functionality predicts patient outcomes. British Journal of Cancer. 2021;124(10):1618-20.
5. Alvarez-Breckenridge C, Markson S, Stocking J, Lastrapes M, Nayyar N, Bertalan M, et al. IMMU-01. SINGLE CELL SEQUENCING OF MELANOMA BRAIN METASTASES UNVEILS HETEROGENEITY OF THE TUMOR MICROENVIRONMENT IN RESPONSE TO IMMUNE CHECKPOINT BLOCKADE. (1522-8517 (Print)).
6. Bushara O, Tidwell J, Wester JR, Miura J. The Current State of Neoadjuvant Therapy in Resectable Advanced Stage Melanoma. Cancers. 2023;15(13):3344.
7. Hieken TJ, Kreidieh F, Aedo-Lopez V, Block MS, McArthur GA, Amaria RN. Neoadjuvant Immunotherapy in Melanoma: The Paradigm Shift. American Society of Clinical Oncology Educational Book. 2023(43):e390614.
8. Thrane K, Eriksson H, Maaskola J, Hansson J, Lundeberg J. Spatially Resolved Transcriptomics Enables Dissection of Genetic Heterogeneity in Stage III Cutaneous Malignant Melanoma. Cancer Research. 2018;78(20):5970-9.
9. Pu Y, Ji Q. Tumor-Associated Macrophages Regulate PD-1/PD-L1 Immunosuppression. Front Immunol. 2022;13:874589.
10. Huang R, Kang T, Chen S. The role of tumor-associated macrophages in tumor immune evasion. J Cancer Res Clin Oncol. 2024;150(5):238.
11. Wang S, Wang J, Chen Z, Luo J, Guo W, Sun L, et al. Targeting M2-like tumor-associated macrophages is a potential therapeutic approach to overcome antitumor drug resistance. NPJ Precis Oncol. 2024;8(1):31.
12. Zhou Q, Fang T, Wei S, Chai S, Yang H, Tao M, et al. Macrophages in melanoma: A double-edged sword and targeted therapy strategies (Review). Exp Ther Med. 2022;24(4):640.
13. Ma RY, Black A, Qian BZ. Macrophage diversity in cancer revisited in the era of single-cell omics. Trends Immunol. 2022;43(7):546-63.
14. Andtbacka RHI, Ross M, Puzanov I, Milhem M, Collichio F, Delman KA, et al. Patterns of Clinical Response with Talimogene Laherparepvec (T-VEC) in Patients with Melanoma Treated in the OPTiM Phase III Clinical Trial. Annals of Surgical Oncology. 2016;23(13):4169-77.
15. Ribas A, Dummer R, Puzanov I, VanderWalde A, Andtbacka RHI, Michielin O, et al. Oncolytic Virotherapy Promotes Intratumoral T Cell Infiltration and Improves Anti-PD-1 Immunotherapy. Cell. 2017;170(6):1109-19.e10.

16. Dummer R, Gyorki DE, Hyngstrom J, Berger AC, Conry R, Demidov L, et al. Neoadjuvant talimogene laherparepvec plus surgery versus surgery alone for resectable stage IIIB-IVM1a melanoma: a randomized, open-label, phase 2 trial. Nature Medicine. 2021;27(10):1789-96.
17. Akalu YT, Rothlin CV, Ghosh S. TAM receptor tyrosine kinases as emerging targets of innate immune checkpoint blockade for cancer therapy. Immunol Rev. 2017;276(1):165-77.
18. Gay CM, Balaji K, Byers LA. Giving AXL the axe: targeting AXL in human malignancy. Br J Cancer. 2017;116(4):415-23.
19. Zhu C, Wei Y, Wei X. AXL receptor tyrosine kinase as a promising anti-cancer approach: functions, molecular mechanisms and clinical applications. Molecular Cancer. 2019;18(1):153.
20. Bhalla S, Gerber DE. AXL Inhibitors: Status of Clinical Development. Curr Oncol Rep. 2023;25(5):521-9.
21. Kirane A, Ludwig KF, Sorrelle N, Haaland G, Sandal T, Ranaweera R, et al. Warfarin Blocks Gas6-Mediated Axl Activation Required for Pancreatic Cancer Epithelial Plasticity and Metastasis. Cancer Research. 2015;75(18):3699-705.
22. Pollack LA, Li J, Berkowitz Z, Weir HK, Wu X-C, Ajani UA, et al. Melanoma survival in the United States, 1992 to 2005. Journal of the American Academy of Dermatology. 2011;65(5 Suppl 1):S78-S86.
23. Wolchok JD, Chiarion-Sileni V, Gonzalez R, Grob JJ, Rutkowski P, Lao CD, et al. Long-Term Outcomes With Nivolumab Plus Ipilimumab or Nivolumab Alone Versus Ipilimumab in Patients With Advanced Melanoma. J Clin Oncol. 2022;40(2):127-37.
24. Hanna TP, Nguyen P, Baetz T, Booth CM, Eisenhauer E. A Population-based Study of Survival Impact of New Targeted and Immune-based Therapies for Metastatic or Unresectable Melanoma. Clin Oncol (R Coll Radiol). 2018;30(10):609-17.
25. Knight A, Karapetyan L, Kirkwood JM. Immunotherapy in Melanoma: Recent Advances and Future Directions. Cancers. 2023;15(4):1106.
26. Bastacky ML, Wang H, Fortman D, Rahman Z, Mascara GP, Brenner T, et al. Immune-Related Adverse Events in PD-1 Treated Melanoma and Impact Upon Anti-Tumor Efficacy: A Real World Analysis. Front Oncol. 2021;11:749064.
27. Thornton J, Chhabra G, Singh CK, Guzmán-Pérez G, Shirley CA, Ahmad N. Mechanisms of Immunotherapy Resistance in Cutaneous Melanoma: Recognizing a Shapeshifter. Frontiers in Oncology. 2022;12:880876.
28. Yan C, Huang M, Swetlik C, Toljan K, Mahadeen AZ, Bena J, et al. Predictors for the development of neurological immune-related adverse events of immune checkpoint inhibitors and impact on mortality. Eur J Neurol. 2023;30(10):3221-7.
29. Deacon DC, Smith EA, Judson-Torres RL. Molecular Biomarkers for Melanoma Screening, Diagnosis and Prognosis: Current State and Future Prospects. Front Med (Lausanne). 2021;8:642380.
30. Maher NG, Vergara IA, Long GV, Scolyer RA. Prognostic and predictive biomarkers in melanoma. Pathology. 2024;56(2):259-73.
31. Naik PP. Role of Biomarkers in the Integrated Management of Melanoma. Dis Markers. 2021;2021:6238317.

32. Lin G, Fan X, Zhu W, Huang C, Zhuang W, Xu H, et al. Prognostic significance of PD-L1 expression and tumor infiltrating lymphocyte in surgically resectable non-small cell lung cancer. Oncotarget. 2017;8(48):83986-94.
33. Placke JM, Kimmig M, Griewank K, Herbst R, Terheyden P, Utikal J, et al. Correlation of tumor PD-L1 expression in different tissue types and outcome of PD-1-based immunotherapy in metastatic melanoma - analysis of the DeCOG prospective multicenter cohort study ADOREG/TRIM. EBioMedicine. 2023;96:104774.
34. Sunshine JC, Nguyen PL, Kaunitz GJ, Cottrell TR, Berry S, Esandrio J, et al. PD-L1 Expression in Melanoma: A Quantitative Immunohistochemical Antibody Comparison. Clin Cancer Res. 2017;23(16):4938-44.
35. Ellebaek E, Khan S, Bastholt L, Schmidt H, Haslund CA, Donia M, et al. PD-L1 is a biomarker of real-world clinical outcomes for anti-CTLA-4 plus anti-PD-1 or anti-PD-1 monotherapy in metastatic melanoma. Eur J Cancer. 2024;198:113476.
36. Andrews MC, Li G, Graf RP, Fisher VA, Mitchell J, Aboosaiedi A, et al. Predictive Impact of Tumor Mutational Burden on Real-World Outcomes of First-Line Immune Checkpoint Inhibition in Metastatic Melanoma. JCO Precis Oncol. 2024;8:e2300640.
37. Chang JW, Huang CJ, Huang WK, Wang YC, Hsieh JJ, Chang YY, et al. Genomic and tumour microenvironmental biomarkers of immune checkpoint inhibitor response in advanced Taiwanese melanoma. Clin Transl Immunology. 2023;12(8):e1465.
38. Zhao P, Li L, Jiang X, Li Q. Mismatch repair deficiency/microsatellite instability-high as a predictor for anti-PD-1/PD-L1 immunotherapy efficacy. J Hematol Oncol. 2019;12(1):54.
39. Greco L, Rubbino F, Dal Buono A, Laghi L. Microsatellite Instability and Immune Response: From Microenvironment Features to Therapeutic Actionability-Lessons from Colorectal Cancer. Genes (Basel). 2023;14(6).
40. Moeckel C, Bakhl K, Georgakopoulos-Soares I, Zaravinos A. The Efficacy of Tumor Mutation Burden as a Biomarker of Response to Immune Checkpoint Inhibitors. Int J Mol Sci. 2023;24(7).
41. Andre T, Cohen R, Salem ME. Immune Checkpoint Blockade Therapy in Patients With Colorectal Cancer Harboring Microsatellite Instability/Mismatch Repair Deficiency in 2022. Am Soc Clin Oncol Educ Book. 2022;42:1-9.
42. Fazio R, Audisio A, Dapra V, Conti C, Benhima N, Abbassi FZ, et al. Non-operative management after immune checkpoint inhibitors for early-stage, dMMR/MSI-H gastrointestinal cancers. Cancer Treat Rev. 2024;128:102752.
43. Killock D. DREAMseq of therapy for BRAF-mutant melanoma. Nat Rev Clin Oncol. 2023;20(1):1.
44. Möller T, Schulze H-J. The Influence of c-Kit and NRAS Mutation on Patients' Survival in Metastatic Melanoma Receiving Immune Checkpoint Inhibitors and Chemotherapy. Dermato. 2022;2(2):53-8.
45. Pilla L, Alberti A, Di Mauro P, Gemelli M, Cogliati V, Cazzaniga ME, et al. Molecular and Immune Biomarkers for Cutaneous Melanoma: Current Status and Future Prospects. Cancers (Basel). 2020;12(11).

46. Rabbie R, Ferguson P, Molina-Aguilar C, Adams DJ, Robles-Espinoza CD. Melanoma subtypes: genomic profiles, prognostic molecular markers and therapeutic possibilities. J Pathol. 2019;247(5):539-51.
47. Liu YT, Sun ZJ. Turning cold tumors into hot tumors by improving T-cell infiltration. Theranostics. 2021;11(11):5365-86.
48. Reijers ILM, Dimitriadis P, Rozeman EA, Krijgsman O, Cornelissen S, Bosch LJW, et al. The interferon-gamma (IFN-y) signature from baseline tumor material predicts pathologic response after neoadjuvant ipilimumab (IPI) + nivolumab (NIVO) in stage III melanoma. Journal of Clinical Oncology. 2022;40(16_suppl):9539-.
49. Reijers ILM, Rao D, Versluis JM, Menzies AM, Dimitriadis P, Wouters MW, et al. IFN-gamma signature enables selection of neoadjuvant treatment in patients with stage III melanoma. J Exp Med. 2023;220(5).
50. Huang AC, Zappasodi R. A decade of checkpoint blockade immunotherapy in melanoma: understanding the molecular basis for immune sensitivity and resistance. Nature immunology. 2022;23(5):660-70.
51. Zhou B, Basu J, Kazmi HR, Chitrala KN, Mo X, Preston-Alp S, et al. Interferon-gamma signaling promotes melanoma progression and metastasis. Oncogene. 2023;42(5):351-63.
52. Blonski PJ, Czarnecka AM, Ostaszewski K, Szumera-Cieckiewicz A, Rutkowski P. Molecular and Clinicopathological Biomarkers in the Neoadjuvant Treatment of Patients with Advanced Resectable Melanoma. Biomedicines. 2024;12(3).
53. Ferraresi V, Vari S. Neoadjuvant immune checkpoint inhibitors in high-risk stage III melanoma. Hum Vaccin Immunother. 2022;18(3):1971015.
54. Reijers ILM, Dimitriadis P, Rozeman EA, Versluis JM, Broeks A, Bosch LJW, et al. Personalized combination of neoadjuvant domatinostat, nivolumab and ipilimumab in macroscopic stage III melanoma patients stratified according to the interferon-gamma signature: The DONIMI study. Journal of Clinical Oncology. 2020;38(15_suppl):TPS10087-TPS.
55. Holder AM, Wargo JA, Ross MI. Timing is Everything: Neoadjuvant Versus Adjuvant Immunotherapy in Patients with Resectable Metastatic Melanoma. Ann Surg Oncol. 2023;30(12):6953-7.
56. Hoeijmakers LL, Reijers ILM, Blank CU. Biomarker-Driven Personalization of Neoadjuvant Immunotherapy in Melanoma. Cancer Discov. 2023;13(11):2319-38.
57. Patel SP, Othus M, Chen Y, Wright GP, Yost KJ, Hyngstrom JR, et al. Neoadjuvant–Adjuvant or Adjuvant-Only Pembrolizumab in Advanced Melanoma. New England Journal of Medicine. 2023;388(9):813-23.
58. Witt RG, Erstad DJ, Wargo JA. Neoadjuvant therapy for melanoma: rationale for neoadjuvant therapy and pivotal clinical trials. Therapeutic Advances in Medical Oncology. 2022;14:17588359221083052.
59. Luke JJ, Rutkowski P, Queirolo P, Vecchio MD, Mackiewicz J, Chiarion-Sileni V, et al. Pembrolizumab versus placebo as adjuvant therapy in completely resected stage IIB or IIC melanoma (KEYNOTE-716): a randomised, double-blind, phase 3 trial. The Lancet. 2022;399(10336):1718-29.
60. Conry RM, Westbrook B, McKee S, Norwood TG. Talimogene laherparepvec: First in class oncolytic virotherapy. Human Vaccines & Immunotherapeutics. 2018;14(4):839-46.

61. Huppert LA, Daud AI. Intratumoral therapies and in-situ vaccination for melanoma. Human Vaccines & Immunotherapeutics. 2022;18(3):1890512.
62. Nelson BE, Adashek JJ, Lin SH, Subbiah V. The abscopal effect in patients with cancer receiving immunotherapy. Med. 2023;4(4):233-44.
63. Dummer R, Gyorki DE, Hyngstrom JR, Ning M, Lawrence T, Ross MI. Final 5-Year Follow-Up Results Evaluating Neoadjuvant Talimogene Laherparepvec Plus Surgery in Advanced Melanoma: A Randomized Clinical Trial. JAMA Oncology. 2023.
64. Cai J, Lin K, Cai W, Lin Y, Liu X, Guo L, et al. Tumors driven by RAS signaling harbor a natural vulnerability to oncolytic virus M1. Mol Oncol. 2020;14(12):3153-68.
65. Lemos de Matos A, Franco LS, McFadden G. Oncolytic Viruses and the Immune System: The Dynamic Duo. Mol Ther Methods Clin Dev. 2020;17:349-58.
66. Kaufman HL, Shalhout SZ, Iodice G. Talimogene Laherparepvec: Moving From First-In-Class to Best-In-Class. Frontiers in Molecular Biosciences. 2022;9:834841.
67. Lee J, Ghonime MG, Wang R, Cassady KA. The Antiviral Apparatus: STING and Oncolytic Virus Restriction. Mol Ther Oncolytics. 2019;13:7-13.
68. Thorne SH. Adding STING to the Tale of Oncolytic Virotherapy. Trends Cancer. 2016;2(2):67-8.
69. Su Y, Su C, Qin L. Current landscape and perspective of oncolytic viruses and their combination therapies. Transl Oncol. 2022;25:101530.
70. Chesney JA, Ribas A, Long GV, Kirkwood JM, Dummer R, Puzanov I, et al. Randomized, Double-Blind, Placebo-Controlled, Global Phase III Trial of Talimogene Laherparepvec Combined With Pembrolizumab for Advanced Melanoma. Journal of Clinical Oncology. 2023;41(3):528-40.
71. Mandala M, Merelli B, Massi D. PD-L1 in melanoma: facts and myths. Melanoma Manag. 2016;3(3):187-94.
72. Vilain RE, Menzies AM, Wilmott JS, Kakavand H, Madore J, Guminski A, et al. Dynamic Changes in PD-L1 Expression and Immune Infiltrates Early During Treatment Predict Response to PD-1 Blockade in Melanoma. Clin Cancer Res. 2017;23(17):5024-33.
73. Li Z, Ding Y, Liu J, Wang J, Mo F, Wang Y, et al. Depletion of tumor associated macrophages enhances local and systemic platelet-mediated anti-PD-1 delivery for post-surgery tumor recurrence treatment. Nat Commun. 2022;13(1):1845.
74. Sheban F. It takes two to tango: the role of tumor-associated macrophages in T cell-directed immune checkpoint blockade therapy. Front Immunol. 2023;14:1183578.
75. Xu S, Wang C, Yang L, Wu J, Li M, Xiao P, et al. Targeting immune checkpoints on tumor-associated macrophages in tumor immunotherapy. Front Immunol. 2023;14:1199631.
76. Sánchez-Magraner L, Miles J, Baker CL, Applebee CJ, Lee D-J, Elsheikh S, et al. High PD-1/PD-L1 Checkpoint Interaction Infers Tumor Selection and Therapeutic Sensitivity to Anti-PD-1/PD-L1 Treatment. Cancer Research. 2020;80(19):4244-57.
77. Sánchez-Magraner L, Gumuzio J, Miles J, Quimi N, Martínez del Prado P, Abad-Villar MT, et al. Functional Engagement of the PD-1/PD-L1 Complex But Not PD-L1 Expression Is Highly Predictive of Patient Response to Immunotherapy in Non–Small-Cell Lung Cancer. Journal of Clinical Oncology. 2023;41(14):2561-70.

78. Miles J, Soubeyran I, Marliot F, Pangon N, Italiano A, Bellera C, et al. Determination of Interactive States of Immune Checkpoint Regulators in Lung Metastases after Radiofrequency Ablation. Cancers. 2022;14(23):5738.
79. Dutta H, Jain N. Post-translational modifications and their implications in cancer. Front Oncol. 2023;13:1240115.
80. Marchese E, Demehri S. Posttranslational protein modifications as gatekeepers of cancer immunogenicity. J Clin Invest. 2024;134(10).
81. Safrygina E, Applebee C, McIntyre A, Padget J, Larijani B. Spatial functional mapping of hypoxia inducible factor heterodimerisation and immune checkpoint regulators in clear cell renal cell carcinoma. BJC Reports. 2024;2(1):10.
82. Li K, Shi H, Zhang B, Ou X, Ma Q, Chen Y, et al. Myeloid-derived suppressor cells as immunosuppressive regulators and therapeutic targets in cancer. Signal Transduction and Targeted Therapy. 2021;6.
83. Planes-Laine G, Rochigneux P, Bertucci F, Chretien AS, Viens P, Sabatier R, et al. PD-1/PD-L1 Targeting in Breast Cancer: The First Clinical Evidences Are Emerging. A Literature Review. Cancers (Basel). 2019;11(7).
84. Asai Y, Yanagawa N, Osakabe M, Yamada N, Sugimoto R, Sato A, et al. The clinicopathological impact of tumor-associated macrophages in patients with cutaneous malignant melanoma. J Surg Oncol. 2024;129(2):381-91.
85. Chen P, Huang Y, Bong R, Ding Y, Song N, Wang X, et al. Tumor-associated macrophages promote angiogenesis and melanoma growth via adrenomedullin in a paracrine and autocrine manner. Clin Cancer Res. 2011;17(23):7230-9.
86. Landry AP, Balas M, Alli S, Spears J, Zador Z. Distinct regional ontogeny and activation of tumor associated macrophages in human glioblastoma. Sci Rep. 2020;10(1):19542.
87. Habib S, Osborn G, Willsmore Z, Chew MW, Jakubow S, Fitzpatrick A, et al. Tumor associated macrophages as key contributors and targets in current and future therapies for melanoma. Expert Rev Clin Immunol. 2024;20(8):895-911.
88. Duan Z, Luo Y. Targeting macrophages in cancer immunotherapy. Signal Transduction and Targeted Therapy. 2021;6(1):127.
89. Gao J, Liang Y, Wang L. Shaping Polarization Of Tumor-Associated Macrophages In Cancer Immunotherapy. Front Immunol. 2022;13:888713.
90. Liu ZL, Chen HH, Zheng LL, Sun LP, Shi L. Angiogenic signaling pathways and anti-angiogenic therapy for cancer. Signal Transduct Target Ther. 2023;8(1):198.
91. Sesarman A, Luput L, Rauca VF, Patras L, Licarete E, Meszaros MS, et al. Targeting of M2 macrophages with IL-13-functionalized liposomal prednisolone inhibits melanoma angiogenesis in vivo. J Liposome Res. 2024:1-12.
92. Hussein MR. Tumour-associated macrophages and melanoma tumourigenesis: integrating the complexity. Int J Exp Pathol. 2006;87(3):163-76.
93. Yang YL, Yang F, Huang ZQ, Li YY, Shi HY, Sun Q, et al. T cells, NK cells, and tumor-associated macrophages in cancer immunotherapy and the current state of the art of drug delivery systems. Front Immunol. 2023;14:1199173.
94. Denton NL, Chen CY, Scott TR, Cripe TP. Tumor-Associated Macrophages in Oncolytic Virotherapy: Friend or Foe? Biomedicines. 2016;4(3).

95. Hofman L, Lawler SE, Lamfers MLM. The Multifaceted Role of Macrophages in Oncolytic Virotherapy. Viruses. 2021;13(8).
96. Shen Z, Liu X, Fan G, Na J, Liu Q, Lin F, et al. Improving the therapeutic efficacy of oncolytic viruses for cancer: targeting macrophages. J Transl Med. 2023;21(1):842.
97. Hong I-S. Stimulatory versus suppressive effects of GM-CSF on tumor progression in multiple cancer types. Experimental & Molecular Medicine. 2016;48(7):e242.
98. Nguyen T-T, Ramsay L, Ahanfeshar-Adams M, Lajoie M, Schadendorf D, Alain T, et al. Mutations in the IFNγ-JAK-STAT Pathway Causing Resistance to Immune Checkpoint Inhibitors in Melanoma Increase Sensitivity to Oncolytic Virus Treatment. Clinical Cancer Research: An Official Journal of the American Association for Cancer Research. 2021;27(12):3432-42.
99. Owen KL, Brockwell NK, Parker BS. JAK-STAT Signaling: A Double-Edged Sword of Immune Regulation and Cancer Progression. Cancers. 2019;11(12):2002.
100. Kumar V, Giacomantonio MA, Gujar S. Role of Myeloid Cells in Oncolytic Reovirus-Based Cancer Therapy. Viruses. 2021;13(4):654.
101. Goyette M-A, Côté J-F. AXL Receptor Tyrosine Kinase as a Promising Therapeutic Target Directing Multiple Aspects of Cancer Progression and Metastasis. Cancers. 2022;14(3):466.
102. Wium M, Ajayi-Smith AF, Paccez JD, Zerbini LF. The Role of the Receptor Tyrosine Kinase Axl in Carcinogenesis and Development of Therapeutic Resistance: An Overview of Molecular Mechanisms and Future Applications. Cancers. 2021;13(7):1521.
103. Jimenez-Garcia L, Mayer C, Burrola PG, Huang Y, Shokhirev MN, Lemke G. The TAM receptor tyrosine kinases Axl and Mer drive the maintenance of highly phagocytic macrophages. Front Immunol. 2022;13:960401.
104. Wei J, Sun H, Zhang A, Wu X, Li Y, Liu J, et al. A novel AXL chimeric antigen receptor endows T cells with anti-tumor effects against triple negative breast cancers. Cell Immunol. 2018;331:49-58.
105. Levin PA, Brekken RA, Byers LA, Heymach JV, Gerber DE. Axl Receptor Axis: A New Therapeutic Target in Lung Cancer. J Thorac Oncol. 2016;11(8):1357-62.
106. Engelsen AST, Lotsberg ML, Abou Khouzam R, Thiery J-P, Lorens JB, Chouaib S, et al. Dissecting the Role of AXL in Cancer Immune Escape and Resistance to Immune Checkpoint Inhibition. Frontiers in Immunology. 2022;13:869676.
107. Ludwig KF, Du W, Sorrelle NB, Wnuk-Lipinska K, Topalovski M, Toombs JE, et al. Small-Molecule Inhibition of Axl Targets Tumor Immune Suppression and Enhances Chemotherapy in Pancreatic Cancer. Cancer Res. 2018;78(1):246-55.
108. Gausdal G, Micklem DR, Blø M, Rayford A, Alzhanova D, Madeleine N, et al. 598 Bemcentinib + pembrolizumab show promising efficacy in metastatic NSCLC harbouring mutations associated with poor prognosis: exploratory sub-analysis from the BGBC008 trial (NCT03184571). Journal for ImmunoTherapy of Cancer. 2023;11(Suppl 1):A680-A1.
109. DeBerge M, Glinton K, Subramanian M, Wilsbacher LD, Rothlin CV, Tabas I, et al. Macrophage AXL receptor tyrosine kinase inflames the heart after reperfused myocardial infarction. The Journal of Clinical Investigation. 2021;131(6):e139576.

110. Fujimori T, Grabiec AM, Kaur M, Bell TJ, Fujino N, Cook PC, et al. The Axl receptor tyrosine kinase is a discriminator of macrophage function in the inflamed lung. Mucosal Immunol. 2015;8(5):1021-30.
111. Tanaka M, Dykes SS, Siemann DW. Inhibition of the Axl pathway impairs breast and prostate cancer metastasis to the bones and bone remodeling. Clin Exp Metastasis. 2021;38(3):321-35.
112. Tanaka T, Koga H, Suzuki H, Iwamoto H, Sakaue T, Masuda A, et al. Anti-PD-L1 antibodies promote cellular proliferation by activating the PD-L1-AXL signal relay in liver cancer cells. Hepatol Int. 2024;18(3):984-97.
113. Rankin EB, Giaccia AJ. The Receptor Tyrosine Kinase AXL in Cancer Progression. Cancers. 2016;8(11):103.
114. Tirado-Gonzalez I, Descot A, Soetopo D, Nevmerzhitskaya A, Schäffer A, Kur I-M, et al. AXL Inhibition in Macrophages Stimulates Host-versus-Leukemia Immunity and Eradicates Naïve and Treatment-Resistant Leukemia. Cancer Discovery. 2021;11(11):2924-43.
115. Boutilier AJ, Elsawa SF. Macrophage Polarization States in the Tumor Microenvironment. International Journal of Molecular Sciences. 2021;22(13):6995.
116. Strizova Z, Benesova I, Bartolini R, Novysedlak R, Cecrdlova E, Foley Lily K, et al. M1/M2 macrophages and their overlaps – myth or reality? Clin Sci (Lond). 2023;137(15):1067-93.
117. Rigoni TS, Vellozo NS, Guimarães-Pinto K, Cabral-Piccin M, Fabiano-Coelho L, Matos-Silva TC, et al. Axl receptor induces efferocytosis, dampens M1 macrophage responses and promotes heart pathology in Trypanosoma cruzi infection. Communications Biology. 2022;5:1421.
118. Zhai X, Pu D, Wang R, Zhang J, Lin Y, Wang Y, et al. Gas6/AXL pathway: immunological landscape and therapeutic potential. Front Oncol. 2023;13:1121130.
119. Chen Y, Miles DH, Udyavar A, Cho S, Becker A, Foley C, et al. Kinetic and Mechanistic Characterization of a Potent and Selective Inhibitor for Human AXL Receptor Tyrosine Kinase. The FASEB Journal. 2020;34(S1):1-.
120. Yi M, Li T, Niu M, Mei Q, Zhao B, Chu Q, et al. Exploiting innate immunity for cancer immunotherapy. Mol Cancer. 2023;22(1):187.
121. Myers SH, Brunton VG, Unciti-Broceta A. AXL Inhibitors in Cancer: A Medicinal Chemistry Perspective. Journal of Medicinal Chemistry. 2016;59(8):3593-608.
122. Sang YB, Kim JH, Kim CG, Hong MH, Kim HR, Cho BC, et al. The Development of AXL Inhibitors in Lung Cancer: Recent Progress and Challenges. Front Oncol. 2022;12:811247.
123. Jerby-Arnon L, Shah P, Cuoco MS, Rodman C, Su MJ, Melms JC, et al. A Cancer Cell Program Promotes T Cell Exclusion and Resistance to Checkpoint Blockade. Cell. 2018;175(4):984-97 e24.
124. Hugo W, Zaretsky JM, Sun L, Song C, Moreno BH, Hu-Lieskovan S, et al. Genomic and Transcriptomic Features of Response to Anti-PD-1 Therapy in Metastatic Melanoma. Cell. 2016;165(1):35-44.
125. Lee CH, Yen CY, Liu SY, Chen CK, Chiang CF, Shiah SG, et al. Axl is a prognostic marker in oral squamous cell carcinoma. Ann Surg Oncol. 2012;19 Suppl 3:S500-8.

126. Elantably D, Wang J, Armashi ARA, Zubaidi AA, Alkrekshi A. The association between body mass index and immune checkpoint inhibitors outcomes in melanoma: Results from real-world data. Journal of Clinical Oncology. 2023;41(16_suppl):e14604-e.
127. Gunjur A, Manrique-Rincon AJ, Klein O, Behren A, Lawley TD, Welsh SJ, et al. 'Know thyself' - host factors influencing cancer response to immune checkpoint inhibitors. J Pathol. 2022;257(4):513-25.
128. Roccuzzo G, Moirano G, Fava P, Maule M, Ribero S, Quaglino P. Obesity and immune-checkpoint inhibitors in advanced melanoma: A meta-analysis of survival outcomes from clinical studies. Semin Cancer Biol. 2023;91:27-34.
129. Scott SC, Shao XM, Niknafs N, Balan A, Pereira G, Marrone KA, et al. Sex-specific differences in immunogenomic features of response to immune checkpoint blockade. Front Oncol. 2022;12:945798.
130. Veeriah S, Leboucher P, de Naurois J, Jethwa N, Nye E, Bunting T, et al. High-throughput time-resolved FRET reveals Akt/PKB activation as a poor prognostic marker in breast cancer. Cancer Res. 2014;74(18):4983-95.
131. Maaten Lvd, Hinton G. Visualizing Data using t-SNE. Journal of Machine Learning Research. 2008;9(86):2579-605.
132. Wallach I, Lilien R. The protein-small-molecule database, a non-redundant structural resource for the analysis of protein-ligand binding. Bioinformatics (Oxford, England). 2009;25(5):615-20.
133. Kirane A, Toombs JE, Larsen JE, Ostapoff KT, Meshaw KR, Zaknoen S, et al. Epithelial-mesenchymal transition increases tumor sensitivity to COX-2 inhibition by apricoxib. Carcinogenesis. 2012;33(9):1639-46.
134. Justus CR, Leffler N, Ruiz-Echevarria M, Yang LV. In vitro Cell Migration and Invasion Assays. J Vis Exp. 2014(88):51046.
135. Heistein JB, Acharya U, Mukkamalla SKR. Malignant Melanoma. StatPearls. Treasure Island (FL): StatPearls Publishing; 2023.
136. Testori AAE, Chiellino S, van Akkooi ACJ. Adjuvant Therapy for Melanoma: Past, Current, and Future Developments. Cancers. 2020;12(7):1994.
137. Poklepovic AS, Luke JJ. Considering adjuvant therapy for stage II melanoma. Cancer. 2020;126(6):1166-74.
138. Gershenwald JE, Scolyer RA, Hess KR, Sondak VK, Long GV, Ross MI, et al. Melanoma Staging: Evidence-Based Changes in the American Joint Committee on Cancer Eighth Edition Cancer Staging Manual. CA: a cancer journal for clinicians. 2017;67(6):472-92.
139. Melanoma Risk Assessment Tool: Online Calculator. Melanoma Risk Assessment Tool.
140. Mueller SN, Rouse BT. Immune responses to viruses. Clinical Immunology. 2008:421-31.
141. van Pul KM, Notohardjo JCL, Fransen MF, Koster BD, Stam AGM, Chondronasiou D, et al. Local delivery of low-dose anti-CTLA-4 to the melanoma lymphatic basin leads to systemic Treg reduction and effector T cell activation. Science Immunology. 2022;7(73):eabn8097.

142. Bateni SB, Walsh AN, Xu AJ, Gingrich AA, Maverakis E, Kirane AR. Association between warfarin and survival in invasive melanoma: a population-based cohort study. Surgical Oncology Insight. 2024;1(3).
143. Rawson RV, Adhikari C, Bierman C, Lo SN, Shklovskaya E, Rozeman EA, et al. Pathological response and tumour bed histopathological features correlate with survival following neoadjuvant immunotherapy in stage III melanoma. Annals of Oncology: Official Journal of the European Society for Medical Oncology. 2021;32(6):766-77.
144. Tetzlaff MT, Messina JL, Stein JE, Xu X, Amaria RN, Blank CU, et al. Pathological assessment of resection specimens after neoadjuvant therapy for metastatic melanoma. Annals of Oncology: Official Journal of the European Society for Medical Oncology. 2018;29(8):1861-8.
145. Koster BD, Lopez Gonzalez M, van den Hout MF, Turksma AW, Sluijter BJ, Molenkamp BG, et al. T cell infiltration on local CpG-B delivery in early-stage melanoma is predominantly related to CLEC9A(+)CD141(+) cDC1 and CD14(+) antigen-presenting cell recruitment. J Immunother Cancer. 2021;9(3).
146. Koster BD, van den Hout M, Sluijter BJR, Molenkamp BG, Vuylsteke R, Baars A, et al. Local Adjuvant Treatment with Low-Dose CpG-B Offers Durable Protection against Disease Recurrence in Clinical Stage I-II Melanoma: Data from Two Randomized Phase II Trials. Clin Cancer Res. 2017;23(19):5679-86.
147. Weber R, Fleming V, Hu X, Nagibin V, Groth C, Altevogt P, et al. Myeloid-Derived Suppressor Cells Hinder the Anti-Cancer Activity of Immune Checkpoint Inhibitors. Front Immunol. 2018;9:1310.
148. Peranzoni E, Ingangi V, Masetto E, Pinton L, Marigo I. Myeloid Cells as Clinical Biomarkers for Immune Checkpoint Blockade. Front Immunol. 2020;11:1590.
149. Kumar A, Taghi Khani A, Sanchez Ortiz A, Swaminathan S. GM-CSF: A Double-Edged Sword in Cancer Immunotherapy. Frontiers in Immunology. 2022;13:901277.
150. Scaltriti M, Elkabets M, Baselga J. Molecular Pathways: AXL, a Membrane Receptor Mediator of Resistance to Therapy. Clin Cancer Res. 2016;22(6):1313-7.
151. Indini A, Rijavec E, Ghidini M, Tomasello G, Cattaneo M, Barbin F, et al. Impact of BMI on Survival Outcomes of Immunotherapy in Solid Tumors: A Systematic Review. Int J Mol Sci. 2021;22(5).
152. Santoni M, Rizzo A, Mollica V, Matrana MR, Rosellini M, Faloppi L, et al. The impact of gender on The efficacy of immune checkpoint inhibitors in cancer patients: The MOUSEION-01 study. Crit Rev Oncol Hematol. 2022;170:103596.
153. Leconet W, Larbouret C, Chardes T, Thomas G, Neiveyans M, Busson M, et al. Preclinical validation of AXL receptor as a target for antibody-based pancreatic cancer immunotherapy. Oncogene. 2014;33(47):5405-14.
154. Du W, Brekken RA. Does Axl have potential as a therapeutic target in pancreatic cancer? Expert Opin Ther Targets. 2018;22(11):955-66.
155. Vick LV, Rosario S, Riess JW, Canter RJ, Mukherjee S, Monjazeb AM, et al. Potential roles of sex-linked differences in obesity and cancer immunotherapy: revisiting the obesity paradox. NPJ Metab Health Dis. 2024;2(1):5.

156. Muller J, Krijgsman O, Tsoi J, Robert L, Hugo W, Song C, et al. Low MITF/AXL ratio predicts early resistance to multiple targeted drugs in melanoma. Nat Commun. 2014;5:5712.
157. Bai X, Fisher DE, Flaherty KT. Cell-state dynamics and therapeutic resistance in melanoma from the perspective of MITF and IFNgamma pathways. Nat Rev Clin Oncol. 2019;16(9):549-62.
158. Ahn A, Chatterjee A, Eccles MR. The Slow Cycling Phenotype: A Growing Problem for Treatment Resistance in Melanoma. Mol Cancer Ther. 2017;16(6):1002-9.
159. Radke J, Schumann E, Onken J, Koll R, Acker G, Bodnar B, et al. Decoding molecular programs in melanoma brain metastases. Nat Commun. 2022;13(1):7304.
160. Tanaka M, Siemann DW. Therapeutic Targeting of the Gas6/Axl Signaling Pathway in Cancer. Int J Mol Sci. 2021;22(18).
161. Repici A, Ardizzone A, De Luca F, Colarossi L, Prestifilippo A, Pizzino G, et al. Signaling Pathways of AXL Receptor Tyrosine Kinase Contribute to the Pathogenetic Mechanisms of Glioblastoma. Cells. 2024;13(4).
162. Li H, Liu Z, Liu L, Zhang H, Han C, Girard L, et al. AXL targeting restores PD-1 blockade sensitivity of STK11/LKB1 mutant NSCLC through expansion of TCF1(+) CD8 T cells. Cell Rep Med. 2022;3(3):100554.
163. Axelrod H, Pienta KJ. Axl as a mediator of cellular growth and survival. Oncotarget. 2014;5(19):8818-52.
164. Sadahiro H, Kang KD, Gibson JT, Minata M, Yu H, Shi J, et al. Activation of the Receptor Tyrosine Kinase AXL Regulates the Immune Microenvironment in Glioblastoma. Cancer Res. 2018;78(11):3002-13.
165. Najafov A, Mookhtiar AK, Luu HS, Ordureau A, Pan H, Amin PP, et al. TAM Kinases Promote Necroptosis by Regulating Oligomerization of MLKL. Mol Cell. 2019;75(3):457-68 e4.
166. Yang X, Wang Z, Zandkarimi F, Liu Y, Duan S, Li Z, et al. Regulation of VKORC1L1 is critical for p53-mediated tumor suppression through vitamin K metabolism. Cell Metab. 2023;35(8):1474-90 e8.
167. Eriksson AS, Eriksson H, Hansson PO, Svardsudd K. Warfarin intake in relation to diagnosis reduces mortality in patients with colorectal cancer - a register-based study. Cancer Treat Res Commun. 2024;40:100820.
168. O'Rorke MA, Murray LJ, Hughes CM, Cantwell MM, Cardwell CR. The effect of warfarin therapy on breast, colorectal, lung, and prostate cancer survival: a population-based cohort study using the Clinical Practice Research Datalink. Cancer Causes Control. 2015;26(3):355-66.
169. Esteban-Fabro R, Willoughby CE, Pique-Gili M, Montironi C, Abril-Fornaguera J, Peix J, et al. Cabozantinib Enhances Anti-PD1 Activity and Elicits a Neutrophil-Based Immune Response in Hepatocellular Carcinoma. Clin Cancer Res. 2022;28(11):2449-60.
170. Mannsaker TA, Hoang T, Aasen SN, Bjornstad OV, Parajuli H, Sundstrom T, et al. Cabozantinib Is Effective in Melanoma Brain Metastasis Cell Lines and Affects Key Signaling Pathways. Int J Mol Sci. 2021;22(22).
171. Schmidinger M, Danesi R. Management of Adverse Events Associated with Cabozantinib Therapy in Renal Cell Carcinoma. Oncologist. 2018;23(3):306-15.

172. Hume DA, MacDonald KP. Therapeutic applications of macrophage colony-stimulating factor-1 (CSF-1) and antagonists of CSF-1 receptor (CSF-1R) signaling. Blood. 2012;119(8):1810-20.
173. Cannarile MA, Weisser M, Jacob W, Jegg AM, Ries CH, Ruttinger D. Colony-stimulating factor 1 receptor (CSF1R) inhibitors in cancer therapy. J Immunother Cancer. 2017;5(1):53.
174. Moeller A, Kurzrock R, Botta GP, Adashek JJ, Patel H, Lee S, et al. Challenges and prospects of CSF1R targeting for advanced malignancies. American Journal of Cancer Research. 2023;13(7):3257-65.
175. Ordentlich P. Clinical evaluation of colony-stimulating factor 1 receptor inhibitors. Semin Immunol. 2021;54:101514.
176. Duong L, Radley-Crabb HG, Gardner JK, Tomay F, Dye DE, Grounds MD, et al. Macrophage Depletion in Elderly Mice Improves Response to Tumor Immunotherapy, Increases Anti-tumor T Cell Activity and Reduces Treatment-Induced Cachexia. Front Genet. 2018;9:526.
177. Egashira M, Hirota Y, Shimizu-Hirota R, Saito-Fujita T, Haraguchi H, Matsumoto L, et al. F4/80+ Macrophages Contribute to Clearance of Senescent Cells in the Mouse Postpartum Uterus. Endocrinology. 2017;158(7):2344-53.
178. Patton EE, Mueller KL, Adams DJ, Anandasabapathy N, Aplin AE, Bertolotto C, et al. Melanoma models for the next generation of therapies. Cancer Cell. 2021;39(5):610-31.
179. Rebecca VW, Somasundaram R, Herlyn M. Pre-clinical modeling of cutaneous melanoma. Nat Commun. 2020;11(1):2858.
180. Meeth K, Wang JX, Micevic G, Damsky W, Bosenberg MW. The YUMM lines: a series of congenic mouse melanoma cell lines with defined genetic alterations. Pigment Cell Melanoma Res. 2016;29(5):590-7.
181. Lelliott EJ, Cullinane C, Martin CA, Walker R, Ramsbottom KM, Souza-Fonseca-Guimaraes F, et al. A novel immunogenic mouse model of melanoma for the preclinical assessment of combination targeted and immune-based therapy. Sci Rep. 2019;9(1):1225.
182. Carlson PM, Mohan M, Rodriguez M, Subbotin V, Sun CX, Patel RB, et al. Depth of tumor implantation affects response to in situ vaccination in a syngeneic murine melanoma model. J Immunother Cancer. 2021;9(4).
183. Wang J, Perry CJ, Meeth K, Thakral D, Damsky W, Micevic G, et al. UV-induced somatic mutations elicit a functional T cell response in the YUMMER1.7 mouse melanoma model. Pigment Cell Melanoma Res. 2017;30(4):428-35.
184. Yuki K, Cheng N, Nakano M, Kuo CJ. Organoid Models of Tumor Immunology. Trends Immunol. 2020;41(8):652-64.
185. Magre L, Verstegen MMA, Buschow S, van der Laan LJW, Peppelenbosch M, Desai J. Emerging organoid-immune co-culture models for cancer research: from oncoimmunology to personalized immunotherapies. J Immunother Cancer. 2023;11(5).
186. Barker RN, Erwig LP, Hill KS, Devine A, Pearce WP, Rees AJ. Antigen presentation by macrophages is enhanced by the uptake of necrotic, but not apoptotic, cells. Clin Exp Immunol. 2002;127(2):220-5.
187. Park J, Wang L, Ho PC. Metabolic guidance and stress in tumors modulate antigen-presenting cells. Oncogenesis. 2022;11(1):62.

Appendix: Copyright documentation

Figure 2-1

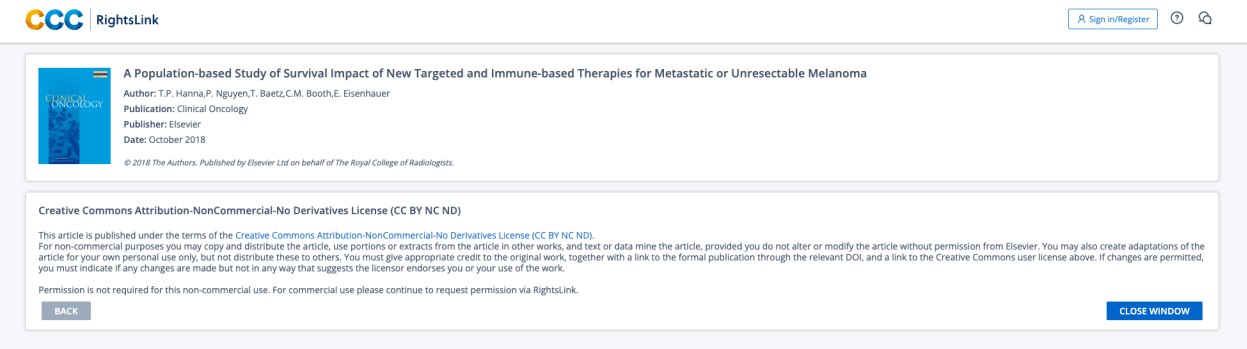

Figure 2-2

SPRINGER NATURE LICENSE
TERMS AND CONDITIONS
Aug 27, 2024

This Agreement between Amanda Kirane ("You") and Springer Nature ("Springer Nature") consists of your license details and the terms and conditions provided by Springer Nature and Copyright Clearance Center.

License Number	5857220663279
License date	Aug 27, 2024
Licensed Content Publisher	Springer Nature
Licensed Content Publication	Annals of Surgical Oncology
Licensed Content Title	Timing is Everything: Neoadjuvant Versus Adjuvant Immunotherapy in Patients with Resectable Metastatic Melanoma
Licensed Content Author	Ashley M. Holder MD et al
Licensed Content Date	Aug 19, 2023

Type of Use	Thesis/Dissertation
Requestor type	academic/university or research institute
Format	electronic
Portion	figures/tables/illustrations
Number of figures/tables/illustrations	2
Will you be translating?	no
Circulation/distribution	1 - 29
Author of this Springer Nature content	no
Title of new work	Targeting macrophages in immunotherapy resistant melanoma
Institution name	UC Davis
Expected presentation date	Sep 2024
Portions	Figure 1 and 2A
The Requesting Person / Organization to Appear on the License	Amanda Kirane Amanda R Kirane Surgery
Requestor Location	PALO ALTO, CA 94304 United States Attn: Stanford
Billing Type	Invoice
Billing Address	Amanda R Kirane Surgery PALO ALTO, CA 94304 United States Attn: Stanford
Total	0.00 USD

Terms and Conditions

Springer Nature Customer Service Centre GmbH Terms and Conditions
The following terms and conditions ("Terms and Conditions") together with the terms specified in your [RightsLink] constitute the License ("License") between you as Licensee and Springer Nature Customer Service Centre GmbH as Licensor. By clicking 'accept' and completing the transaction for your use of the material ("Licensed Material"), you confirm your acceptance of and obligation to be bound by these Terms and Conditions.

Grant and Scope of License
1. 1. The Licensor grants you a personal, non-exclusive, non-transferable, nonsublicensable, revocable, world-wide License to reproduce, distribute, communicate to the public, make available, broadcast, electronically transmit or create derivative works using the Licensed Material for the purpose(s) specified in your RightsLink Licence Details only. Licenses are granted for the specific use requested in the order and for no other use, subject to these Terms and Conditions. You acknowledge and agree that the rights granted to you under this License do not include the right to modify, edit, translate, include in collective works, or create derivative works of the Licensed Material in whole or in part unless expressly stated in your RightsLink
Licence Details. You may use the Licensed Material only as permitted under this Agreement and will not reproduce, distribute, display, perform, or otherwise use or exploit any Licensed Material in any way, in whole or in part, except as expressly permitted by this License.
1. 2. You may only use the Licensed Content in the manner and to the extent permitted by these Terms and Conditions, by your RightsLink Licence Details and by any applicable laws.
1. 3. A separate license may be required for any additional use of the Licensed Material, e.g. where a license has been purchased for print use only, separate permission must be obtained for electronic re-use. Similarly, a License is only valid in the language selected and does not apply for editions in other languages unless additional translation rights have been granted separately in the License.
1. 4. Any content within the Licensed Material that is owned by third parties is expressly excluded from the License.
1. 5. Rights for additional reuses such as custom editions, computer/mobile applications, film or TV reuses and/or any other derivative rights requests require additional permission and may be subject to an additional fee. Please apply to
journalpermissions@springernature.com or bookpermissions@springernature.com for these rights.

Reservation of Rights
Licensor reserves all rights not expressly granted to you under this License. You acknowledge and agree that nothing in this License limits or restricts Licensor's rights in or use of the Licensed Material in any way. Neither this License, nor any act, omission, or statement by Licensor or you, conveys any ownership right to you in any Licensed Material, or to any element or portion thereof. As between Licensor and you, Licensor owns and retains all right, title, and interest in and to the Licensed Material subject to the license

granted in Section 1.1. Your permission to use the Licensed Material is expressly conditioned on you not impairing Licensor's or the applicable copyright owner's rights in the Licensed Material in any way.

Restrictions on use

3. 1. Minor editing privileges are allowed for adaptations for stylistic purposes or formatting purposes provided such alterations do not alter the original meaning or intention of the Licensed Material and the new figure(s) are still accurate and representative of the Licensed Material. Any other changes including but not limited to, cropping, adapting, and/or omitting material that affect the meaning, intention or moral rights of the author(s) are strictly prohibited.
3. 2. You must not use any Licensed Material as part of any design or trademark.
3. 3. Licensed Material may be used in Open Access Publications (OAP), but any such reuse must include a clear acknowledgment of this permission visible at the same time as the figures/tables/illustration or abstract and which must indicate that the Licensed Material is not part of the governing OA license but has been reproduced with permission. This may be indicated according to any standard referencing system but must include at a minimum 'Book/Journal title, Author, Journal Name (if applicable), Volume (if applicable), Publisher, Year, reproduced with permission from SNCSC'.

STM Permission Guidelines

4. 1. An alternative scope of license may apply to signatories of the STM Permissions Guidelines ("STM PG") as amended from time to time and made available at https://www.stm-assoc.org/intellectualproperty/permissions/permissions-guidelines/.
4. 2. For content reuse requests that qualify for permission under the STM PG, and which may be updated from time to time, the STM PG supersede the terms and conditions contained in this License.
4. 3. If a License has been granted under the STM PG, but the STM PG no longer apply at the time of publication, further permission must be sought from the Rightsholder. Contact journalpermissions@springernature.com or bookpermissions@springernature.com for these rights.

Duration of License

5. 1. Unless otherwise indicated on your License, a License is valid from the date of purchase ("License Date") until the end of the relevant period in the below table:

Reuse in a medical communications project	Reuse up to distribution or time period indicated in License
Reuse in a dissertation/thesis	Lifetime of thesis
Reuse in a journal/magazine	Lifetime of journal/magazine
Reuse in a book/textbook	Lifetime of edition

Reuse on a website	1 year unless otherwise specified in the License
Reuse in a presentation/slide kit/poster	Lifetime of presentation/slide kit/poster. Note: publication whether electronic or in print of presentation/slide kit/poster may require further permission.
Reuse in conference proceedings	Lifetime of conference proceedings
Reuse in an annual report	Lifetime of annual report
Reuse in training/CME materials	Reuse up to distribution or time period indicated in License
Reuse in newsmedia	Lifetime of newsmedia
Reuse in coursepack/classroom materials	Reuse up to distribution and/or time period indicated in license

Acknowledgement

6. 1. The Licensor's permission must be acknowledged next to the Licensed Material in print. In electronic form, this acknowledgement must be visible at the same time as the figures/tables/illustrations or abstract and must be hyperlinked to the journal/book's homepage.

6. 2. Acknowledgement may be provided according to any standard referencing system and at a minimum should include "Author, Article/Book Title, Journal name/Book imprint, volume, page number, year, Springer Nature".

Reuse in a dissertation or thesis

7. 1. Where 'reuse in a dissertation/thesis' has been selected, the following terms apply: Print rights of the Version of Record are provided for; electronic rights for use only on institutional repository as defined by the Sherpa guideline (www.sherpa.ac.uk/romeo/) and only up to what is required by the awarding institution.

7. 2. For theses published under an ISBN or ISSN, separate permission is required. Please contact journalpermissions@springernature.com or bookpermissions@springernature.com for these rights.

7. 3. Authors must properly cite the published manuscript in their thesis according to current citation standards and include the following acknowledgement: '*Reproduced with permission from Springer Nature*'.

License Fee

You must pay the fee set forth in the License Agreement (the "License Fees"). All amounts payable by you under this License are exclusive of any sales, use, withholding, value added

or similar taxes, government fees or levies or other assessments. Collection and/or remittance of such taxes to the relevant tax authority shall be the responsibility of the party who has the legal obligation to do so.

Warranty

9. 1. The Licensor warrants that it has, to the best of its knowledge, the rights to license reuse of the Licensed Material. You are solely responsible for ensuring that the material you wish to license is original to the Licensor and does not carry the copyright of another entity or third party (as credited in the published version). If the credit line on any part of the Licensed Material indicates that it was reprinted or adapted with permission from another source, then you should seek additional permission from that source to reuse the material.

9. 2. EXCEPT FOR THE EXPRESS WARRANTY STATED HEREIN AND TO THE EXTENT PERMITTED BY APPLICABLE LAW, LICENSOR PROVIDES THE LICENSED MATERIAL "AS IS" AND MAKES NO OTHER REPRESENTATION OR WARRANTY. LICENSOR EXPRESSLY DISCLAIMS ANY LIABILITY FOR ANY CLAIM ARISING FROM OR OUT OF THE CONTENT, INCLUDING BUT NOT LIMITED TO ANY ERRORS, INACCURACIES, OMISSIONS, OR DEFECTS CONTAINED THEREIN, AND ANY IMPLIED OR EXPRESS WARRANTY AS TO MERCHANTABILITY OR FITNESS FOR A PARTICULAR PURPOSE. IN NO EVENT SHALL LICENSOR BE LIABLE TO YOU OR ANY OTHER PARTY OR ANY OTHER PERSON OR FOR ANY SPECIAL, CONSEQUENTIAL, INCIDENTAL, INDIRECT, PUNITIVE, OR EXEMPLARY DAMAGES, HOWEVER CAUSED, ARISING OUT OF OR IN CONNECTION WITH THE DOWNLOADING, VIEWING OR USE OF THE LICENSED MATERIAL REGARDLESS OF THE FORM OF ACTION, WHETHER FOR BREACH OF CONTRACT, BREACH OF WARRANTY, TORT, NEGLIGENCE, INFRINGEMENT OR OTHERWISE (INCLUDING, WITHOUT LIMITATION, DAMAGES BASED ON LOSS OF PROFITS, DATA, FILES, USE, BUSINESS OPPORTUNITY OR CLAIMS OF THIRD PARTIES), AND WHETHER OR NOT THE PARTY HAS BEEN ADVISED OF THE POSSIBILITY OF SUCH DAMAGES. THIS LIMITATION APPLIES NOTWITHSTANDING ANY FAILURE OF ESSENTIAL PURPOSE OF ANY LIMITED REMEDY PROVIDED HEREIN.

Termination and Cancellation

10. 1. The License and all rights granted hereunder will continue until the end of the applicable period shown in Clause 5.1 above. Thereafter, this license will be terminated and all rights granted hereunder will cease.

10. 2. Licensor reserves the right to terminate the License in the event that payment is not received in full or if you breach the terms of this License.

General

11. 1. The License and the rights and obligations of the parties hereto shall be construed, interpreted and determined in accordance with the laws of the Federal

Republic of Germany without reference to the stipulations of the CISG (United Nations Convention on Contracts for the International Sale of Goods) or to Germaný s choice-of-law principle.
11. 2. The parties acknowledge and agree that any controversies and disputes arising out of this License shall be decided exclusively by the courts of or having jurisdiction for Heidelberg, Germany, as far as legally permissible.
11. 3. This License is solely for Licensor's and Licensee's benefit. It is not for the benefit of any other person or entity.

Questions? For questions on Copyright Clearance Center accounts or website issues please contact springernaturesupport@copyright.com or +1-855-239-3415 (toll free in the US) or +1-978-646-2777. For questions on Springer Nature licensing please visit https://www.springernature.com/gp/partners/rights-permissions-third-party-distribution
Other Conditions:
Version 1.4 - Dec 2022
Questions? customercare@copyright.com.

Figure 2-4

SPRINGER NATURE LICENSE
TERMS AND CONDITIONS
Aug 27, 2024

This Agreement between Amanda R Kirane ("You") and Springer Nature ("Springer Nature") consists of your license details and the terms and conditions provided by Springer Nature and Copyright Clearance Center.

License Number	5857221207065
License date	Aug 27, 2024
Licensed Content Publisher	Springer Nature
Licensed Content Publication	Nature Medicine
Licensed Content Title	Neoadjuvant talimogene laherparepvec plus surgery versus surgery alone for resectable stage IIIB–IVM1a melanoma: a randomized, open-label, phase 2 trial

Licensed Content Author	R. Dummer et al
Licensed Content Date	Oct 4, 2021
Type of Use	Thesis/Dissertation
Requestor type	academic/university or research institute
Format	electronic
Portion	figures/tables/illustrations
Number of figures/tables/illustrations	1
Would you like a high resolution image with your order?	no
Will you be translating?	no
Circulation/distribution	1 - 29
Author of this Springer Nature content	no
Title of new work	Targeting macrophages in immunotherapy resistant melanoma
Institution name	UC Davis
Expected presentation date	Sep 2024
	Figure 1
Portions	
The Requesting Person /	

Organization to Appear on the License	Amanda R Kirane
Requestor Location	Amanda R Kirane Surgery PALO ALTO, CA 94304 United States Attn: Stanford
	Invoice Amanda R Kirane Surgery

Billing Type
Billing Address
PALO ALTO, CA 94304
United States
Attn: Stanford
Total 0.00 USD

Terms and Conditions

Springer Nature Customer Service Centre GmbH Terms and Conditions
The following terms and conditions ("Terms and Conditions") together with the terms specified in your [RightsLink] constitute the License ("License") between you as Licensee and Springer Nature Customer Service Centre GmbH as Licensor. By clicking 'accept' and completing the transaction for your use of the material ("Licensed Material"), you confirm your acceptance of and obligation to be bound by these Terms and Conditions.

Grant and Scope of License

1. 1. The Licensor grants you a personal, non-exclusive, non-transferable, nonsublicensable, revocable, world-wide License to reproduce, distribute, communicate to the public, make available, broadcast, electronically transmit or create derivative works using the Licensed Material for the purpose(s) specified in your RightsLink Licence Details only. Licenses are granted for the specific use requested in the order and for no other use, subject to these Terms and Conditions. You acknowledge and agree that the rights granted to you under this License do not include the right to modify, edit, translate, include in collective works, or create derivative works of the Licensed Material in whole or in part unless expressly stated in your RightsLink
Licence Details. You may use the Licensed Material only as permitted under this Agreement and will not reproduce, distribute, display, perform, or otherwise use or exploit

any Licensed Material in any way, in whole or in part, except as expressly permitted by this License.
1. 2. You may only use the Licensed Content in the manner and to the extent permitted by these Terms and Conditions, by your RightsLink Licence Details and by any applicable laws.
1. 3. A separate license may be required for any additional use of the Licensed Material, e.g. where a license has been purchased for print use only, separate permission must be obtained for electronic re-use. Similarly, a License is only valid in the language selected and does not apply for editions in other languages unless additional translation rights have been granted separately in the License.
1. 4. Any content within the Licensed Material that is owned by third parties is expressly excluded from the License.
1. 5. Rights for additional reuses such as custom editions, computer/mobile applications, film or TV reuses and/or any other derivative rights requests require additional permission and may be subject to an additional fee. Please apply to journalpermissions@springernature.com or bookpermissions@springernature.com for these rights.

Reservation of Rights
Licensor reserves all rights not expressly granted to you under this License. You acknowledge and agree that nothing in this License limits or restricts Licensor's rights in or use of the Licensed Material in any way. Neither this License, nor any act, omission, or statement by Licensor or you, conveys any ownership right to you in any Licensed Material, or to any element or portion thereof. As between Licensor and you, Licensor owns and retains all right, title, and interest in and to the Licensed Material subject to the license granted in Section 1.1. Your permission to use the Licensed Material is expressly conditioned on you not impairing Licensor's or the applicable copyright owner's rights in the Licensed Material in any way.

Restrictions on use
3. 1. Minor editing privileges are allowed for adaptations for stylistic purposes or formatting purposes provided such alterations do not alter the original meaning or intention of the Licensed Material and the new figure(s) are still accurate and representative of the Licensed Material. Any other changes including but not limited to, cropping, adapting, and/or omitting material that affect the meaning, intention or moral rights of the author(s) are strictly prohibited.
3. 2. You must not use any Licensed Material as part of any design or trademark.
3. 3. Licensed Material may be used in Open Access Publications (OAP), but any such reuse must include a clear acknowledgment of this permission visible at the same time as the figures/tables/illustration or abstract and which must indicate that the Licensed Material is not part of the governing OA license but has been reproduced with permission. This may be indicated according to any standard referencing system but must include at a minimum 'Book/Journal title, Author, Journal Name (if applicable), Volume (if applicable), Publisher, Year, reproduced with permission from SNCSC'.

STM Permission Guidelines

4. 1. An alternative scope of license may apply to signatories of the STM Permissions Guidelines ("STM PG") as amended from time to time and made available at https://www.stm-assoc.org/intellectualproperty/permissions/permissions-guidelines/.

4. 2. For content reuse requests that qualify for permission under the STM PG, and which may be updated from time to time, the STM PG supersede the terms and conditions contained in this License.

4. 3. If a License has been granted under the STM PG, but the STM PG no longer apply at the time of publication, further permission must be sought from the Rightsholder. Contact journalpermissions@springernature.com or bookpermissions@springernature.com for these rights.

Duration of License

5. 1. Unless otherwise indicated on your License, a License is valid from the date of purchase ("License Date") until the end of the relevant period in the below table:

Reuse in a medical communications project	Reuse up to distribution or time period indicated in License
Reuse in a dissertation/thesis	Lifetime of thesis
Reuse in a journal/magazine	Lifetime of journal/magazine
Reuse in a book/textbook	Lifetime of edition
Reuse on a website	1 year unless otherwise specified in the License
Reuse in a presentation/slide kit/poster	Lifetime of presentation/slide kit/poster. Note: publication whether electronic or in print of presentation/slide kit/poster may require further permission.
Reuse in conference proceedings	Lifetime of conference proceedings
Reuse in an annual report	Lifetime of annual report
Reuse in training/CME materials	Reuse up to distribution or time period indicated in License
Reuse in newsmedia	Lifetime of newsmedia
Reuse in coursepack/classroom materials	Reuse up to distribution and/or time period indicated in license

Acknowledgement

6. 1. The Licensor's permission must be acknowledged next to the Licensed Material in print. In electronic form, this acknowledgement must be visible at the same time as the figures/tables/illustrations or abstract and must be hyperlinked to the journal/book's homepage.

6. 2. Acknowledgement may be provided according to any standard referencing system and at a minimum should include "Author, Article/Book Title, Journal name/Book imprint, volume, page number, year, Springer Nature".

Reuse in a dissertation or thesis

7. 1. Where 'reuse in a dissertation/thesis' has been selected, the following terms apply: Print rights of the Version of Record are provided for; electronic rights for use only on institutional repository as defined by the Sherpa guideline (www.sherpa.ac.uk/romeo/) and only up to what is required by the awarding institution.

7. 2. For theses published under an ISBN or ISSN, separate permission is required. Please contact journalpermissions@springernature.com or bookpermissions@springernature.com for these rights.

7. 3. Authors must properly cite the published manuscript in their thesis according to current citation standards and include the following acknowledgement: '*Reproduced with permission from Springer Nature*'.

License Fee

You must pay the fee set forth in the License Agreement (the "License Fees"). All amounts payable by you under this License are exclusive of any sales, use, withholding, value added or similar taxes, government fees or levies or other assessments. Collection and/or remittance of such taxes to the relevant tax authority shall be the responsibility of the party who has the legal obligation to do so.

Warranty

9. 1. The Licensor warrants that it has, to the best of its knowledge, the rights to license reuse of the Licensed Material. You are solely responsible for ensuring that the material you wish to license is original to the Licensor and does not carry the copyright of another entity or third party (as credited in the published version). If the credit line on any part of the Licensed Material indicates that it was reprinted or adapted with permission from another source, then you should seek additional permission from that source to reuse the material.

9. 2. EXCEPT FOR THE EXPRESS WARRANTY STATED HEREIN AND TO THE EXTENT PERMITTED BY APPLICABLE LAW, LICENSOR PROVIDES THE LICENSED MATERIAL "AS IS" AND MAKES NO OTHER REPRESENTATION OR WARRANTY. LICENSOR EXPRESSLY DISCLAIMS ANY LIABILITY FOR ANY CLAIM ARISING FROM OR OUT OF THE CONTENT, INCLUDING BUT NOT LIMITED TO ANY ERRORS, INACCURACIES, OMISSIONS, OR DEFECTS CONTAINED THEREIN, AND ANY IMPLIED OR EXPRESS WARRANTY AS TO MERCHANTABILITY OR FITNESS FOR A PARTICULAR PURPOSE. IN NO EVENT SHALL LICENSOR

BE LIABLE TO YOU OR ANY OTHER PARTY OR ANY OTHER PERSON OR FOR ANY SPECIAL, CONSEQUENTIAL, INCIDENTAL, INDIRECT, PUNITIVE, OR EXEMPLARY DAMAGES, HOWEVER CAUSED, ARISING OUT OF OR IN CONNECTION WITH THE DOWNLOADING, VIEWING OR USE OF THE LICENSED MATERIAL REGARDLESS OF THE FORM OF ACTION, WHETHER FOR BREACH OF CONTRACT, BREACH OF WARRANTY, TORT, NEGLIGENCE, INFRINGEMENT OR OTHERWISE (INCLUDING, WITHOUT LIMITATION, DAMAGES BASED ON LOSS OF PROFITS, DATA, FILES, USE, BUSINESS OPPORTUNITY OR CLAIMS OF THIRD PARTIES), AND WHETHER OR NOT THE PARTY HAS BEEN ADVISED OF THE POSSIBILITY OF SUCH DAMAGES. THIS LIMITATION APPLIES NOTWITHSTANDING ANY FAILURE OF ESSENTIAL PURPOSE OF ANY LIMITED REMEDY PROVIDED HEREIN.

Termination and Cancellation

10. 1. The License and all rights granted hereunder will continue until the end of the applicable period shown in Clause 5.1 above. Thereafter, this license will be terminated and all rights granted hereunder will cease.

10. 2. Licensor reserves the right to terminate the License in the event that payment is not received in full or if you breach the terms of this License.

General

11. 1. The License and the rights and obligations of the parties hereto shall be construed, interpreted and determined in accordance with the laws of the Federal Republic of Germany without reference to the stipulations of the CISG (United Nations Convention on Contracts for the International Sale of Goods) or to Germaný s choice-of-law principle.

11. 2. The parties acknowledge and agree that any controversies and disputes arising out of this License shall be decided exclusively by the courts of or having jurisdiction for Heidelberg, Germany, as far as legally permissible.

11. 3. This License is solely for Licensor's and Licensee's benefit. It is not for the benefit of any other person or entity.

Questions? For questions on Copyright Clearance Center accounts or website issues please contact springernaturesupport@copyright.com or +1-855-239-3415 (toll free in the US) or +1-978-646-2777. For questions on Springer Nature licensing please visit https://www.springernature.com/gp/partners/rights-permissions-third-party-distribution

Other Conditions:

Version 1.4 - Dec 2022

Questions? customercare@copyright.com.

Figure 2-5

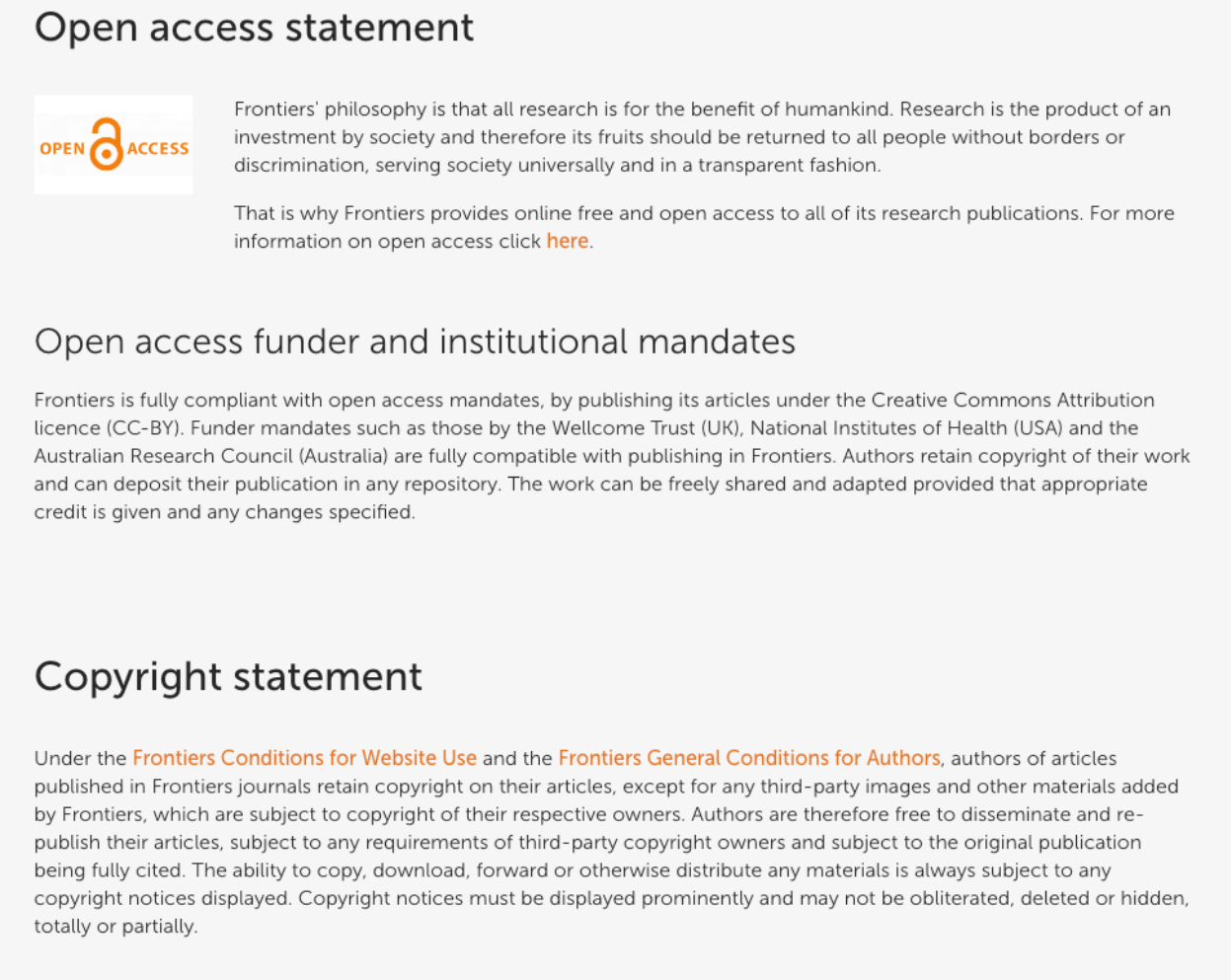

Open access statement

Frontiers' philosophy is that all research is for the benefit of humankind. Research is the product of an investment by society and therefore its fruits should be returned to all people without borders or discrimination, serving society universally and in a transparent fashion.

That is why Frontiers provides online free and open access to all of its research publications. For more information on open access click here.

Open access funder and institutional mandates

Frontiers is fully compliant with open access mandates, by publishing its articles under the Creative Commons Attribution licence (CC-BY). Funder mandates such as those by the Wellcome Trust (UK), National Institutes of Health (USA) and the Australian Research Council (Australia) are fully compatible with publishing in Frontiers. Authors retain copyright of their work and can deposit their publication in any repository. The work can be freely shared and adapted provided that appropriate credit is given and any changes specified.

Copyright statement

Under the Frontiers Conditions for Website Use and the Frontiers General Conditions for Authors, authors of articles published in Frontiers journals retain copyright on their articles, except for any third-party images and other materials added by Frontiers, which are subject to copyright of their respective owners. Authors are therefore free to disseminate and re-publish their articles, subject to any requirements of third-party copyright owners and subject to the original publication being fully cited. The ability to copy, download, forward or otherwise distribute any materials is always subject to any copyright notices displayed. Copyright notices must be displayed prominently and may not be obliterated, deleted or hidden, totally or partially.

Figure 2-8 and 2-9

AMERICAN ASSOCIATION FOR CANCER RESEARCH LICENSE
TERMS AND CONDITIONS
Aug 28, 2024

This Agreement between Amanda R Kirane ("You") and American Association for Cancer Research ("American Association for Cancer Research") consists of your license details and the terms and conditions provided by American Association for Cancer Research and Copyright Clearance Center.

License Number	5857630027277
License date	Aug 28, 2024

Licensed Content Publisher	American Association for Cancer Research
Licensed Content Publication	Cancer Research
Licensed Content Title	High PD-1/PD-L1 Checkpoint Interaction Infers Tumor Selection and Therapeutic Sensitivity to Anti-PD-1/PD-L1 Treatment
Licensed Content Author	Sánchez-Magraner, Lissete; Miles, James
Licensed Content Date	Oct 2, 2020
Licensed Content Volume	80
Licensed Content Issue	19
Type of Use	Thesis/Dissertation
Requestor type	academic/educational
Format Portion	electronic figures/tables/illustrations
Number of figures/tables/illustrations	1
Will you be translating?	no
Circulation	1
Territory of distribution	North America

Title of new work	Targeting macrophages in immunotherapy resistant melanoma
Institution name	UC Davis
Expected presentation date	Sep 2024
Portions	4c, 7a

The Requesting Person / Organization Amanda R Kirane to Appear on the License
Amanda R Kirane
Surgery
Requestor Location
PALO ALTO, CA 94304
United States
Attn: Stanford
Billing Type Invoice
Amanda R Kirane
Surgery
Billing Address
PALO ALTO, CA 94304
United States
Attn: Stanford
Total 0.00 USD
Terms and Conditions
American Association for Cancer Research (AACR) Terms and Conditions

INTRODUCTION
The Publisher for this copyright material is the American Association for Cancer Research (AACR). By clicking "accept" in connection with completing this licensing transaction, you agree to the following terms and conditions applying to this transaction. You also agree to

the Billing and Payment terms and conditions established by Copyright Clearance Center (CCC) at the time you opened your Rightslink account.

LIMITED LICENSE
The AACR grants exclusively to you, the User, for onetime, non-exclusive use of this material for the purpose stated in your request and used only with a maximum distribution equal to the number you identified in the permission process. Any form of republication must be completed within one year although copies made before then may be distributed thereafter and any electronic posting is limited to a period of one year. Reproduction of this material is confined to the purpose and/or media for which permission is granted. Altering or modifying this material is not permitted. However, figures and illustrations may be minimally altered or modified to serve the new work.

GEOGRAPHIC SCOPE
Licenses may be exercised as noted in the permission process

RESERVATION OF RIGHTS
The AACR reserves all rights not specifically granted in the combination of 1) the license details provided by you and accepted in the course of this licensing transaction, 2) these terms and conditions , and 3) CCC's Billing and Payment terms and conditions.

DISCLAIMER
You may obtain permission via Rightslink to use material owned by AACR. When you are requesting permission to reuse a portion for an AACR publication, it is your responsibility to examine each portion of content as published to determine whether a credit to, or copyright notice of a third party owner is published next to the item. You must obtain permission from the third party to use any material which has been reprinted with permission from the said third party. If you have not obtained permission from the third party, AACR disclaims any responsibility for the use you make of items owned by them.

LICENSE CONTINGENT ON PAYMENT
While you may exercise the rights licensed immediately upon issuance of the license at the end of the licensing process for the transaction, provided that you have disclosed complete and accurate details of your proposed use, no license is finally effective unless and until full payment is received from you, either by the publisher or by the CCC, as provided in CCC's Billing and Payment terms and conditions. If full payment is not received on a timely basis, then any license preliminarily granted shall be deemed automatically revoked and shall be void as if never granted. Further, in the event that you breach any of these terms and conditions, or any of the CCC's Billing and Payment terms and conditions, the license is automatically revoked and shall be void as if never granted. Use of materials as described in a revoked license, as well as any use of the materials beyond the scope of an unrevoked license, may constitute copyright infringement and the publisher reserves the right to take any and all action to protect its copyright in the materials.

COPYRIGHT NOTICE
You must include the following credit line in connection with your reproduction of the licensed material: "Reprinted (or adapted) from Publication Title, Copyright Year, Volume/Issue, Page Range, Author, Title of Article, with permission from AACR".

TRANSLATION
This permission is granted for non-exclusive world English rights only.

WARRANTIES
Publisher makes no representations or warranties with respect to the licensed material.

INDEMNIFICATION
You hereby indemnify and agree to hold harmless the publisher and CCC, and their respective officers, directors, employees and agents, from and against any and all claims arising out of your use of the licensed material other than as specifically authorized pursuant to this license.

REVOCATION
The AACR reserves the right to revoke a license for any reason, including but not limited to advertising and promotional uses of AACR content, third party usage and incorrect figure source attribution.

NO TRANSFER OF LICENSE
This license is personal to you and may not be sublicensed, assigned, or transferred by you to any other person without publisher's written permission.

NO AMENDMENT EXCEPT IN WRITING
This license may not be amended except in a writing signed by both parties (or, in the case of publisher, by CCC on publisher's behalf).

OBJECTION TO CONTRARY TERMS
Publishers hereby objects to any terms contained in any purchase order, acknowledgement, check endorsement or other writing prepared by you, which terms are inconsistent with these terms and conditions or CCC's Billing and Payment terms and conditions. These terms and conditions together with CCC's Billing and Payment terms and conditions (which are incorporated herein) comprise the entire agreement between you and publisher (and CCC) concerning this licensing transaction. In the event of any conflict between your obligations established by these terms and conditions, and those established by CCC's Billing and Payment terms and conditions, these terms and conditions shall control.

THESIS/DISSERTATION TERMS

If your request is to reuse an article authored by you and published by the AACR in your dissertation/thesis, your thesis may be submitted to your institution in either in print or electronic form. Should your thesis be published commercially, please reapply.

ELECTRONIC RESERVE
If this license is made in connection with a course, and the Licensed Material or any portion thereof is to be posted to a website, the website is to be password protected and made available only to the students registered for the relevant course. The permission is granted for the duration of the course. All content posted to the website must maintain the copyright information notice.

JURISDICTION
This license transaction shall be governed by and construed in accordance with the laws of Pennsylvania. You hereby agree to submit to the jurisdiction of the federal and state courts located in Pennsylvania for purposes of resolving any disputes that may arise in connection with this licensing transaction.
Other Terms and Conditions: v1.0
Questions? customercare@copyright.com.

Figure 2-10 and 2-12

MDPI Open Access Information and Policy

All articles published by MDPI are made immediately available worldwide under an open access license. This means:

- everyone has free and unlimited access to the full-text of *all* articles published in MDPI journals;
- everyone is free to re-use the published material if proper accreditation/citation of the original publication is given;
- open access publication is supported by the authors' institutes or research funding agencies by payment of a comparatively low **Article Processing Charge (APC)** for accepted articles.

Permissions

No special permission is required to reuse all or part of article published by MDPI, including figures and tables. For articles published under an open access Creative Common CC BY license, any part of the article may be reused without permission provided that the original article is clearly cited. Reuse of an article does not imply endorsement by the authors or MDPI.

External Open Access Resources

Those who are new to the concept of open access might find the following websites or the *Open Access Explained!* video informative:

- **Wikipedia article on Open Access**
- **Open Access Network**

Meaning of Open Access

In accordance with major definitions of open access in scientific literature (namely the Budapest, Berlin, and Bethesda declarations), MDPI defines *open access* by the following conditions:

- peer-reviewed literature is freely available without subscription or price barriers,
- literature is immediately released in open access format (no embargo period), and
- published material can be re-used without obtaining permission as long as a correct citation to the original publication is given.

Open Access Explained!



Until 2008, most articles published by MDPI contained the note: "© *year* by MDPI (http://www.mdpi.org). Reproduction is permitted for noncommercial purposes". During 2008, MDPI journals started to publish articles under the **Creative Commons Attribution License** and are now using the latest version of the CC BY license, which grants authors the most extensive rights. All articles published by MDPI before and during 2008 should now be considered as having been released under the post-2008 Creative Commons Attribution License.

Figure 2-13

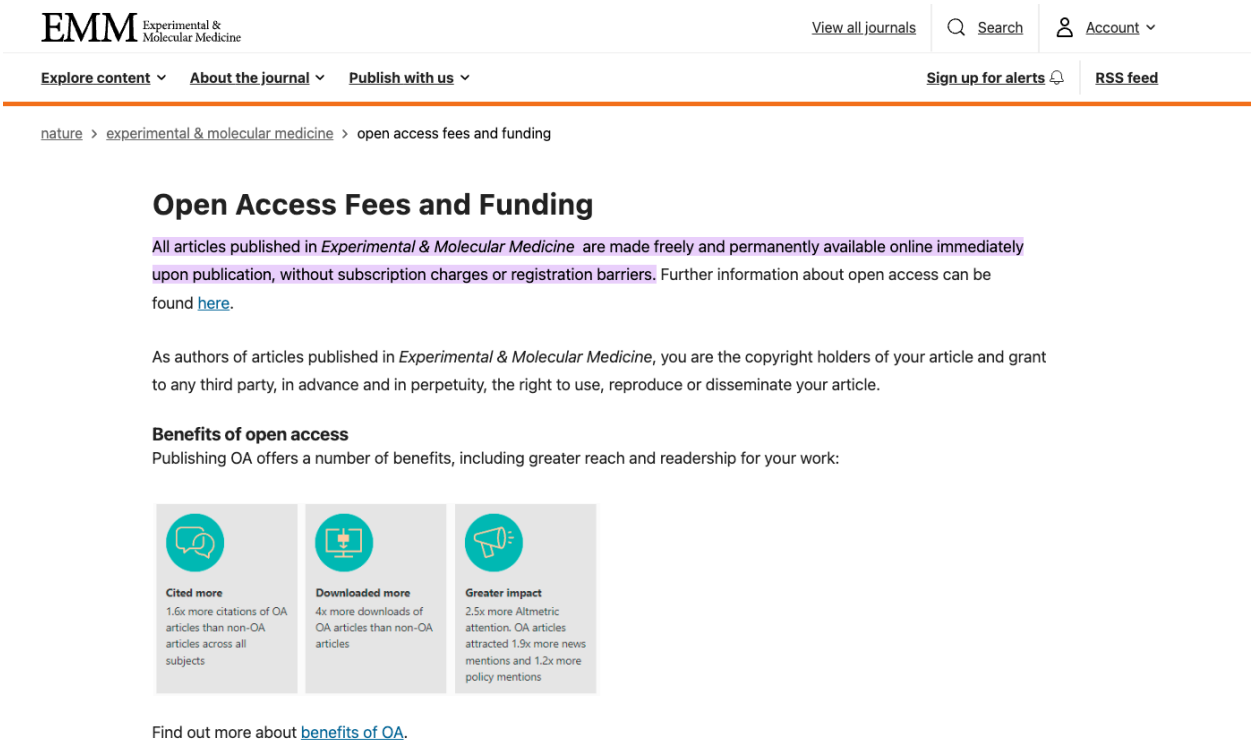

Figure 2-14

ELSEVIER LICENSE
TERMS AND CONDITIONS
Aug 27, 2024

This Agreement between Amanda R Kirane ("You") and Elsevier ("Elsevier") consists of your license details and the terms and conditions provided by Elsevier and Copyright Clearance Center.

License Number	5857240402419
License date	Aug 27, 2024
Licensed Content Publisher	Elsevier
Licensed Content Publication	Journal of Thoracic Oncology

Licensed Content Title	Axl Receptor Axis: A New Therapeutic Target in Lung Cancer
Licensed Content Author	Pavel A. Levin,Rolf A. Brekken,Lauren Averett Byers,John V. Heymach,David E. Gerber
Licensed Content Date	Aug 1, 2016
Licensed Content Volume	11
Licensed Content Issue	8
Licensed Content Pages	6
Start Page	1357
End Page	1362
Type of Use	reuse in a thesis/dissertation
Portion	figures/tables/illustrations
Number of figures/tables/illustrations	1
Format	electronic
Are you the author of this Elsevier article?	No
Will you be translating?	No
Title of new work	Targeting macrophages in immunotherapy resistant melanoma

Institution name	UC Davis
Expected presentation date	Sep 2024
Portions	Figure 1
The Requesting Person / Organization to Appear on the License	Amanda R Kirane
Requestor Location	Amanda R Kirane Surgery PALO ALTO, CA 94304 United States Attn: Stanford
Publisher Tax ID	98-0397604
Total	0.00 USD

Terms and Conditions

INTRODUCTION

1. The publisher for this copyrighted material is Elsevier. By clicking "accept" in connection with completing this licensing transaction, you agree that the following terms and conditions apply to this transaction (along with the Billing and Payment terms and conditions established by Copyright Clearance Center, Inc. ("CCC"), at the time that you opened your RightsLink account and that are available at any time at https://myaccount.copyright.com).

GENERAL TERMS

Elsevier hereby grants you permission to reproduce the aforementioned material subjectto the terms and conditions indicated.

Acknowledgement: If any part of the material to be used (for example, figures) has appeared in our publication with credit or acknowledgement to another source, permission must also be sought from that source. If such permission is not obtained then that material may not be included in your publication/copies. Suitable acknowledgement to the source must be made, either as a footnote or in a reference list at the end of your publication, as follows:

"Reprinted from Publication title, Vol /edition number, Author(s), Title of article / title of chapter, Pages No., Copyright (Year), with permission from Elsevier [OR APPLICABLE SOCIETY COPYRIGHT OWNER]." Also Lancet special credit - "Reprinted from The Lancet, Vol. number, Author(s), Title of article, Pages No., Copyright (Year), with permission from Elsevier."

Reproduction of this material is confined to the purpose and/or media for which permission is hereby given. The material may not be reproduced or used in any other way, including use in combination with an artificial intelligence tool (including to train an algorithm, test, process, analyse, generate output and/or develop any form of artificial intelligence tool), or to create any derivative work and/or service (including resulting from the use of artificial intelligence tools).

Altering/Modifying Material: Not Permitted. However figures and illustrations may be altered/adapted minimally to serve your work. Any other abbreviations, additions, deletions and/or any other alterations shall be made only with prior written authorization of Elsevier Ltd. (Please contact Elsevier's permissions helpdesk here). No modifications can be made to any Lancet figures/tables and they must be reproduced in full.
If the permission fee for the requested use of our material is waived in this instance,please be advised that your future requests for Elsevier materials may attract a fee.
Reservation of Rights: Publisher reserves all rights not specifically granted in the combination of (i) the license details provided by you and accepted in the course of this licensing transaction, (ii) these terms and conditions and (iii) CCC's Billing and Payment terms and conditions.

License Contingent Upon Payment: While you may exercise the rights licensedimmediately upon issuance of the license at the end of the licensing process for the transaction, provided that you have disclosed complete and accurate details of your proposed use, no license is finally effective unless and until full payment is received from you (either by publisher or by CCC) as provided in CCC's Billing and Payment terms and conditions. If full payment is not received on a timely basis, then any license preliminarily granted shall be deemed automatically revoked and shall be void as if never granted. Further, in the event that you breach any of these terms and conditions or any of CCC's Billing and Payment terms and conditions, the license is automatically revoked and shall be void as if never granted. Use of materials as described in a revoked license, as well as any use of the materials beyond the scope of an unrevoked license, may constitute copyright infringement and publisher reserves the right to take any and all action to protect its copyright in the materials.

Warranties: Publisher makes no representations or warranties with respect to thelicensed material.

Indemnity: You hereby indemnify and agree to hold harmless publisher and CCC, andtheir respective officers, directors, employees and agents, from and against any and all claims

arising out of your use of the licensed material other than as specifically authorized pursuant to this license.

No Transfer of License: This license is personal to you and may not be sublicensed,assigned, or transferred by you to any other person without publisher's written permission.

No Amendment Except in Writing: This license may not be amended except in a writing signed by both parties (or, in the case of publisher, by CCC on publisher's behalf).

Objection to Contrary Terms: Publisher hereby objects to any terms contained in any purchase order, acknowledgment, check endorsement or other writing prepared by you, which terms are inconsistent with these terms and conditions or CCC's Billing and Payment terms and conditions. These terms and conditions, together with CCC's Billing and Payment terms and conditions (which are incorporated herein), comprise the entire agreement between you and publisher (and CCC) concerning this licensing transaction. In the event of any conflict between your obligations established by these terms and conditions and those established by CCC's Billing and Payment terms and conditions, these terms and conditions shall control.

Revocation: Elsevier or Copyright Clearance Center may deny the permissions described in this License at their sole discretion, for any reason or no reason, with a full refund payable to you. Notice of such denial will be made using the contact information provided by you. Failure to receive such notice will not alter or invalidate the denial. In no event will Elsevier or Copyright Clearance Center be responsible or liable for any costs, expenses or damage incurred by you as a result of a denial of your permission request, other than a refund of the amount(s) paid by you to Elsevier and/or Copyright Clearance Center for denied permissions.

LIMITED LICENSE
The following terms and conditions apply only to specific license types:
Translation: This permission is granted for non-exclusive world English rights only unless your license was granted for translation rights. If you licensed translation rights you may only translate this content into the languages you requested. A professional translator must perform all translations and reproduce the content word for word preserving the integrity of the article.

Posting licensed content on any Website: The following terms and conditions apply as follows: Licensing material from an Elsevier journal: All content posted to the web site must maintain the copyright information line on the bottom of each image; A hyper-text must be included to the Homepage of the journal from which you are licensing at http://www.sciencedirect.com/science/journal/xxxxx or the Elsevier homepage for books at http://www.elsevier.com; Central Storage: This license does not include permission for

a scanned version of the material to be stored in a central repository such as that provided by Heron/XanEdu.

Licensing material from an Elsevier book: A hyper-text link must be included to the Elsevier homepage at http://www.elsevier.com . All content posted to the web site must maintain the copyright information line on the bottom of each image.
Posting licensed content on Electronic reserve: In addition to the above the following clauses are applicable: The web site must be password-protected and made available only to bona fide students registered on a relevant course. This permission is granted for 1 year only. You may obtain a new license for future website posting.
For journal authors: the following clauses are applicable in addition to the above:
Preprints:
A preprint is an author's own write-up of research results and analysis, it has not been peer-reviewed, nor has it had any other value added to it by a publisher (such as formatting, copyright, technical enhancement etc.).
Authors can share their preprints anywhere at any time. Preprints should not be added to or enhanced in any way in order to appear more like, or to substitute for, the final versions of articles however authors can update their preprints on arXiv or RePEc with their Accepted Author Manuscript (see below).

If accepted for publication, we encourage authors to link from the preprint to their formal publication via its DOI. Millions of researchers have access to the formal publications on ScienceDirect, and so links will help users to find, access, cite and use the best available version. Please note that Cell Press, The Lancet and some society-owned have different preprint policies. Information on these policies is available on the journal homepage.
Accepted Author Manuscripts: An accepted author manuscript is the manuscript of an article that has been accepted for publication and which typically includes authorincorporated changes suggested during submission, peer review and editor-author communications.
Authors can share their accepted author manuscript:

- immediately via their non-commercial person homepage or blog
    - by updating a preprint in arXiv or RePEc with the accepted manuscript via their
    - research institute or institutional repository for internal institutional uses or as
    - part of an invitation-only research collaboration work-group directly by
    - providing copies to their students or to research collaborators for their personal use
    - for private scholarly sharing as part of an invitation-only work group on commercial sites with which Elsevier has an agreement
- After the embargo period via non-commercial hosting platforms such as their institutional repository via commercial sites with which Elsevier has an agreement In all cases accepted manuscripts should:
    - link to the formal publication via its DOI bear a CC-BY-NC-ND license - this is easy to
    - do
    -

if aggregated with other manuscripts, for example in a repository or other site, be shared in alignment with our hosting policy not be added to or enhanced in any way to appear more like, or to substitute for, the published journal article.
Published journal article (JPA): A published journal article (PJA) is the definitive final record of published research that appears or will appear in the journal and embodies all value-adding publishing activities including peer review co-ordination, copy-editing, formatting, (if relevant) pagination and online enrichment.
Policies for sharing publishing journal articles differ for subscription and gold open access articles:

Subscription Articles: If you are an author, please share a link to your article rather than the full-text. Millions of researchers have access to the formal publications on ScienceDirect, and so links will help your users to find, access, cite, and use the best available version. Theses and dissertations which contain embedded PJAs as part of the formal submission can be posted publicly by the awarding institution with DOI links back to the formal publications on ScienceDirect.

If you are affiliated with a library that subscribes to ScienceDirect you have additional private sharing rights for others' research accessed under that agreement. This includes use for classroom teaching and internal training at the institution (including use in course packs and courseware programs), and inclusion of the article for grant funding purposes.
Gold Open Access Articles: May be shared according to the author-selected end-user license and should contain a CrossMark logo, the end user license, and a DOI link to the formal publication on ScienceDirect.
Please refer to Elsevier's posting policy for further information.

For book authors the following clauses are applicable in addition to the above: Authors are permitted to place a brief summary of their work online only. You are not allowed to download and post the published electronic version of your chapter, nor may you scan the printed edition to create an electronic version. Posting to a repository: Authors are permitted to post a summary of their chapter only in their institution's repository.
Thesis/Dissertation: If your license is for use in a thesis/dissertation your thesis may be submitted to your institution in either print or electronic form. Should your thesis be published commercially, please reapply for permission. These requirements include permission for the Library and Archives of Canada to supply single copies, on demand, of the complete thesis and include permission for Proquest/UMI to supply single copies, on demand, of the complete thesis. Should your thesis be published commercially, please reapply for permission. Theses and dissertations which contain embedded PJAs as part of the formal submission can be posted publicly by the awarding institution with DOI links back to the formal publications on ScienceDirect.

Elsevier Open Access Terms and Conditions
You can publish open access with Elsevier in hundreds of open access journals or in nearly 2000 established subscription journals that support open access publishing. Permitted

third party re-use of these open access articles is defined by the author's choice of Creative Commons user license. See our open access license policy for more information.
Terms & Conditions applicable to all Open Access articles published with Elsevier:
Any reuse of the article must not represent the author as endorsing the adaptation of the article nor should the article be modified in such a way as to damage the author's honour or reputation. If any changes have been made, such changes must be clearly indicated.
The author(s) must be appropriately credited and we ask that you include the end user license and a DOI link to the formal publication on ScienceDirect.
If any part of the material to be used (for example, figures) has appeared in our publication with credit or acknowledgement to another source it is the responsibility of the user to ensure their reuse complies with the terms and conditions determined by the rights holder.

Additional Terms & Conditions applicable to each Creative Commons user license:

CC BY: The CC-BY license allows users to copy, to create extracts, abstracts and new works from the Article, to alter and revise the Article and to make commercial use of the Article (including reuse and/or resale of the Article by commercial entities), provided the user gives appropriate credit (with a link to the formal publication through the relevant DOI), provides a link to the license, indicates if changes were made and the licensor is not represented as endorsing the use made of the work. The full details of the license are available at http://creativecommons.org/licenses/by/4.0.

CC BY NC SA: The CC BY-NC-SA license allows users to copy, to create extracts, abstracts and new works from the Article, to alter and revise the Article, provided this is not done for commercial purposes, and that the user gives appropriate credit (with a link to the formal publication through the relevant DOI), provides a link to the license, indicates if changes were made and the licensor is not represented as endorsing the use made of the work. Further, any new works must be made available on the same conditions. The full details of the license are available at http://creativecommons.org/licenses/by-nc-sa/4.0.

CC BY NC ND: The CC BY-NC-ND license allows users to copy and distribute the Article, provided this is not done for commercial purposes and further does not permit distribution of the Article if it is changed or edited in any way, and provided the user gives appropriate credit (with a link to the formal publication through the relevant DOI), provides a link to the license, and that the licensor is not represented as endorsing the use made of the work. The full details of the license are available at http://creativecommons.org/licenses/by-nc-nd/4.0. Any commercial reuse of Open Access articles published with a CC BY NC SA or CC BY NC ND license requires permission from Elsevier and will be subject to a fee.
Commercial reuse includes:

- Associating advertising with the full text of the Article
- Charging fees for document delivery or access
- Article aggregation
- Systematic distribution via e-mail lists or share buttons

Posting or linking by commercial companies for use by customers of those companies.

20. Other Conditions:

v1.10
Questions? customercare@copyright.com.

Figure 2-15

AMERICAN ASSOCIATION FOR CANCER RESEARCH LICENSE
TERMS AND CONDITIONS
Aug 27, 2024

This Agreement between Amanda R Kirane ("You") and American Association for Cancer Research ("American Association for Cancer Research") consists of your license details and the terms and conditions provided by American Association for Cancer Research and Copyright Clearance Center.

License Number 5857240619679
License date Aug 27, 2024
Licensed Content Publisher American Association for Cancer Research
Licensed Content Publication Cancer Research
Licensed Content Title Small-Molecule Inhibition of Axl Targets Tumor Immune Suppression and Enhances Chemotherapy in Pancreatic Cancer
Licensed Content Author Ludwig, Kathleen F.; Du, Wenting
Licensed Content Date Jan 2, 2018
Licensed Content Volume 78
Licensed Content Issue 1
Type of Use Thesis/Dissertation
Requestor type academic/educational
Format electronic
Portion figures/tables/illustrations
Number of figures/tables/illustrations 1
Will you be translating? no
Circulation 1
Territory of distribution North America
Title of new work Targeting macrophages in immunotherapyresistant melanoma
Institution name UC Davis
Expected presentation date Sep 2024
Portions Figure 4
The Requesting Person / Organization Amanda R Kirane

to Appear on the License
Amanda R Kirane
Surgery
Requestor Location
PALO ALTO, CA 94304
United States
Attn: Stanford
Billing Type Invoice
Amanda R Kirane
Surgery
Billing Address
PALO ALTO, CA 94304
United States
Attn: Stanford
Total 0.00 USD
Terms and Conditions
American Association for Cancer Research (AACR) Terms and Conditions

INTRODUCTION
The Publisher for this copyright material is the American Association for Cancer Research (AACR). By clicking "accept" in connection with completing this licensing transaction, you agree to the following terms and conditions applying to this transaction. You also agree to the Billing and Payment terms and conditions established by Copyright Clearance Center (CCC) at the time you opened your Rightslink account.

LIMITED LICENSE
The AACR grants exclusively to you, the User, for onetime, non-exclusive use of this material for the purpose stated in your request and used only with a maximum distribution equal to the number you identified in the permission process. Any form of republication must be completed within one year although copies made before then may be distributed thereafter and any electronic posting is limited to a period of one year. Reproduction of this material is confined to the purpose and/or media for which permission is granted. Altering or modifying this material is not permitted. However, figures and illustrations may be minimally altered or modified to serve the new work.

GEOGRAPHIC SCOPE
Licenses may be exercised as noted in the permission process

RESERVATION OF RIGHTS
The AACR reserves all rights not specifically granted in the combination of 1) the license details provided by you and accepted in the course of this licensing transaction, 2) these terms and conditions , and 3) CCC's Billing and Payment terms and conditions.

DISCLAIMER

You may obtain permission via Rightslink to use material owned by AACR. When you are requesting permission to reuse a portion for an AACR publication, it is your responsibility to examine each portion of content as published to determine whether a credit to, or copyright notice of a third party owner is published next to the item. You must obtain permission from the third party to use any material which has been reprinted with permission from the said third party. If you have not obtained permission from the third party, AACR disclaims any responsibility for the use you make of items owned by them.

LICENSE CONTINGENT ON PAYMENT
While you may exercise the rights licensed immediately upon issuance of the license at the end of the licensing process for the transaction, provided that you have disclosed complete and accurate details of your proposed use, no license is finally effective unless and until full payment is received from you, either by the publisher or by the CCC, as provided in CCC's Billing and Payment terms and conditions. If full payment is not received on a timely basis, then any license preliminarily granted shall be deemed automatically revoked and shall be void as if never granted. Further, in the event that you breach any of these terms and conditions, or any of the CCC's Billing and Payment terms and conditions, the license is automatically revoked and shall be void as if never granted. Use of materials as described in a revoked license, as well as any use of the materials beyond the scope of an unrevoked license, may constitute copyright infringement and the publisher reserves the right to take any and all action to protect its copyright in the materials.

COPYRIGHT NOTICE
You must include the following credit line in connection with your reproduction of the licensed material: "Reprinted (or adapted) from Publication Title, Copyright Year, Volume/Issue, Page Range, Author, Title of Article, with permission from AACR".

TRANSLATION
This permission is granted for non-exclusive world English rights only.

WARRANTIES
Publisher makes no representations or warranties with respect to the licensed material.

INDEMNIFICATION
You hereby indemnify and agree to hold harmless the publisher and CCC, and their respective officers, directors, employees and agents, from and against any and all claims arising out of your use of the licensed material other than as specifically authorized pursuant to this license.

REVOCATION
The AACR reserves the right to revoke a license for any reason, including but not limited to advertising and promotional uses of AACR content, third party usage and incorrect figure source attribution.

NO TRANSFER OF LICENSE
This license is personal to you and may not be sublicensed, assigned, or transferred by you to any other person without publisher's written permission.

NO AMENDMENT EXCEPT IN WRITING
This license may not be amended except in a writing signed by both parties (or, in the case of publisher, by CCC on publisher's behalf).

OBJECTION TO CONTRARY TERMS
Publishers hereby objects to any terms contained in any purchase order, acknowledgement, check endorsement or other writing prepared by you, which terms are inconsistent with these terms and conditions or CCC's Billing and Payment terms and conditions. These terms and conditions together with CCC's Billing and Payment terms and conditions (which are incorporated herein) comprise the entire agreement between you and publisher (and CCC) concerning this licensing transaction. In the event of any conflict between your obligations established by these terms and conditions, and those established by CCC's Billing and Payment terms and conditions, these terms and conditions shall control.

THESIS/DISSERTATION TERMS
If your request is to reuse an article authored by you and published by the AACR in your dissertation/thesis, your thesis may be submitted to your institution in either in print or electronic form. Should your thesis be published commercially, please reapply.

ELECTRONIC RESERVE
If this license is made in connection with a course, and the Licensed Material or any portion thereof is to be posted to a website, the website is to be password protected and made available only to the students registered for the relevant course. The permission is granted for the duration of the course. All content posted to the website must maintain the copyright information notice.

JURISDICTION
This license transaction shall be governed by and construed in accordance with the laws of Pennsylvania. You hereby agree to submit to the jurisdiction of the federal and state courts located in Pennsylvania for purposes of resolving any disputes that may arise in connection with this licensing transaction.
Other Terms and Conditions: v1.0
Questions? customercare@copyright.com.

Figure 2-16

ELSEVIER LICENSE
TERMS AND CONDITIONS

Aug 28, 2024

This Agreement between Amanda R Kirane ("You") and Elsevier ("Elsevier") consists of your license details and the terms and conditions provided by Elsevier and Copyright Clearance Center.

License Number	5857900293722
License date	Aug 28, 2024
Licensed Content Publisher	Elsevier
Licensed Content Publication	Cell
Licensed Content Title	Genomic and Transcriptomic Features of Response toAnti-PD-1 Therapy in Metastatic Melanoma
Licensed Content Author	Willy Hugo,Jesse M. Zaretsky,Lu Sun,Chunying Song,Blanca Homet Moreno,Siwen Hu-Lieskovan,Beata Berent-Maoz,Jia Pang,Bartosz Chmielowski,GraceCherry,Elizabeth Seja,Shirley Lomeli,Xiangju Kong,Mark C. Kelley,Jeffrey A. Sosman,Douglas B. Johnson et al.
Licensed Content Date	Mar 24, 2016
Licensed Content Volume	165
Licensed Content Issue	1
Licensed Content Pages	10
Start Page	35
End Page	44
Type of Use	reuse in a thesis/dissertation
Portion	figures/tables/illustrations
Number of figures/tables/illustrations	1
Format	electronic
Are you the author of this Elsevier article?	No
Will you be translating?	No
Title of new work	Targeting macrophages in immunotherapy resistantmelanoma
Institution name	UC Davis
Expected presentation date	Sep 2024
Portions	2B
The Requesting Person / Organization to Appear on the License	Amanda R Kirane Amanda R Kirane Surgery Requestor Location PALO ALTO, CA 94304 United States

Attn: Stanford
Publisher Tax ID 98-0397604
Total 0.00 USD
Terms and Conditions

INTRODUCTION
1. The publisher for this copyrighted material is Elsevier. By clicking "accept" in connection with completing this licensing transaction, you agree that the following terms and conditions apply to this transaction (along with the Billing and Payment terms and conditions established by Copyright Clearance Center, Inc. ("CCC"), at the time that you opened your RightsLink account and that are available at any time at https://myaccount.copyright.com).

GENERAL TERMS
Elsevier hereby grants you permission to reproduce the aforementioned material subjectto the terms and conditions indicated.
Acknowledgement: If any part of the material to be used (for example, figures) has appeared in our publication with credit or acknowledgement to another source, permission must also be sought from that source. If such permission is not obtained then that material may not be included in your publication/copies. Suitable acknowledgement to the source must be made, either as a footnote or in a reference list at the end of your publication, as follows:
"Reprinted from Publication title, Vol /edition number, Author(s), Title of article / title of chapter, Pages No., Copyright (Year), with permission from Elsevier [OR APPLICABLE SOCIETY COPYRIGHT OWNER]." Also Lancet special credit - "Reprinted from The Lancet, Vol. number, Author(s), Title of article, Pages No., Copyright (Year), with permission from Elsevier."
Reproduction of this material is confined to the purpose and/or media for which permission is hereby given. The material may not be reproduced or used in any other way, including use in combination with an artificial intelligence tool (including to train an algorithm, test, process, analyse, generate output and/or develop any form of artificial intelligence tool), or to create any derivative work and/or service (including resulting from the use of artificial intelligence tools).

Altering/Modifying Material: Not Permitted. However figures and illustrations may be altered/adapted minimally to serve your work. Any other abbreviations, additions, deletions and/or any other alterations shall be made only with prior written authorization of Elsevier Ltd. (Please contact Elsevier's permissions helpdesk here). No modifications can be made to any Lancet figures/tables and they must be reproduced in full.
If the permission fee for the requested use of our material is waived in this instance,please be advised that your future requests for Elsevier materials may attract a fee.
Reservation of Rights: Publisher reserves all rights not specifically granted in the combination of (i) the license details provided by you and accepted in the course of this

licensing transaction, (ii) these terms and conditions and (iii) CCC's Billing and Payment terms and conditions.

License Contingent Upon Payment: While you may exercise the rights licensedimmediately upon issuance of the license at the end of the licensing process for the transaction, provided that you have disclosed complete and accurate details of your proposed use, no license is finally effective unless and until full payment is received from you (either by publisher or by CCC) as provided in CCC's Billing and Payment terms and conditions. If full payment is not received on a timely basis, then any license preliminarily granted shall be deemed automatically revoked and shall be void as if never granted. Further, in the event that you breach any of these terms and conditions or any of CCC's Billing and Payment terms and conditions, the license is automatically revoked and shall be void as if never granted. Use of materials as described in a revoked license, as well as any use of the materials beyond the scope of an unrevoked license, may constitute copyright infringement and publisher reserves the right to take any and all action to protect its copyright in the materials.

Warranties: Publisher makes no representations or warranties with respect to the licensed material.

Indemnity: You hereby indemnify and agree to hold harmless publisher and CCC, and their respective officers, directors, employees and agents, from and against any and all claims arising out of your use of the licensed material other than as specifically authorized pursuant to this license.

No Transfer of License: This license is personal to you and may not be sublicensed,assigned, or transferred by you to any other person without publisher's written permission.

No Amendment Except in Writing: This license may not be amended except in awriting signed by both parties (or, in the case of publisher, by CCC on publisher's behalf).
Objection to Contrary Terms: Publisher hereby objects to any terms contained in any purchase order, acknowledgment, check endorsement or other writing prepared by you, which terms are inconsistent with these terms and conditions or CCC's Billing and Payment terms and conditions. These terms and conditions, together with CCC's Billing and Payment terms and conditions (which are incorporated herein), comprise the entire agreement between you and publisher (and CCC) concerning this licensing transaction. In the event of any conflict between your obligations established by these terms and conditions and those established by CCC's Billing and Payment terms and conditions, these terms and conditions shall control.

Revocation: Elsevier or Copyright Clearance Center may deny the permissions described in this License at their sole discretion, for any reason or no reason, with a full refund payable to you. Notice of such denial will be made using the contact information provided

by you. Failure to receive such notice will not alter or invalidate the denial. In no event will Elsevier or Copyright Clearance Center be responsible or liable for any costs, expenses or damage incurred by you as a result of a denial of your permission request, other than a refund of the amount(s) paid by you to Elsevier and/or Copyright Clearance Center for denied permissions.

LIMITED LICENSE

The following terms and conditions apply only to specific license types:

Translation: This permission is granted for non-exclusive world English rights only unless your license was granted for translation rights. If you licensed translation rights you may only translate this content into the languages you requested. A professional translator must perform all translations and reproduce the content word for word preserving the integrity of the article.

Posting licensed content on any Website: The following terms and conditions apply as follows: Licensing material from an Elsevier journal: All content posted to the web site must maintain the copyright information line on the bottom of each image; A hyper-text must be included to the Homepage of the journal from which you are licensing at http://www.sciencedirect.com/science/journal/xxxxx or the Elsevier homepage for books at http://www.elsevier.com; Central Storage: This license does not include permission for a scanned version of the material to be stored in a central repository such as that provided by Heron/XanEdu.

Licensing material from an Elsevier book: A hyper-text link must be included to the Elsevier homepage at http://www.elsevier.com . All content posted to the web site must maintain the copyright information line on the bottom of each image.

Posting licensed content on Electronic reserve: In addition to the above the following clauses are applicable: The web site must be password-protected and made available only to bona fide students registered on a relevant course. This permission is granted for 1 year only. You may obtain a new license for future website posting.

For journal authors: the following clauses are applicable in addition to the above:

Preprints:

A preprint is an author's own write-up of research results and analysis, it has not been peer-reviewed, nor has it had any other value added to it by a publisher (such as formatting, copyright, technical enhancement etc.).

Authors can share their preprints anywhere at any time. Preprints should not be added to or enhanced in any way in order to appear more like, or to substitute for, the final versions of articles however authors can update their preprints on arXiv or RePEc with their Accepted Author Manuscript (see below).

If accepted for publication, we encourage authors to link from the preprint to their formal publication via its DOI. Millions of researchers have access to the formal publications on ScienceDirect, and so links will help users to find, access, cite and use the best available version. Please note that Cell Press, The Lancet and some society-owned have different preprint policies. Information on these policies is available on the journal homepage.

Accepted Author Manuscripts: An accepted author manuscript is the manuscript of an article that has been accepted for publication and which typically includes author

incorporated changes suggested during submission, peer review and editor-author communications.

Authors can share their accepted author manuscript:

- immediately via their non-commercial person homepage or blog
  - by updating a preprint in arXiv or RePEc with the accepted manuscript via their
  - research institute or institutional repository for internal institutional uses or as
  - part of an invitation-only research collaboration work-group directly by
  - providing copies to their students or to research collaborators for their personal use
- for private scholarly sharing as part of an invitation-only work group on commercial sites with which Elsevier has an agreement
- After the embargo period via non-commercial hosting platforms such as their institutional repository via commercial sites with which Elsevier has an agreement In all cases accepted manuscripts should:
  - link to the formal publication via its DOI bear a CC-BY-NC-ND license - this is easy to
  - do
  - if aggregated with other manuscripts, for example in a repository or other site, be shared in alignment with our hosting policy not be added to or enhanced in any way to appear more like, or to substitute for, the published journal article.

Published journal article (JPA): A published journal article (PJA) is the definitive final record of published research that appears or will appear in the journal and embodies all value-adding publishing activities including peer review co-ordination, copy-editing, formatting, (if relevant) pagination and online enrichment.

Policies for sharing publishing journal articles differ for subscription and gold open access articles:

Subscription Articles: If you are an author, please share a link to your article rather than the full-text. Millions of researchers have access to the formal publications on ScienceDirect, and so links will help your users to find, access, cite, and use the best available version. Theses and dissertations which contain embedded PJAs as part of the formal submission can be posted publicly by the awarding institution with DOI links back to the formal publications on ScienceDirect.

If you are affiliated with a library that subscribes to ScienceDirect you have additional private sharing rights for others' research accessed under that agreement. This includes use for classroom teaching and internal training at the institution (including use in course packs and courseware programs), and inclusion of the article for grant funding purposes.

Gold Open Access Articles: May be shared according to the author-selected end-user license and should contain a CrossMark logo, the end user license, and a DOI link to the formal publication on ScienceDirect.

Please refer to Elsevier's posting policy for further information.

For book authors the following clauses are applicable in addition to the above: Authors are permitted to place a brief summary of their work online only. You are not allowed to download and post the published electronic version of your chapter, nor may you scan the printed edition to create an electronic version. Posting to a repository: Authors are permitted to post a summary of their chapter only in their institution's repository.

Thesis/Dissertation: If your license is for use in a thesis/dissertation your thesis may be submitted to your institution in either print or electronic form. Should your thesis be published commercially, please reapply for permission. These requirements include permission for the Library and Archives of Canada to supply single copies, on demand, of the complete thesis and include permission for Proquest/UMI to supply single copies, on demand, of the complete thesis. Should your thesis be published commercially, please reapply for permission. Theses and dissertations which contain embedded PJAs as part of the formal submission can be posted publicly by the awarding institution with DOI links back to the formal publications on ScienceDirect.

Elsevier Open Access Terms and Conditions
You can publish open access with Elsevier in hundreds of open access journals or in nearly 2000 established subscription journals that support open access publishing. Permitted third party re-use of these open access articles is defined by the author's choice of Creative Commons user license. See our open access license policy for more information.
Terms & Conditions applicable to all Open Access articles published with Elsevier:
Any reuse of the article must not represent the author as endorsing the adaptation of the article nor should the article be modified in such a way as to damage the author's honour or reputation. If any changes have been made, such changes must be clearly indicated.
The author(s) must be appropriately credited and we ask that you include the end user license and a DOI link to the formal publication on ScienceDirect.
If any part of the material to be used (for example, figures) has appeared in our publication with credit or acknowledgement to another source it is the responsibility of the user to ensure their reuse complies with the terms and conditions determined by the rights holder.

Additional Terms & Conditions applicable to each Creative Commons user license:

CC BY: The CC-BY license allows users to copy, to create extracts, abstracts and new works from the Article, to alter and revise the Article and to make commercial use of the Article (including reuse and/or resale of the Article by commercial entities), provided the user gives appropriate credit (with a link to the formal publication through the relevant DOI), provides a link to the license, indicates if changes were made and the licensor is not represented as endorsing the use made of the work. The full details of the license are available at http://creativecommons.org/licenses/by/4.0.

CC BY NC SA: The CC BY-NC-SA license allows users to copy, to create extracts, abstracts and new works from the Article, to alter and revise the Article, provided this is not done for commercial purposes, and that the user gives appropriate credit (with a link to the formal publication through the relevant DOI), provides a link to the license, indicates if changes were made and the licensor is not represented as endorsing the use made of the work. Further, any new works must be made available on the same conditions. The full details of the license are available at http://creativecommons.org/licenses/by-nc-sa/4.0.

CC BY NC ND: The CC BY-NC-ND license allows users to copy and distribute the Article, provided this is not done for commercial purposes and further does not permit distribution of the Article if it is changed or edited in any way, and provided the user gives appropriate credit (with a link to the formal publication through the relevant DOI), provides a link to the license, and that the licensor is not represented as endorsing the use made of the work. The full details of the license are available at http://creativecommons.org/licenses/by-nc-nd/4.0. Any commercial reuse of Open Access articles published with a CC BY NC SA or CC BY NC ND license requires permission from Elsevier and will be subject to a fee.
Commercial reuse includes:

- Associating advertising with the full text of the Article
- Charging fees for document delivery or access
- Article aggregation
- Systematic distribution via e-mail lists or share buttons

Posting or linking by commercial companies for use by customers of those companies.

20. Other Conditions:

v1.10
Questions? customercare@copyright.com.